Electronic Thesis and Dissertation Repository

12-11-2017 1:00 PM

Neuronal Correlates for Neuroendocrine Habituation to Repeated Stress

Sara Matovic, *The University of Western Ontario*

Supervisor: Inoue, Wataru, *The University of Western Ontario*
A thesis submitted in partial fulfillment of the requirements for the Master of Science degree in Neuroscience
© Sara Matovic 2017

Follow this and additional works at: https://ir.lib.uwo.ca/etd

Part of the Behavior and Behavior Mechanisms Commons, Biological Phenomena, Cell Phenomena, and Immunity Commons, Mental Disorders Commons, Neurosciences Commons, Physiological Processes Commons, and the Psychiatric and Mental Health Commons

Abstract

One way that the body actively responds to an impending stressor is by increasing systemic glucocorticoids through the activation of the hypothalamic-pituitary-adrenal (HPA) axis. While it is essential for short-term adaptation to stress, the sustained activation of the HPA axis during chronic stress can be detrimental and is linked to stress-related psychiatric conditions such as anxiety and depression. Therefore, it is important that the HPA axis adapts, or habituates, during chronic stress to minimize the negative consequences. Corticotropin releasing hormone (CRH) neurons in the paraventricular nucleus of the hypothalamus (PVN) function to assimilate incoming information from the stress circuitry and initiate the HPA axis by releasing CRH to the circulation. Here, we report a neurophysiological correlate for the habituation of the HPA axis to daily repeated restraint stress in mice. By using immunohistochemistry, we first show that 21 days of repeated restraint stress decreases restraint-induced c-fos expression in PVN-CRH neurons (i.e. habituation of PVN-CRH neurons to restraint). We then show that this neuronal habituation to repeated restraint stress is accompanied by a robust decrease in the intrinsic excitability of PVN-CRH neurons. Mechanistically, the stress-induced decrease in the intrinsic excitability correlates with a decrease in whole-cell membrane resistance. Surprisingly, the decrease in the membrane resistance is not due to the changes in specific properties of the cell membrane but is best explained by the changes in cell surface area (i.e. cell size), suggesting that stress-induced changes in cell size promote attenuation of incoming stress signals. Together these findings support stress-induced changes during habituation that promote stress resilience.

Keywords: stress, resilience, habituation, HPA axis, paraventricular nucleus of the hypothalamus, corticotropin releasing hormone, intrinsic excitability

Co-Authorship Statement

This thesis includes material that is result of joint research, as follows:

Xue-Fan Wang and Aoi Ichiyama conducted the experiments and data analysis presented in Chapter 3, section 3.1, as part of their honors thesis projects. Eric Salter generated data and contributed to the initial development of the projects investigating the plasticity of PVN-CRH neurons' plasticity, as well as conducted synaptic stimulation experiments (Figure 3.2.1), as a part of his honors thesis project.

Acknowledgments

Table of Contents

List of Figures

List of Tables

List of Appendices

Chapter 1

1. Introduction

1.1 The Stress Response

The activation of the hypothalamic-pituitary-adrenal (HPA) axis is a fundamental survival mechanism that coordinates physiological and psychological responses to manage impending threats. Although this immediate reaction to stress is essential for our survival, protracted activation of the HPA axis during chronic stress can become detrimental and contribute to psychophysiological mal-adaptations, particularly in vulnerable subjects (B. S. McEwen, 2000; Munck, Guyre, & Holbrook, 1984; Sapolsky, Romero, & Munck, 2000). For example, a meta-analysis of 361 human studies implicated the hyperactivity of the HPA axis in depression etiology (Stetler & Miller, 2011); HPA axis hyperactivity may also be a link between depression and its prevalent comorbidities such as diabetes, dementia and coronary heart disease (Brown, Varghese, & McEwen, 2004). However, it is important to note that the majority of people maintain normal psychophysiological functioning and avoid mental illnesses, even under high levels of stress. Indeed, it has become increasingly clear that there are a number of active adaptation mechanisms promoted by prior exposure to stress (Covington et al., 2010; Lehmann & Herkenham, 2011; Russo, Murrough, Han, Charney, & Nestler, 2012). For example, it has been shown that mild early-life stressors can promote resilient behaviours when encountering a novel stressor later in life, as indicated by increased exploratory behaviour and lower cortisol levels under stress (Parker, Buckmaster, Schatzberg, & Lyons, 2004). Therefore, our survival and resilience to psychiatric illnesses relies on the ability to integrate and learn from our past experiences and accordingly fine-tune the stress response in a longer time scale to be able to adapt to a dynamic environment.

In line with the idea that stress exposure can promote adaptive changes that can serve as a mechanism for resilience, human studies show that the HPA axis normally responds less and less (i.e. becomes habituated) to repeated encounters of psychological stress (Kirschbaum et al., 1995). Also it has been shown that the lack of habituation is associated with stress vulnerability (Epel et al., 2000; Gianferante et al., 2014; Kudielka,

Bellingrath, & Hellhammer, 2006; B. S. McEwen & Seeman, 1999). In animal models, it is well established that the HPA axis gradually habituates to restraint stress, a primarily psychological stressor, when repeated over days to weeks (Aguilera, 1994a; Bhatnagar, Huber, Nowak, & Trotter, 2002a; X. Chen & Herbert, 1995; Kim & Han, 2006; Uchida et al., 2008). Similar to human studies, impairment of HPA axis habituation during chronic stress is associated with the development of anxiety-related symptoms (Uchida et al., 2008). This suggests that habituation of the HPA axis in response to long-term stress exposure, is one way by which stress resiliency can be promoted. Stress-induced changes in HPA axis function is a form of learning; therefore, established animal models of stress habituation provide a useful model to examine the underlying neural plasticity.

This project investigates the neural plasticity that may underlie habituation of the HPA axis to repeated stress by using a mouse model. In order to outline the framework of this project, I will first describe the general mechanisms underlying HPA axis activation during stress. Next, I will narrow my focus on one brain region, the paraventricular nucleus of the hypothalamus (PVN), which serves as a key regulator of the HPA axis. Lastly, I will describe neural plasticity at the level of the PVN with relevance to HPA axis habituation and ultimately how this may serve as a potential cellular mechanism for stress resilience.

1.2. The HPA axis

The brain regulates the elevation of circulating glucocorticoids (GCs) through activation of the HPA axis. The HPA axis consists of three components: the hypothalamus, pituitary and adrenal gland (Figure 1.1). The apex of the HPA axis is a population of neuroendocrine neurons localized in the PVN that synthesize corticotropin-releasing hormone (CRH). Upon activation of these neuroendocrine neurons, CRH is released into the hypophyseal portal circulation, and reaches the anterior pituitary to stimulate the release of adrenocorticotropic hormone (ACTH). The CRH-induced release of ACTH can also be enhanced by a co-secretagogue arginine vasopressin (AVP), which is produced by and released from neurons in the PVN (Herman & Cullinan, 1997). ACTH released into the general circulation, in turn, stimulates the release of GCs from the adrenal cortex (Figure 1.1).

Figure 1.1
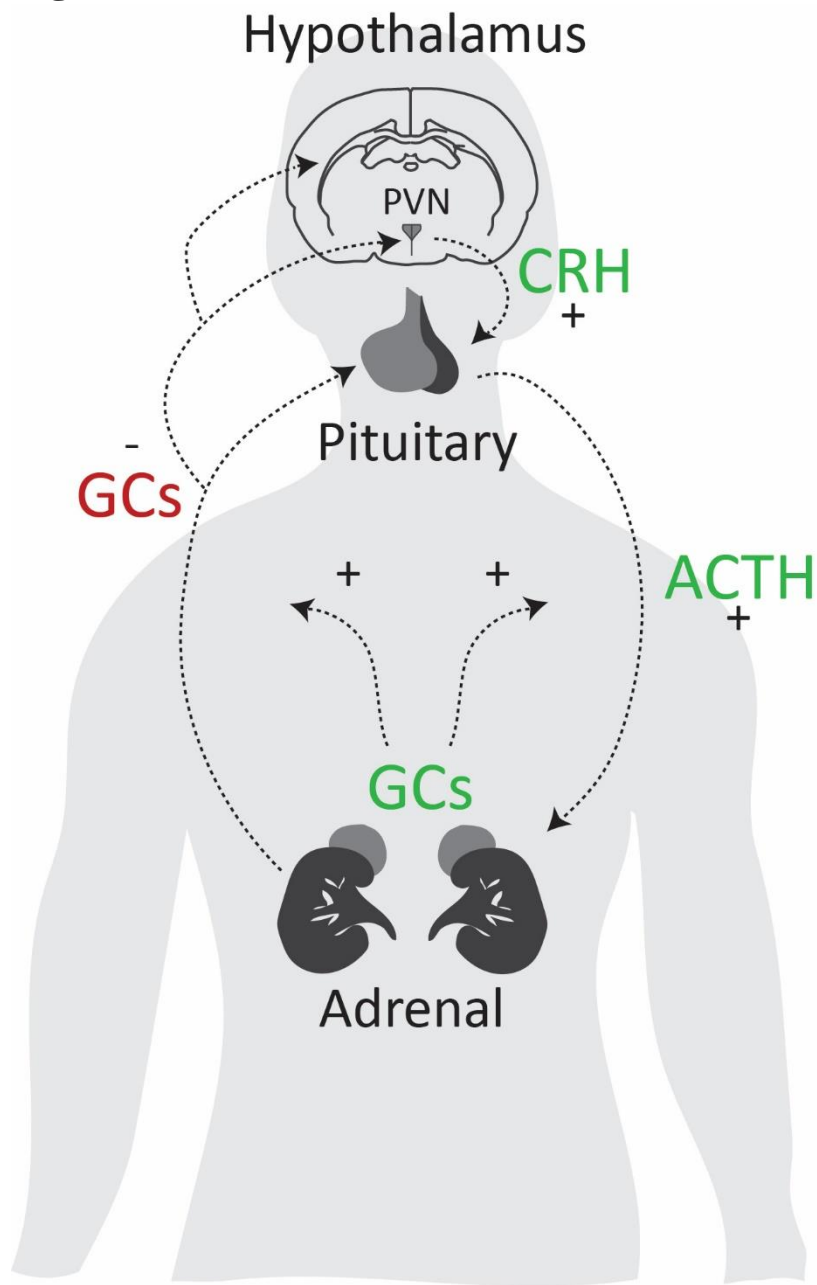
Figure 1.1 The Hypothalamic-Pituitary-Adrenal (HPA) Axis.

The HPA axis is regulated through the actions of neurons from the paraventricular nucleus (PVN) of the hypothalamus. These neurons secrete corticotrophin releasing hormone (CRH) in accordance with daily circadian rhythms or in response to stress. CRH secretion reaches the anterior pituitary via the hypophyseal portal system and stimulates the secretion of adrenocorticotropic hormone (ACTH). ACTH then acts on the adrenal cortex to secrete glucocorticoids (GCs). GCs serve as a negative feedback mechanism through their actions on the brain and pituitary gland. Adopted from https://www.integrativepro.com/Resources/Integrative-Blog/2016/The-HPA-Axis

GCs are a type of steroid hormone (corticosteroid) which exert their effects by binding GC receptors. GCs are an important mediator of the stress response with widespread actions throughout the body including the brain. In the brain, GCs have three important actions during stress: they 1) elicit cognitive, emotional and physiological changes associated with stress; 2) inhibit the HPA axis, serving as a negative feedback signal; and 3) promote long-lasting plasticity of these systems (Bruce S. McEwen, 2012; Sapolsky et al., 2000). The plasticity-related actions of GCs provide a way to self-tune the HPA axis based on the history of stress (Dallman, Akana, Strack, Hanson, & Sebastian, 1995; de Kloet, Joëls, & Holsboer, 2005; Bruce S. McEwen, 2012). Almost all cells in the body express GC receptors in the cytoplasm with slightly varying functions (i.e., in some cells GC receptor binding activates gene transcription, while in other cells it represses gene transcription); this promotes different GC actions in different organs and orchestrates different outcomes (Cain & Cidlowski, 2017). In order to prepare the body to survive an impending stressor, a classic action of GCs is to mobilize energy stores (glycogenolysis and lipolysis) to supply resources to the body during stress (Herman et al., 2003; Tanaka, Shimizu, & Yoshikawa, 2017). In addition, GCs exert powerful anti-inflammatory and immunosuppressive effects as well as modulate cardiovascular tones (Buttgereit, Burmester, & Lipworth, 2009). The adverse consequences of excess GCs action are well documented in Cushing Syndrome, a condition with chronic high levels of GCs, that leads to various psychophysiological symptoms including ulcers, hypertension, immunosuppression, glucose intolerance, insulin insensitivity, osteoporosis, impaired wound healing, depression and mood changes (Cain & Cidlowski, 2017). Although Cushing Syndrome differs from chronic stress, the symptoms of the hypercortisolemia share striking similarities with the maladaptive consequences of chronic stress. This points to the importance of the mechanisms that constrain HPA axis hyperactivity in promoting stress resilience.

It is important to mention that under normal non-stress conditions, low-level, circadian cycles of glucocorticoids also play many physiological roles including food intake, learning, attention and cognition that are not associated with stressful experiences (Dallman et al., 1987; De Kloet, Vreugdenhil, Oitzl, & Joëls, 1998). For the purpose of this project, we narrow the discussion of HPA axis activity as it relates to stress.

1.3 Paraventricular Nucleus of the Hypothalamus: the apex of the HPA axis

1.3.1 Inputs to the PVN

Virtually any type of stress activates the HPA axis. In other words, a diverse range of sensory information, such as visual, auditory and olfactory signals associated with predator threats, somatosensory cues associated with pain, and humoral cues associated with inflammation, are all processed in various brain regions which ultimately recruit the same neuronal mechanism that lead to the activation of CRH neurons in the PVN. These various brain regions, which are implicated in the convergence of stress related signals, process and relay stress information through both direct and indirect projections to the PVN (Figure 1.2). Herman and colleagues (2003) proposed a model which organizes the neuro-circuitry underlying the activation of the HPA axis under two different circumstances: "real" stress and "perceived" stress. Generally, these different types of stressors recruit distinct circuits leading to the activation of the PVN.

Figure 1.2
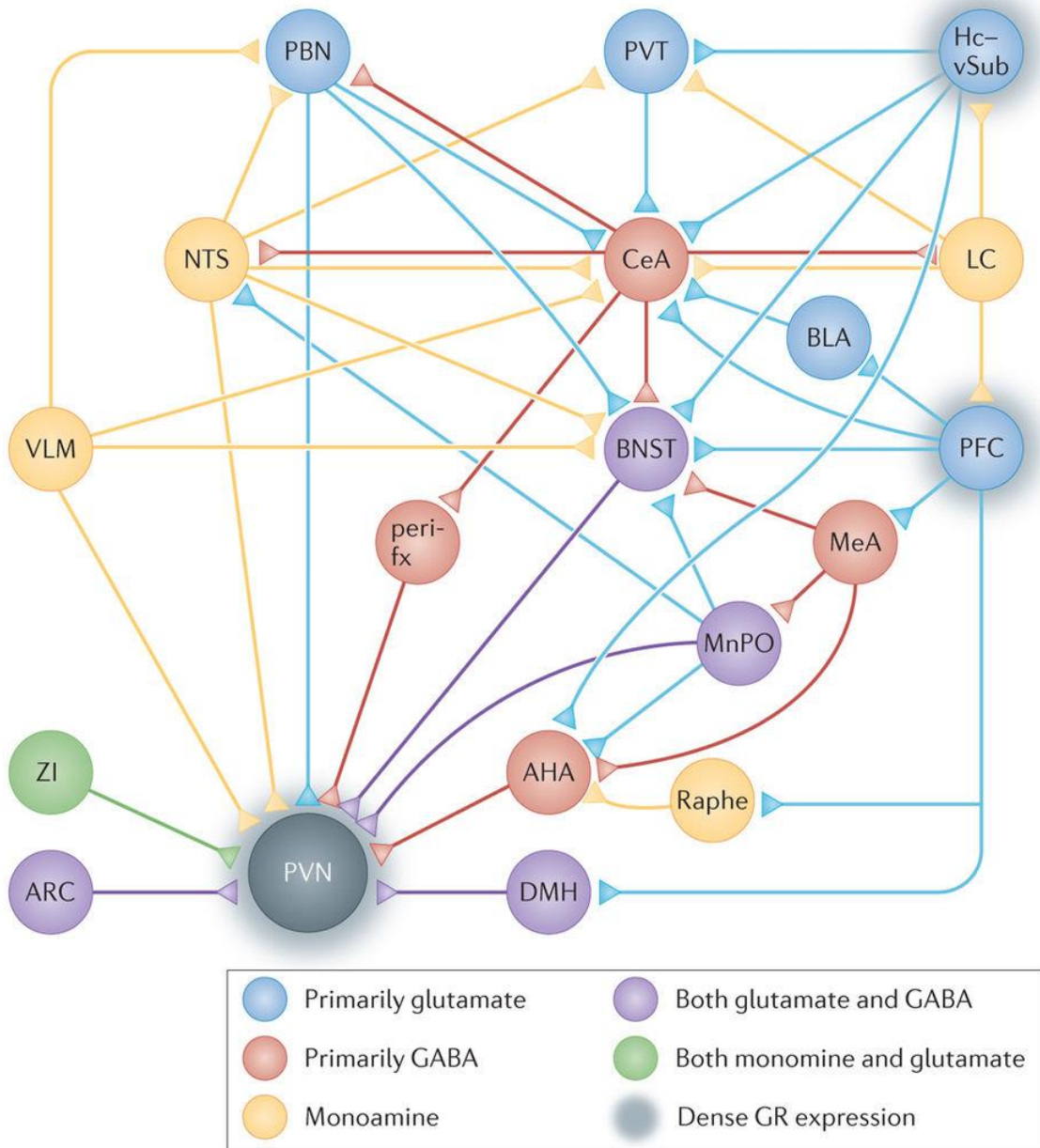
Figure 1.2 Brain circuitry involved in the HPA axis response to stress.

Various direct and indirect inputs to the paraventricular nucleus (PVN) of the hypothalamus are involved in regulating the HPA axis response to stress.

Abbreviations: AHA, anterior hypothalamus; ARC, arcuate nucleus; BLA, basolateral amygdala; BNST, bed nucleus of the stria terminalis; CeA, central amygdala; DMH, dorsomedial hypothalamus; Hc, hippocampus; LC, locus coeruleus; MeA, medial amygdala; MnPO, medial preoptic nucleus; NTS, nucleus tractus solitarius; PBN, parabrachial nucleus; PVT, paraventricular thalamus; peri-fx, peri-fornical area; PFC, prefrontal cortex; Raphe, Raphe nuclei; VLM, ventrolateral medulla; vSub, ventral subiculum; ZI, zona incerta.

Real stress is defined as physiological challenges such as inflammation, injury and pain, as well as deviation of cardiovascular, respiratory and metabolic functions from the normal homeostatic range. These real stressors trigger a rapid, reflexive activation of the brain areas that mostly send direct projections to the PVN. While determining the exact interplay between the different brain regions involved in regulating stress has yet to be fully understood, there is a general proposal of how these different stress regions interact. For example, it is believed that direct inputs to the PVN that are involved in reflexive stress integration come from the arcuate nucleus, dorsal medial hypothalamus, and medial preoptic nucleus, which all send both glutamatergic and GABAergic projections to the PVN; the anterior hypothalamus and peri-fornical area, which send primarily GABAergic projections; ventrolateral medulla and nucleus tractus solitarus, which send primarily monoamine projections; the zona incerta, which sends monoamine and glutamatergic projections; and the bed nucleus of the stria terminalis (BNST), which sends primarily GABAergic projections and serves as an important relay station connecting the limbic forebrain structures to the PVN (Cunningham, Bohn, & Sawchenko, 1990; Herman et al., 2003).

On the other hand, perceived stress is an anticipatory response to a potential threat. Perceived stress has greater involvement of the limbic and forebrain structures that do not send direct projection to the PVN, but rather through major stress integrating relay stations such as the BNST. Examples of limbic forebrain structures involved in perceived stress include the ventral subiculum of the hippocampus and the prefrontal cortex, which contain primarily glutamatergic projections to major stress integrating deep brain structures (e.g. amygdala, thalamus, locus coerulus and BNST); the central and medial amygdala which receive inputs from almost all limbic forebrain structures, and sends primarily GABAergic projections to stress integrating deep brain structures (e.g. BNST, parabrachial nucleus, locus coerulus and nucleus tractus solitarius); and the locus coeruleus, which sends monoamine projections to stress integrating nuclei such as the amygdala and thalamus (Bains, Cusulin, & Inoue, 2015; Herman et al., 2003a). These two "distinct" stress activation routes are not mutually exclusive; rather, some brain areas can mediate information from both pathways. For example, the nucleus tractus solitarius serves both a reflexive function for real homeostatic stressors by receiving inputs from

9

cardiovascular afferents and medullary neurons controlling autonomic functions, and also serves an anticipatory, perceived stress role by receiving afferent inputs from the limbic forebrain brain areas (Herman et al., 2003).

Although ideas about the involvement of different brain regions in different types of stress responses have been proposed (Bains, Cusulin, & Inoue, 2015; Herman et al., 2003), a lot of work remains in establishing the relationship and roles of these various stress regions during stress integration. Despite the complexity of the stress circuitry, one commonality among all elicited stressors is that the stress signals ultimately converge on the neurons within the PVN. For this reason, neural plasticity that occurs in the PVN itself has the capacity to serve a major role in regulating the HPA axis. Therefore, my project will be investigating the neuroplasticity occurring specifically at these PVN neurons.

1.3.2 Neuronal subtypes of the PVN

Besides neuroendocrine neurons that release CRH to initiate the HPA axis, the PVN contains other types of neurons that are involved in vital physiological functions such as fluid homeostasis (Bourque, 2008), lactation (Walker, Toufexis, & Burlet, 2001), metabolism (Billington, Briggs, Harker, Grace, & Levine, 1994) and the regulation of the autonomic nervous system (Ulrich-Lai & Herman, 2009). The PVN neurons are highly heterogeneous: there are > 10 different populations of neurons that can be defined based on their neurochemical and neuroanatomical features (Biag et al., 2012; Simmons & Swanson, 2009). However, conventionally these populations are classified into three major categories based on their gross phenotype. These include 1) magnocellular neuroendocrine neurons, 2) parvocellular neuroendocrine neurons, and 3) parvocellular pre-autonomic neurons. The magnocellular neurons are characterized by their large cell body size (from which "magno" comes from), the expression of two neuropeptides AVP and oxytocin, and their axonal projection to the posterior pituitary. AVP is an important regulator for water retention in the body, and also functions synergistically with CRH to stimulate ACTH release (Abou-Samra, Harwood, Manganiello, Catt, & Aguilera, 1987; Lee, Tse, & Tse, 2015). Oxytocin mediates the milk ejection reflex during breastfeeding as well as cervical dilation before the birth and uterine contractions during labor (Gimpl

& Fahrenholz, 2001). The second population are the parvocellular neurosecretory neurons. Morphologically, they tend to be smaller than magnocellular neurons with a more complex dendritic architecture (Tasker & Dudek, 1991). Parvocellular neurons project to the median eminence and secrete various releasing hormones into the pituitary portal circulation for neuroendocrine regulations. These includes, CRH for the HPA axis as well as thyrotropin releasing hormone (TRH), somatostatin, and dopamine (Daftary, Boudaba, & Tasker, 2000). The third subtype are the pre-autonomic descending parvocellular neurons that project to the brainstem and spinal cord and regulate the sympathetic nerve tone (Sawchenko & Swanson, 1982; Stern, 2001). These pre-autonomic neurons contain three subtypes which are identified based on their localization in different sub-nuclei of the PVN and also based on their morphology (Stern, 2001). The plasticity of these neurons has been implicated in elevated sympathetic activity that is associated with heart failure (Nunn, Womack, Dart, & Barrett-Jolley, 2011).

Since the parvocellular neuroendocrine neurons are responsible for the stimulation of ACTH release and consequently GC production through the actions of CRH, my project will specifically examine changes in CRH secreting PVN neuron: the neurons that form the apex of the HPA axis.

1.3.3 The electrophysiological properties of PVN neuronal subtypes

Earlier studies that conducted electrophysiological recording from histologically identified neurons in the PVN have identified unique electrophysiological properties (i.e. electrophysiological "fingerprints") associated with different classes of PVN neurons (N. W. Hoffman, Tasker, & Dudek, 1991; J A Luther et al., 2002; Jason A. Luther & Tasker, 2000; Stern, 2001; J. G. Tasker & Dudek, 1991). I will give a brief overview of these electrophysiological "fingerprints" that have been the standard of the field (Hewitt & Bains, 2006; Hewitt, Wamsteeker, Kurz, & Bains, 2009; Hoyda & Ferguson, 2010; Inoue et al., 2013; Latchford, 2008; Levy & Tasker, 2012; Loewen & Ferguson, 2017; Price, Hoyda, Samson, & Ferguson, 2008; Senst, Baimoukhametova, Sterley, & Bains, 2016a; Taylor et al., 2005; Yuill, Hoyda, Ferri, Zhou, & Ferguson, 2007).

Magnocellular neurons are characterized by a strong outward rectifying current upon sufficient depolarization due to a large transient inactivating potassium current (A-

type current, I_A; Figure 1.3, A; Luther & Tasker, 2000). On the other hand, parvocellular pre-autonomic neurons exhibit a large low-threshold Ca^{2+} current (T-type current, I_T). Additionally this depolarizing I_T current contributes to low-threshold spiking (LTS), which is characteristic of parvocellular pre-autonomic neurons (Figure 1.3,C; Stern, 2001) and has been implicated in generating rhythmicity and oscillatory behaviour in the brain (Gutnick & Yarom, 1989). Lastly, parvocellular neurosecretory neurons are characterized by minimal I_A current upon depolarization and consequently a lack of outward rectification. Additionally, they sometimes contain a small I_T current upon depolarization. However, this current is not large enough to induce LTS as is defined above (Figure 1.3, B; Luther et al., 2002).

Figure 1.3

+30 to +80 pA

0 pA

-60 to -30 pA

-30 to -15 pA

A Magnocellular
A-type component

B Parvocellular
Neurosecretory

C Parvocellular Pre-Autonomic
Low-threshold Ca2+ component

40 mV

100 ms
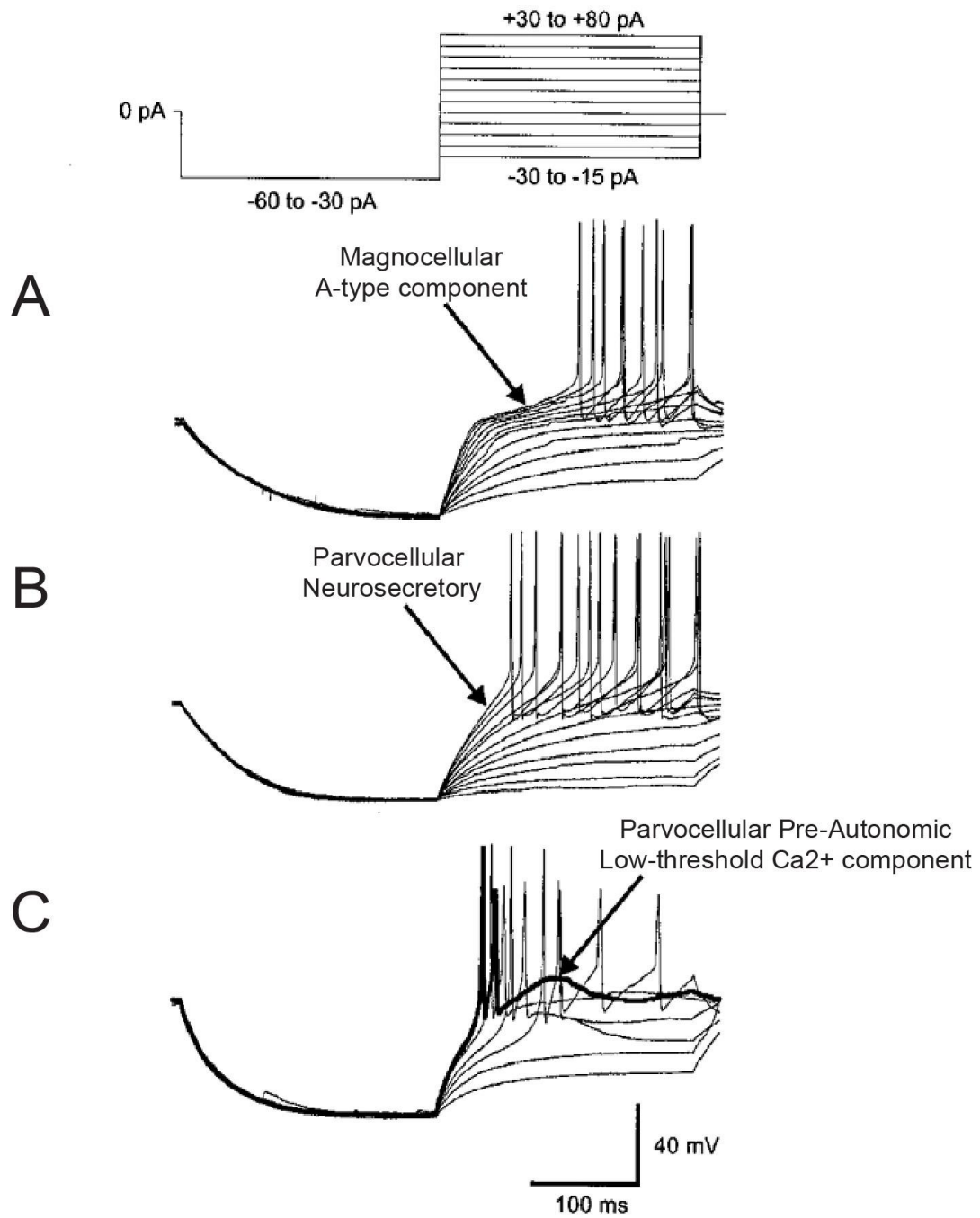
Figure 1.3 Electrophysiological Fingerprints in the Paraventricular Nucleus (PVN) of the Hypothalamus.

Top, current clamp protocol used to investigate the electrophysiological fingerprints of PVN neurons. **(A)** Magnocellular neurons of the PVN contain a strong outward rectifying current (I_A) upon depolarization. **(B)** Parvocellular neurosecretory neurons of the PVN lack a strong outward rectifying current and can contain minimal low threshold T-type Ca^{2+} conductance (I_T). **(C)** Parvocellular pre-autonomic neurons show large low threshold T-type Ca^{2+} current (I_T).

Modified from "Voltage-gated currents distinguish parvocellular from magnocellular neurones in the rat hypothalamic paraventricular nucleus," by J. A. Luther & J. G. Tasker. 2000. *The Journal of Physiology*. *523*(1): 193–209. Copyright (2000) The Journal of Physiology. Reprinted with permission.

These electrophysiological fingerprints have tremendously benefitted electrophysiological research in the PVN by providing an easy way (without the need for post-hoc histological analysis of filled cells) to identify specific subpopulation of neurons in slice during electrophysiology experiments. However, the limitation to this approach is that it cannot differentiate between neurochemical phenotypes of PVN neurons. For example, among parvocellular neuroendocrine neurons, there are neurons that express CRH, TRH, somatostatin, and dopamine that are involved in distinct physiological functions. Recently, reporter mouse lines for these neuropeptides have been generated. For my thesis research, which focuses on CRH neurons, three independent groups have validated a CRH neuron reporter line (Crh-IRES-Cre crossed with floxed tdTomato) which drives the expression of bright red fluorescent protein tdTomato in CRH neurons (Chen, Molet, Gunn, Ressler, & Baram, 2015; Itoi et al., 2014; Wamsteeker Cusulin, Füzesi, Watts, & Bains, 2013). The tdTomato labelled CRH neurons in this reporter mouse line follow an established rostral-caudal pattern of activation of CRH neurons (Biag et al., 2012). Also, when neurons in this mouse line were immunofluorescently labelled for CRH, they showed high co-localization with tdTomato in nearly all CRH-expressing somata (96.0±0.3%; Wamsteeker Cusulin et al., 2013). To add, tdTomato neurons showed a high co-localization with fluorogold, a retrograde marker for neuroendocrine neurons (85.9±0.2%; Wamsteeker Cusulin et al., 2013). These findings support the specificity for tdTomato labelling within CRH neurons. With the development of this mouse line, this now allows me to identify CRH neurons in mice so that I can study the intrinsic plasticity changes that occur with stress. Stress can potentially change the electrophysiological properties of CRH neurons, therefore this study would be impossible without the development of the CRH reporter mouse that allows for CRH neuron identification without reliance on the electrophysiological fingerprint.

1.4 Habituation

As mentioned earlier, excessive activation of the HPA axis during chronic stress has been implicated in psychological and physical maladaptation to stress. Therefore, the mechanisms that limit the activity of the HPA axis during chronic stress are an important

aspect of adaptation, providing stress resiliency. A prominent example is the decrease of the HPA axis response to a mild stressor following repeated exposures to that same stressor, a phenomenon commonly known as habituation of the HPA axis. The term "habituation" refers to a wide range of behavioral adaptations during which an organism decreases its innate response to a stimulus after repeated presentations, as defined in a landmark review by Thompson & Spencer (1966). Recently, Grissom and Bhatnagar (2009) surveyed extensive literature in neuroendocrinology and summarized several characteristics of HPA axis habituation. Here, I will discuss these characteristics with relevance to the adaptive advantages of HPA axis habituation for stress resiliency.

1. Habituation is specific for "perceived" but not for "real" stress.

The HPA axis response habituates to repeated exposures to varieties of stressors including restraint, immobilization, social defeat, and loud noise (Grissom & Bhatnagar, 2009). An important common feature of these stressors is that they are "perceived" or psychological stress and do not involve major physiological challenges. By contrast, "real" or physiological stressors generally do not cause habituation of the HPA axis. These example includes repeated administration of hypertonic saline (Kiss & Aguilera, 1993) and foot shock (Kant, Bunnell, Mougey, Pennington, & Meyerhoff, 1983). From the perspective of the adaptive advantages of habituation, specificity for the category of stressors is reasonable: habituation is an active learning process that applies to non-threatening stimuli to minimize the cost of mounting the HPA axis response; whereas, for the challenges that indeed require the actions of GCs, the HPA axis does not habituate. The mechanisms for stress selectivity remain unknown. However, one possibility is that it relates to the "severity" of stress. An earlier study showed that the speed of habituation is inversely correlated with the severity of stressor (Natelson et al., 1988). Another possibility is that the specificity of habituation arises from the difference in the underlying neural circuits for "real" and "perceived" stressors as described earlier.

2. Habituation is context-dependent and stressor-specific

While various types of stressors cause, when repeated, habituation of the HPA axis, the development of habituation to repeated stressor is specific to the stressor within a given series of repeated stress. Indeed, it has also been reported that animals that had

been habituated to restraint stress or cold stress respond to a novel stressor with a sensitized HPA axis activation (Bhatnagar & Dallman, 1998; Kiss & Aguilera, 1993; Melia, Ryabinin, Schroeder, Bloom, & Wilson, 1994). Moreover, a recent study reported that habituation to a repeated stressor also depends on the physical context of the previous stressor such that when habituated rats were stressed with the same stressor but novel context (i.e. a different odor in the room), they exhibited less habituation (Grissom & Bhatnagar, 2009). The stressor- and context-specificity of HPA axis habituation provides strong evidence that habituation is not due to a simple run down of the endocrine function or sensory inactivation, but rather an active process to attenuate the endocrine response to specific stressor.

3. Habituation is reversible

The stressor and context specificity also indicates that the habituation of the HPA axis is quickly reversible (by a new stressor). Along the same line, it has been predicted that HPA axis habituation spontaneously reverses once the repeated stress is terminated. However, to date few studies have addressed this issue. One available study, indeed, indicated the opposite and found that habituation to repeated restraint stress showed only a partial recovery after 3 weeks of no stress recovery period. In my thesis, I characterized the spontaneous recovery from habituation in a mouse model of repeated restraint.

Habituation, as it has been described in the context of repeated restraint stress, describes an attenuation of a stress response that is learned to be harmless, while maintaining the capacity to respond optimally to other forms of potentially harmful stressors. In this respect, habituation of the stress response can serve as a mechanism to promote resilience within a dynamically changing environment.

1.5. Rationale, Hypothesis, Aims

1.5.1 Rationale: Habituation, as a mechanism for resilience

A number of mechanisms occurring during stress exposure actively promote future resilience to stress. Habituation of the HPA axis is one mechanism by which the brain learns about stress and diminishes the future stress response (Aguilera, 1994; Grissom & Bhatnagar, 2009). While the stress-circuitry regulating activity of the HPA

axis is complex, one area that integrates all stress-relevant information and initiates the HPA axis is the PVN. However, the potential involvement of the plasticity of PVN-CRH neurons in the development of HPA axis habituation remains obscure. Habituation, by nature, is a diminished responsiveness of neurons to a given stimuli. Thus, one possibility is that HPA axis habituation involves a reduced responsiveness of the CRH neurons to excitatory inputs (i.e. a decrease in intrinsic excitability).

1.5.2 Hypothesis

The development of the HPA axis habituation to repeated stress involves a decrease in the intrinsic excitability of PVN-CRH neurons.

1.5.3 Aims

1. To establish a timeline looking at habituation to repeated restraint stress by examining neuronal excitability.

2. To investigate the neurophysiological intrinsic excitability changes that occur with repeated restraint stress.

3. To investigate the mechanisms related to these intrinsic excitability changes that occur with repeated stress.

Chapter 2

2. Materials and Methods

2.1 Animals

All experimental procedures were approved by the University of Western Ontario Animal Use Subcommittee and University Council on Animal Care in accordance with the Canadian Council on Animal Care guidelines. Homozygous *Crh-IRES-Cre* (Stock No: 012704, the Jackson Laboratory) and *Ai14* (Stock No: 007908, the Jackson Laboratory) mice were mated, and the resulting heterozygous crh-IRES-Cre;Ai14 offspring were used as CRH-reporter mice as characterized in detail previously (Chen, Molet, Gunn, Ressler, & Baram, 2015; Itoi et al., 2014; Wamsteeker Cusulin et al., 2013). The bright tdTomato expression allows for visual identification of CRH neurons in brain slices prepared for immunohistochemistry as well as *ex vivo* electrophysiology recordings (Figure 2.1). All animals used were male and between 8-12 weeks old at the time of sacrifice. They were group housed (2-4 mice per cage) in a standard shoebox mouse cage supplied with a mouse housing, paper nesting materials and wood chip bedding. The mice were housed on a 12/12 hour light/dark cycle (lights on 07:00) in a temperature-controlled ($23 \pm 1°C$) room with free access to food and water. Cages were cleaned every 7 days.

Figure 2.1
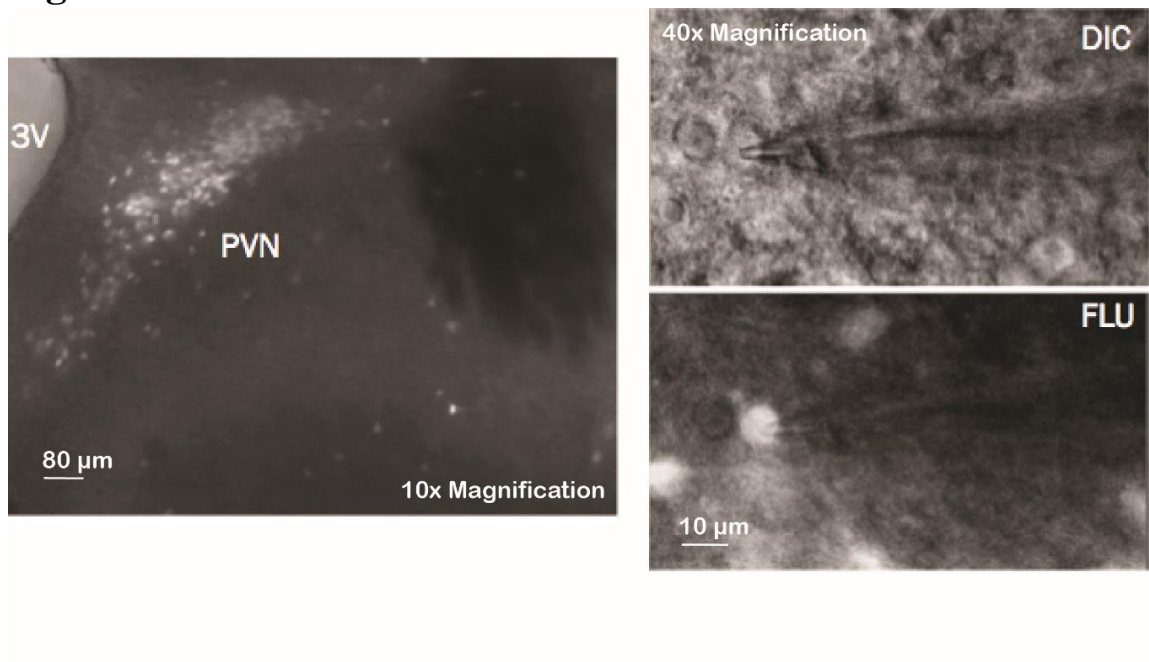
Figure 2.1 Visual Identification of Fluorescent PVN CRH neurons.

Fluorescent PVN CRH neurons shown at 10x magnification (left). PVN CRH neurons shown under both differential interference contrast (DIC) conditions and fluorescent (FLU) conditions while patch-clamped (right).

2.2 Stress protocols

For restraint stress, mice were placed in a restrainer constructed from a 50 mL conical tube with multiple ventilation holes. In order to restrict the forward/backward movement of mice, the inner space length of the restrainer was adjusted by moving a disc wall that forms the one end of the restrainer (Figure 2.2). For a single session of restraint stress, mice were restrained in an empty, clean breeding cage (cage base dimensions = 45cm length x 35cm width x 20cm height) with up to 12 mice per cage for one hour (between 13:00-14:00 during the light phase). For repeated restraint stress, the one hour restraint stress session was repeated for 7 or 21 consecutive days. For stress recovery assessments, an additional group of mice were first subjected to 21 days of repeated restraint stress and then left undisturbed in their home cage for 7 days. The control mice were kept in their home cage in the animal housing facility.

Figure 2.2

Figure 2.2 Repeated Restraint Stress Tube.

Stress tube is constructed using a 50mL conical tube with drilled ventilation holes. Mice are placed with their tail out from the top of the conical tube and movement is restricted by using an adjustable disc wall constructed from a button and wooden stick. Mice were tied to a platform to prevent turning of the tube.

2.3 Immunohistochemistry

Immunohistochemistry and subsequent image analysis was conducted by two undergraduate students Xue Fan Wang and Aoi Ichiyama in the Inoue Lab as a part of their honors thesis projects. Our goal was to determine the time course of PVN-CRH neuron habituation to repeated restraint stress. To this end, we examined c-fos expression in PVN-CRH neurons following one-hour restraint stress in mice that were naïve to the stressor, repeatedly exposed to the stressor for 7 and 21 consecutive days, and received no stress for 7 days after 21-day repeated stress. Accordingly, on the following day of the last repeated stress session, mice received an additional one-hour restraint stress as a probe stress (e.g. on 8th and 22nd day, and 8th day of stress recovery period), and were perfused for brain collection immediately after the end of the probe stress. The mice were deeply anaesthetized with sodium pentobarbital (50mg/kg, i.p.). A tail-pinch test was performed to ensure the depth of the anesthesia. (Blood samples were collected from the right ventricle using a 1 mL syringe containing 10μL of ethylenediaminetetraacetic acid (EDTA). The mice were transcardially perfused with ice-cold saline solution (0.9% NaCl) followed by 4% paraformaldehyde (PFA) dissolved in phosphate-buffered saline (PBS, pH 7.4). The brains were removed and fixed in 4% PFA at 4°C overnight. The fixed tissue was then transferred to PBS and supplemented with 0.03 % sodium azide and kept at 4°C for a short-term storage (up to 4 weeks). The brains were coronally sectioned into 50μm thick slices using a vibratome (VT1000s, Leica). Sections were stored in a cryoprotectant solution (30% glycerol, 30% ethylene glycol, in 20 mM PB) at -20°C until used for immunohistochemistry. Immunohistochemistry was performed on free-floating sections. Sections were rinsed in PBS 3 times for 5 minutes each and then incubated in a blocking solution (3% normal donkey serum, 0.3% triton and 0.03% NaN_3 in PBS) for 1 hour to minimize non-specific binding. Slices were then incubated with anti-c-fos rabbit monoclonal antibody (Cell Signalling Technology, cat: 2250S, 1:1000 dilution in blocking solution) overnight at room temperature. After three washes in PBS on the next day, the sections were incubated with Alexa Fluor 647 donkey anti-rabbit IgG (ThermoFisher Scientific, cat: A-31573, 1:500 dilution in blocking solution). Then after three washes with PBS, the sections were incubated in 4',6-diamidino-2-phenylindole (DAPI; Sigma, cat: 28718-90-3, 1:5000 in PBS) for 10 minutes. After two final rinses

with PBS, the sections were mounted (VWR Micro Slides) and air-dried overnight. The slides were cover slipped using Fluoromount-G mounting medium (Electron Microscopy Sciences).

2.4 Slice preparation

For the electrophysiology experiments, our goal was to investigate lasting plasticity due to the stress paradigm. For this purpose, we sacrificed the mice the day after the last restraint stress (i.e., on day 22 without stressing the mouse on that day). To collect the brain tissue, the mice were deeply anesthetized with isoflurane and decapitated. Brains were then quickly removed from the skull and placed in icy slicing solution containing (in mM): 87 NaCl, 2.5 KCl, 25 $NaHCO_3$, 0.5 $CaCl_2$*2H2O, 7 $MgCl_2$*6H2O, 1.25 NaH_2PO + H2O, 25 glucose and 75 sucrose (Osmolarity: 315-320 mOsm), saturated with 95% O_2/5% CO_2. 250µm thick coronal sections containing the paraventricular nucleus of the hypothalamus (PVN) were obtained using a vibratome (VT1200 S, Leica). Sections were then placed in artificial cerebral spinal fluid (aCSF) containing (in mM): 126 NaCl, 2.5 KCl, 1.25 NaH_2PO_4+H2O, 26 $NaHCO_3$, 10 glucose, 2.5 $CaCl_2$*H2O and 1.5 $MgCl_2$*6H2O (OsM: 295-300), saturated in 95% O_2/5% CO_2, maintained at 36°C for 30 minutes, and thereafter kept at room temperature in the same aCSF for the rest of the day.

2.5 Electrophysiology

PVN slices were transferred to a recording chamber superfused with aCSF (flow rate 1-2 mL/min, 28-32°C). Slices were visualized using an upright microscope (BX51WI, Olympus) equipped with infrared differential interference contrast (DIC) and epifluorescence (FLU) optics as well as a digital camera (Rolera-XR, Q-Imaging). CRH neurons were identified by their expression of tdTomato. Patch clamp recording pipettes were pulled from borosilicate glass (Cat#: BF150-86-10, Sutter Instrument) using a Flaming/Brown Micropipette Puller (P-1000, Sutter Instrument) to a tip resistance of 3-5 MΩ. Electrodes were filled with an internal solution containing (in mM): 108 K-gluconate, 2 $MgCl_2$, 8 Na-gluconate, 8 KCl, 1 K_2- ethylene glycol-bis(β-aminoethyl ether)-N,N,N',N'-tetraacetic acid (EGTA), 4 K_2-ATP, 0.3 Na_3-GTP, and 10 HEPES (Osmolarity: 283-289 mOsm, and pH: 7.2-7.4). In some experiments, 1,2-bis(o-

aminophenoxy)ethane-N,N,N′,N′-tetraacetic acid (BAPTA, 10 mM, Molecular Probes) and EGTA (10 mM, Molecular Probes) were added to the internal solution (by substituting an equimolar amount of K-gluconate) in order to chelate free intracellular Ca^{2+}. The calculated liquid junction potential was –12 mV, and was not corrected for when reporting membrane potentials.

Whole-cell patch-clamp recordings were obtained using a Multiclamp 700B amplifier (Molecular Devices), digitized at 10 kHz (Digidata 1440, Molecular Devices) and recorded on a PC using pClamp 10 software (Molecular Devices). Whole-cell capacitance (C_m) was measured using Membrane Test protocol implemented in pClamp. Specifically, the electrode capacitance was compensated following gigaseal formation and before establishing the whole-cell configuration. Under whole-cell voltage clamp mode (holding potential at -68 mV to account for a -12 mV junction potential), a continuous square pulse voltage command (5mV, 10ms) was applied at 50 Hz. Signals were low-pass filtered at 10 kHz and averaged 100 times. C_m was derived from the total charge divided by ΔV("Membrane Test Algorithms," n.d.). Resting membrane potential was measured in $I = 0$ current clamp about 2 min after breaking the membrane to achieve a whole-cell configuration. To study neural excitability, a series of current injection steps were applied under current clamp (Figure 2.3, 2.4). Rheobase current was defined as the first current step eliciting one action potential.

Figure 2.3
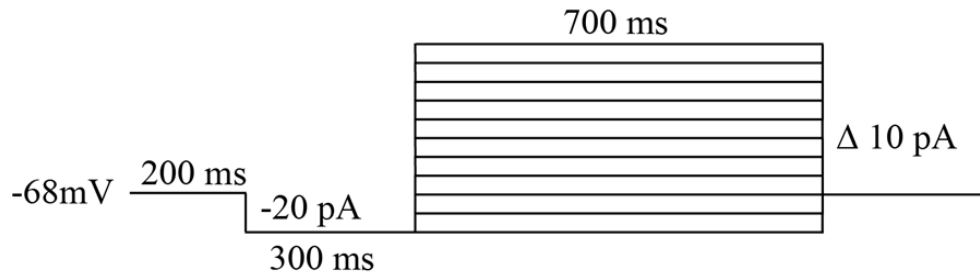
Figure 2.3 Current Clamp Protocol.

Membrane was held at a holding potential of -68 mV. First a -20pA hyperpolarizing current was injected (300ms) to de-inactivate any contributing voltage-activating/inactivating channels. From this hyperpolarized potential (~88mV), a series of current steps increasing in 10pA increments were applied for 700ms (10 sweeps).

Figure 2.4
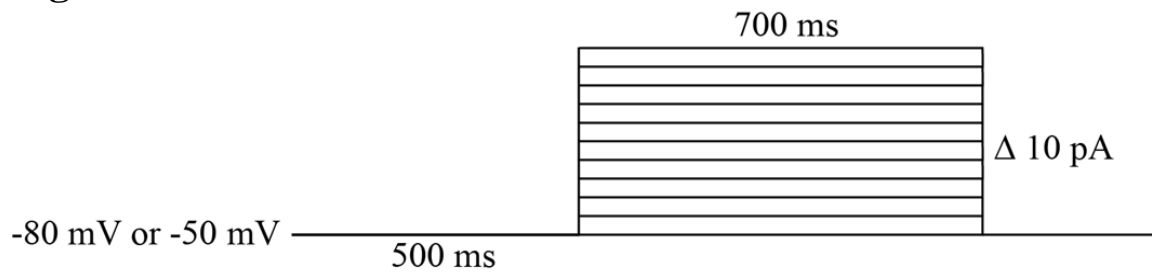
Figure 2.4 Current Clamp Protocol with no hyperpolarization.

During experiments investigating the contribution of voltage-activating channels, membranes were held at both a holding potential of -80 mV and -50 mV (500ms). Subsequently, a series of current steps increasing in 10pA increments were applied for 700ms (10 sweeps).

To investigate voltage-dependent changes in membrane conductance, a series of voltage steps were applied in voltage clamp mode (Figure 2.5). For these experiments, kynurenic acid (2mM, Sigma) and picrotoxin (100μM, Sigma) were added to block ionotropic glutamate and GABA receptors, respectively. Whole cell current was measured from 3 different areas within the 10-second voltage clamp protocol. Early current was measured between t = 0.003s - 0.0031s after the onset of voltage steps, mid current was measured between t = 0.116s - 0.117s after the onset of voltage steps and end current was measured at t = 9.996s - 9.997s seconds after the onset of voltage steps. All values were compared relative to baseline current values measured from t=0.0-0.1 seconds. Both early and mid current were measured by subtracting the end current from the values obtained at their specific time point. The early current represents fast activating and potentially fast inactivating current. One example would be the group of Kv4, fast-activating and fast-inactivating voltage-dependent potassium channels. The mid current represents slower activating channels, such as those from the Ca^{2+}-activated potassium channel (KCa) family. Finally end current reflects any residual non-inactivating currents.

Figure 2.5
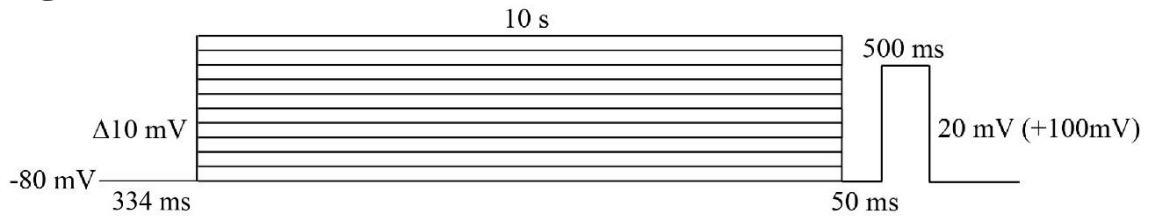
Figure 2.5 Voltage Clamp Protocol.

To investigate voltage-dependent changes in membrane conductance, a series of voltage steps increasing in 10mV increments were applied for 10 seconds. Whole cell current from 3 different areas from the 10-second voltage clamp protocol. Early current was measured between $t = 0.003s - 0.0031s$ after the onset of voltage steps, mid current was measured between $t = 0.116s - 0.117s$ after the onset of voltage steps and end current was measured at $t = 9.996s - 9.997s$ after the onset of voltage steps. All values were compared relative to baseline current values measured from $t = 0.0s - 0.1s$.

In order to examine neural excitation in response to an excitatory neurotransmitter glutamate, L-glutamic acid (5 mM, Sigma) was pressure applied from a glass pipette whose tip was placed 20μm-50μm away from the soma of the recorded neurons using a Picospritzer II (10 psi, 500ms; Figure 2.6). For individual trials, the location of the pipette tip was adjusted so that a single application generated varying amplitudes (50pA and 100pA) of peak current response. Thereafter, neural excitation was examined under current clamp (the membrane potential prior to glutamate application was set near -55 mV).

Figure 2.6
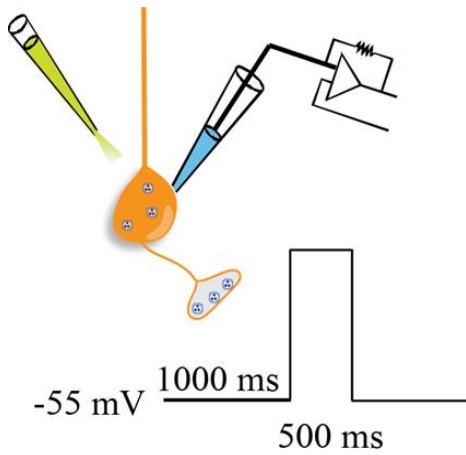
Figure 2.6 Glutamate Puff Protocol.

During glutamate puff experiments, L-glutamic acid (5mM, Sigma) was pressure applied from a glass pipette whose tip was placed 20μm-50μm away from the soma of the recorded neurons. Membranes were held just below the action potential firing threshold at -55mV. Pressure was applied for 500ms at 10psi.

The following experiments were performed by an undergraduate in our lab, Eric Salter as a part of his honors thesis project. In order to examine postsynaptic spike responses to synaptically-driven excitation, the afferent synapses were stimulated at various frequencies (5Hz, 10Hz and 20Hz for 2s) using an extracellular electrode placed 50μm-100μm away from the postsynaptic neurons. For individual trials, we first recorded excitatory postsynaptic current (EPSCs) in voltage clamp configuration. We then performed current clamp experiments to examine excitatory postsynaptic potential (EPSP)-spike coupling by delivering trains of synaptic stimulation (Figure 2.7). Prior to the synaptic stimulation, the membrane potential was held near -55mV, just below action potential threshold.

Figure 2.7
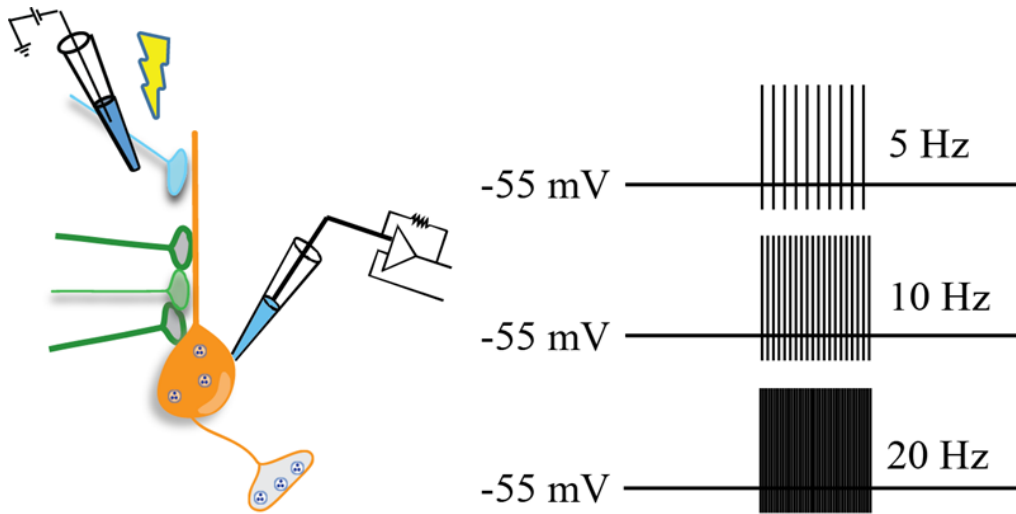
Figure 2.7 Train Stimulation Protocol.

During synaptic stimulation experiments, an extracellular electrode was placed amongst the afferent synapses, 50μm -100μm away from the postsynaptic neurons. Membrane were held just below the action potential firing threshold at -55mV. Afferent synapses were stimulated at various frequencies (5 Hz, 10 Hz and 20 Hz) for 2 seconds.

2.6 Data collection, analysis and statistics

To examine the degree of c-fos expression in tdTomato-positive PVN CRH neurons, immunohistochemistry samples were analyzed as follows. Z stack images (0.685 µm thick optical slices, 20-25 slices) were obtained with a confocal microscope (CIAN Leica SP8, acquisition software LAS X) using a 20x objective (0.75 NA dry). Two to four images of the PVN were obtained per animal. All confocal images were blinded for treatment prior to image analysis. Each image was reconstructed in 3D and quantified using Imaris v7.6.4 (Bitplane). The region of interest (ROI) was positioned based on positive signals of tdTomato in order to best capture the CRH neurons within the PVN (area of ROI set at x = 283.8 µm, y = 227.1 µm, z = 13.1 µm – 15.0 µm). To estimate the volume positive for tdTomato and c-fos expression, automatic thresholding was applied and a surface was created for each (Figure 2.8). The threshold values were then used to create a co-localization channel dual-positive for tdTomato and c-fos. A third surface was then created for the co-localization channel, determining the volume of the co-localization (Figure 2.8). The degree of c-fos expression by CRH neurons was derived from the co-localization volume divided by tdTomato volume for individual images.

Figure 2.8
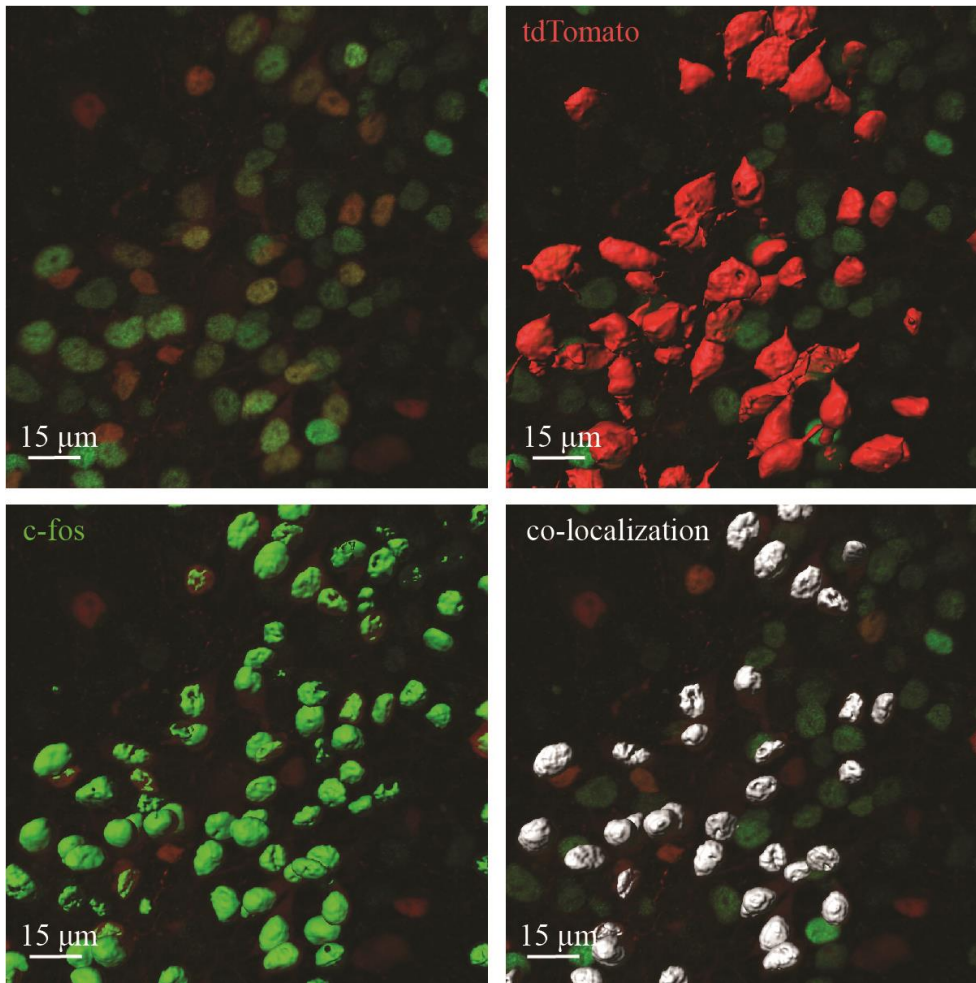
Figure 2.8 Image analysis for c-fos quantification.

Surfaces positive for tdTomato (red), c-Fos (green), and both (colocalization, white) were created in Imaris to quantify the volume of each.

To estimate cell surface size of recorded cells, Alexa-488 hydrazide (0.2 mM, Molecular Probes) and biocytin (0.5 % w/v, Life Technologies Inc.) were included in the internal solution. These dye-filled slices were fixated in 4% PFA at 4°C for 24 hours or longer. The filled cells were then visualized by incubating slices with streptavidin-A488 (1:500, Molecular Probes) diluted in PBS containing 2% TritonX-100. Dye-filled cells were imaged on a confocal microscope (Leica TCS SP8) using a 63x (1.3 NA oil-immersion) objective lens with optical section thickness at 0.3μm. The confocal Z-stack images were 3D reconstructed using Imaris software (Imaris v7.6.4, Bitplane) and surface area was calculated by applying automatic thresholds. Regions of interest (x = 40.7 µm, y = 40.7 µm, z = 9.4 µm – 26.6 µm) were applied to encompass the soma and proximal dendrites (Figure 2.9).

Figure 2.9
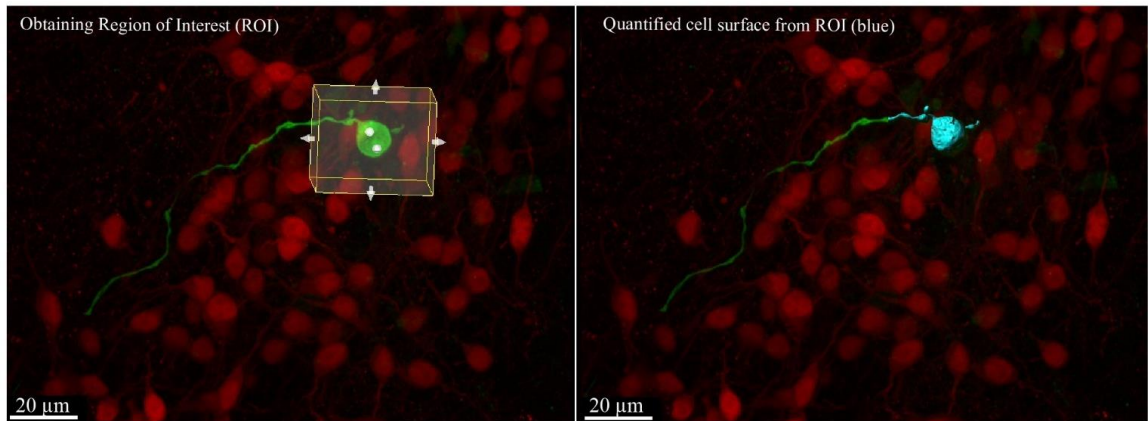
Figure 2.9 Image analysis for biocytin cell surface area quantification.

From left to right: regions of interest (ROI, x = 40.7 µm, y = 40.7 µm, z = 9.4 µm – 26.6 µm) were used to quantify surfaces positive for biocytin (Alexa 488); surface area quantified within ROI is identified with a blue surface colour.

For offline analysis of electrophysiological data, Clampfit (Molecular Devices) and MATLAB (The MathWorks Inc.) were used. The delay to first spike and frequency of firing was manually measured by counting action potential spikes and measuring the delay to spike using the cursors built into the Clampfit software. The spike threshold and peak amplitude were calculated using MATLAB. Spike threshold was calculated as the first millivolt value where the slope was greater than 5mV/ms for at least four consecutive points derived from the 10kHz digitized data. Peak amplitude was calculated as the difference between the spike threshold value and the peak millivolt value for that particular action potential.

Electrophysiological recordings were obtained from at least 3 animals in each comparison group. The number of cells and mice were denoted by n and N, respectively. For all data sets, the mean and the standard error of mean (SEM) was calculated using the number of cells (n) as the population. To perform a two-group comparison, an unpaired t-test was used during which a Gaussian distribution was assumed. To compare multiple groups, a one-way ANOVA was performed, with Dunnett's and Tukey's multiple comparisons post-hoc tests. For multiple group comparisons with an additional factor (ex. 4AP, holding potential, stimulation frequency, peak evoked current, Ca^{2+} chelator and current injection), a two-way ANOVA was used with Tukey's multiple comparisons post-hoc test. Finally, to examine linear correlations, a linear regression analysis was conducted. For all statistical analyses, GraphPad Prism 7 software (Graphpad Software Inc., CA, USA) was used and $p < 0.05$ was considered statistically significant.

Chapter 3

3. Results

3.1 PVN-CRH neurons habituate to repeated restraint stress in a reversible manner.

The activation of the HPA axis during stress relies on the activity of PVN-CRH neurons that convert neuronal signaling into the release of neuroendocrine hormones. We hypothesized that the habituation of the HPA axis to repeated stress exposure involves a decrease in the responsiveness of PVN-CRH neurons to that same stressor. To characterize the 'habituation' of PVN-CRH neurons to repeated restraint stress, we first conducted a comprehensive time course study over weeks of repeated restraint stress. To measure PVN-CRH neuron activity *in vivo*, we used immunohistochemistry for an immediate early gene c-fos, whose up-regulation represents the recent history of neuronal activity. For the identification of CRH neurons, we used a CRH reporter mouse line that expresses bright red fluorescent protein tdTomato in CRH neurons: the specificity of this mouse line to label PVN-CRH neurons has been validated by multiple laboratories (Chen, Molet, Gunn, Ressler, & Baram, 2015; Itoi et al., 2014; Wamsteeker Cusulin, Füzesi, Watts, & Bains, 2013). We quantified the co-localization of c-fos and tdTomato following 1 h of restraint stress in four groups of mice that previously received (or did not receive) the same stressor. These groups are outlined in Figure 3.1 and include: a single 1 h restraint stress (1 day), daily 1 h restraint stress for seven days (7 days) plus 1 h restraint stress on 8th day, 21 days of repeated restraint stress (21 days) plus 1 h restraint on 22nd day, and 21 days of repeated restraint stress followed by a one-week no stress period plus 1 h restraint stress on the 29th day (recovery). An additional group of mice that received no stress was included as a control. We found that in the control group, with no prior exposure to a stressor, c-fos protein expression in CRH neurons was almost undetectable (values represent % c-fos in tdTomato-positive volume ± S.E.M: $0.93 \pm 0.58\%$, N = 3; Figure 3.1, A). After exposure to a single stress, c-fos was robustly up-regulated in CRH neurons ($37.86 \pm 2.90\%$, N = 8, $p < 0.0001$, 1 day vs. Control, Tukey's post-hoc test; Figure 3.1, B). After seven days of repeated stress, c-fos induction in CRH

neurons still remains elevated in response to the stressor, showing no signs of habituation (35.76 ± 2.90%, N = 6; Figure 3.1, C). By contrast, after 21 days of repeated restraint stress, c-fos induction in CRH neurons was significantly attenuated (19.67 ± 3.80%, N = 7, p = 0.002, 1 day vs. 21 days), demonstrating a neuronal habituation to the repeated stressor (Figure 3.1, D). This habituation was reversible, since allowing these mice to recover for one week significantly increased c-fos upregulation in CRH neurons to a level similar to 1 day group (37.10 ± 3.30%, N = 6, p = 1.0, Recovery vs. 1 day; Figure 3.1, E). These results provided a proof of principle that our repeated restraint stress paradigm in mice effectively induces habituation at the level of PVN-CRH neurons. Importantly, these results also suggested that the PVN-CRH neuron habituation in mice was a slow process, not evident after 7 days of repeated stress, but rather required a more protracted period of repeated stress (21 days). This provided a timeline during which we could compare neurophysiological changes in response to habituation.

Figure 3.1
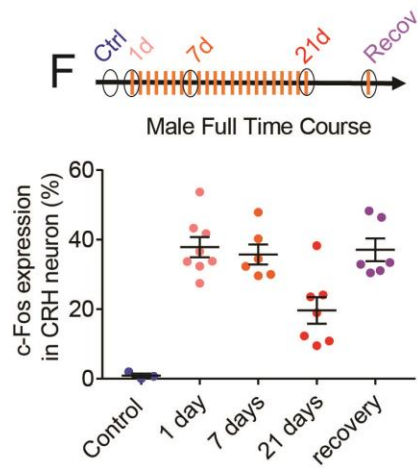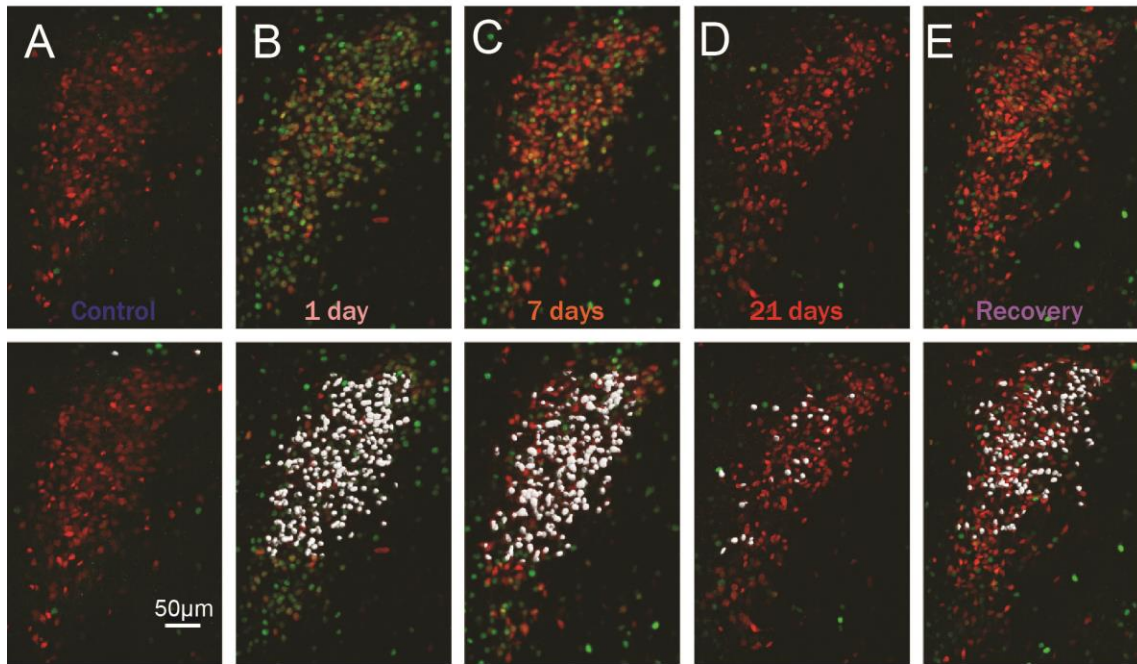
Figure 3.1 CRH-PVN neurons show habituation after 21 days of repeated restraint stress and begin to recover after 1 week without stress

CRH neurons in the PVN habituate to repeated stress in a reversible manner. **(A-E)** Sample images of tdTomato (reporter for CRH, red), c-fos immunoreactivity (green) and their co-localization (reconstructed in 3D surface, white). **(F)** Summary of c-fos co-localization with tdTomato. Note that values represent % c-fos in tdTomato-positive volume. 3-4 images were obtained and averaged for individual animals. One-way ANOVA between groups, $p < 0.0001$. **(A)** Control (no exposure to a stressor, N=3). **(B)** 1 day (immediately after a single 1 h stress, N=8). $p < 0.0001$, Tukey's post-hoc test vs Control. **(C)** 7 day (7 day prior repeated stress followed by additional 1 h stress on 8th day, N=6). $p < 0.0001$, Tukey's post-hoc test vs Control. **(D)** 21 days (21 day prior repeated stress followed by additional 1 h stress on 22nd day, N=7). $p = 0.02$, Tukey's post-hoc test vs Control. **(E)** Recovery (7 day no-stress recovery period after 21 day repeated stress, followed by an additional 1 h stress on 29th day, N = 6). $p < 0.0001$, Tukey's post-hoc test vs Control; $p = 1.00$, Tukey's post-hoc test vs. 1 day stress; $p = 0.006$, Tukey's post-hoc test vs 21 day stress. N represents the number of mice.

3.2 Repeated restraint stress decreases the responsiveness of PVN-CRH neurons to excitatory stimuli

The c-fos time course study indicated that 21 day repeated restraint stress decreased the responsiveness of PVN-CRH neurons to that same stressor administered on the next (22nd) day. This suggested that the repeated stress caused a lasting form of plasticity in the mechanisms that drive the activities of PVN-CRH neurons. To study the neurophysiological mechanisms underlying this, we conducted patch clamp electrophysiology in acute brain slices prepared on the 22nd day of repeated restraint stress without subjecting the animal to the stressor on the day of sacrifice. Slices from stress naïve mice were prepared as a control. Glutamate synapses are the major afferent excitatory inputs to PVN-CRH neurons (van den Pol, Wuarin, & Dudek, 1990) and mediate the HPA axis response to restraint stress (Ziegler & Herman, 2000). Thus, we investigated the responsiveness of PVN-CRH neurons to glutamatergic synaptic excitation by examining excitatory postsynaptic potential (EPSP)-spike coupling. We obtained whole cell patch clamp recordings from tdTomato-expressing PVN-CRH neurons, and stimulated their afferent inputs using an extracellular glass electrode placed on the neuropil ventromedial to the recorded neurons as described elsewhere (Kuzmiski, Marty, Baimoukhametova, & Bains, 2010; Marty, Kuzmiski, Baimoukhametova, & Bains, 2011). These recordings were obtained in the presence a $GABA_A$ receptor antagonist picrotoxin (100μM) in order to pharmacologically isolate fast glutamatergic synaptic transmission. Figure 3.2, D shows that in slices from control (stress naïve) mice, afferent stimulations at various frequencies (5, 10, 20 Hz) elicited a frequency-dependent postsynaptic firing. 21 day repeated restraint stress significantly reduced this EPSP-spike coupling across all stimulation frequencies (Two-way ANOVA, Stimulation frequency: $p < 0.0001$, Control vs. Stress: $p = 0.006$, Interaction: $p = 0.003$; Figure 3.2, D). In the same set of neurons, we also recorded initial evoked excitatory postsynaptic currents (eEPSCs) under the voltage-clamp mode and found no difference in their average amplitude between control and 21 day stress group (Two-way ANOVA, Stimulation Frequency: $p = 0.16$, Control vs. Stress: $p = 1.00$, Interaction: $p = 0.36$; Figure 3.2, B). Similarly, the dynamics of short-term synaptic plasticity of eEPSCs, as measured using paired-pulse-

ratio (PPR) during a train of varying frequencies (5, 10, 20 Hz) was not different between the two groups (Two-way ANOVA, Stimulation Frequency: $p = 0.82$, Control vs. Stress: $p = 0.68$, Interaction: $p = 0.19$; Figure 3.2, C). These results suggested that 21 day repeated stress did not significantly change the properties of excitatory synaptic transmission at the stimulation paradigms we used, and that the decrease of EPSP-spike coupling was primarily due to the changes in postsynaptic excitability.

Figure 3.2.1
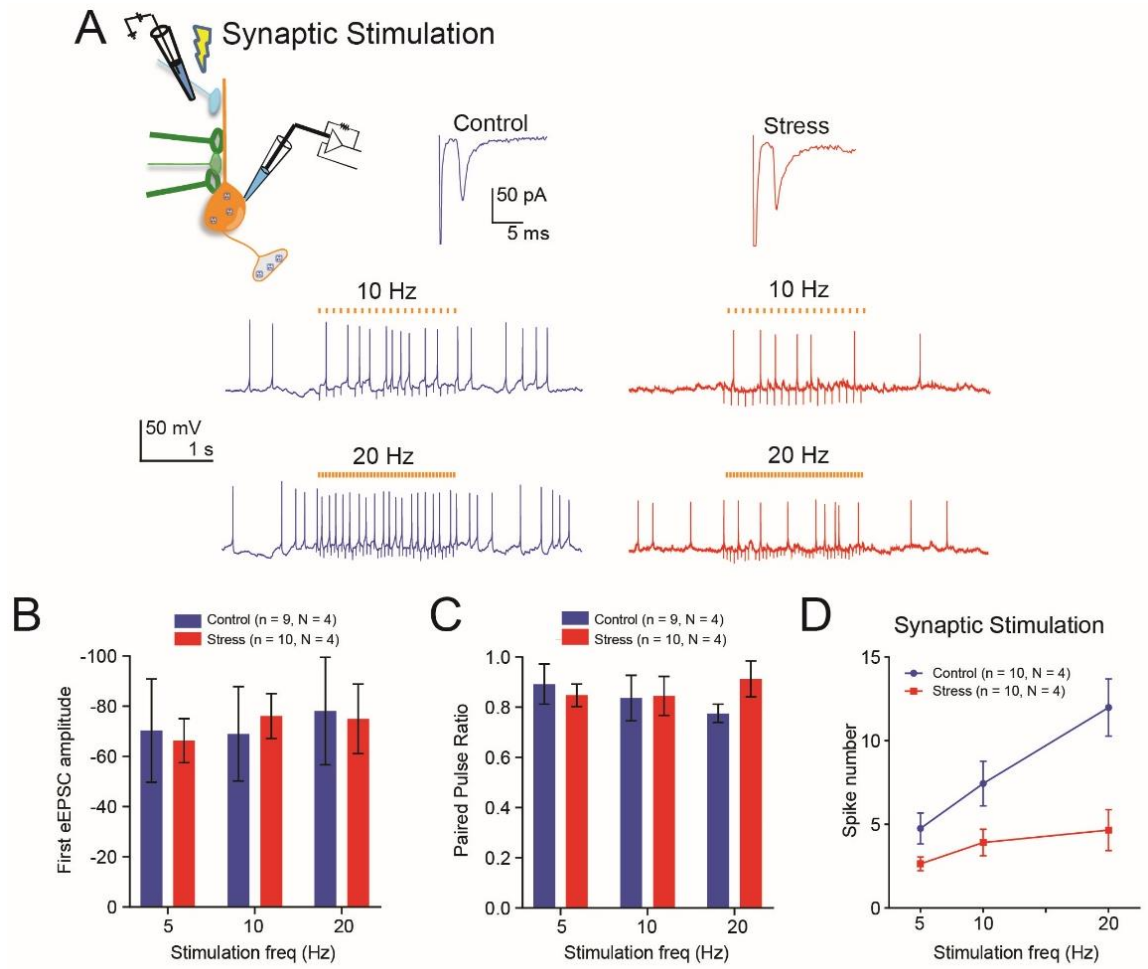
Figure 3.2.1 Repeated restraint stress decreases EPSP-spike coupling in response to synaptic stimulations at different frequencies.

Neural excitation in response to synaptic stimulation is reduced following 21 day stress despite no differences in initial evoked excitatory post-synaptic current (eEPSC). **(A)** Sample eEPSCs (top) and spike response to various frequency of synaptic stimulation. **(B)** Initial eEPSC amplitude does not differ between control and stress at each stimulation frequency (Two-way ANOVA, Stimulation Frequency: $p = 0.16$, Control vs. Stress: $p = 1.00$, Interaction: $p = 0.36$). **(C)** Paired pulse ratio also does not differ between control and stress at each stimulation frequency (Two-way ANOVA, Stimulation Frequency: $p = 0.82$, Control vs. Stress: $p = 0.68$, Interaction: $p = 0.19$). **(D)** Summary graph of spike number at various stimulation frequencies. (Two-way ANOVA, Stimulation Frequency: $p < 0.0001$, Control vs. Stress: $p = 0.006$, Interaction: $p = 0.003$). n and N represent the number of cells and mice, respectively.

In line with this, we also found that the firing response of PVN-CRH neurons to a direct activation of the postsynaptic glutamate receptor by L-glutamic acid was significantly reduced after 21 days of repeated restraint stress. In this experiment, we first adjusted the location of the glass pipette for focal pressure applications of L-glutamic acid (10 psi for 500ms) relative to the postsynaptic cells so that a single pressure application generated postsynaptic current response with its peak amplitude near -50pA and -100pA under voltage clamp (Figure 3.2.2, top-right subset of each trace). To ensure equal charge transfer evoked by the excitatory glutamate puff, we calculated the amount of charge elicited for the duration of the evoked current and found no differences between control and stress (Two-way ANOVA, Peak current: $p < 0.0001$, Control vs. Stress: $p = 0.93$, Interaction: $p = 0.60$; Figure 3.2.2, B). Thereafter, the postsynaptic firing responses were measured in current clamp. We found that the number of action potentials elicited during the first second of evoked current was significantly less in 21 day repeated stress groups compared to control (Two-way ANOVA, Control vs. Stress: $p = 0.0002$; Figure 3.2.2, A and C). These results suggest that 21 days of repeated restraint stress decreases the responsiveness of PVN-CRH neurons to an excitatory neurotransmitter, glutamate.

Figure 3.2.2
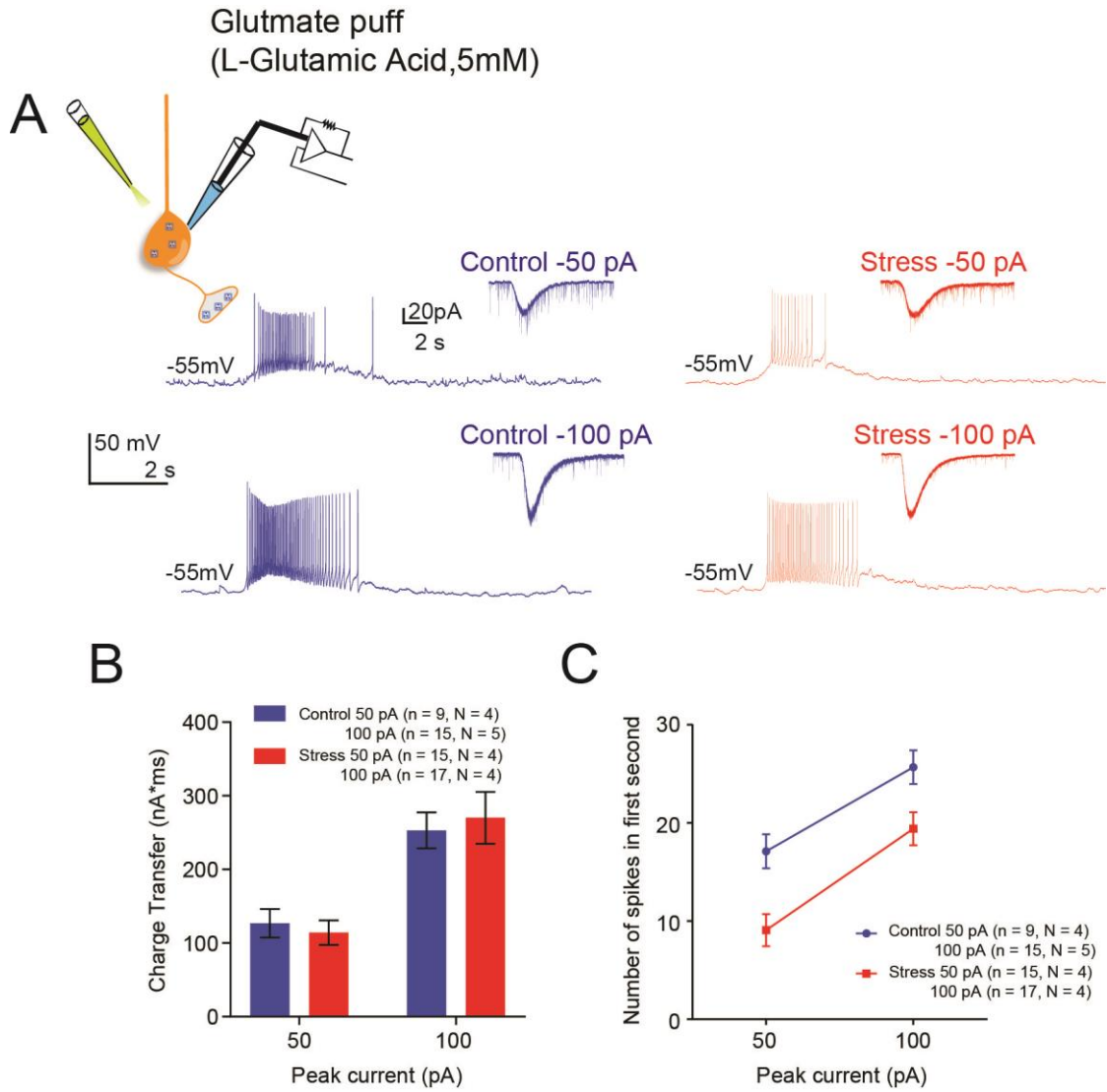
Figure 3.2.2 Repeated restraint decreases EPSP-spike coupling in response to a glutamate puff.

Neural excitation in response to focal application of glutamate is reduced following 21 day stress. **(A)** Focal glutamate application was adjusted to generate 50pA and 100pA inward current in voltage clamp. In the same cell, current clamp response was measured. **(B)** The amount of charge transferred during a focal application of glutamate was the same between stress and control at both 50pA and 100pA inward current. (Two-way ANOVA, Peak current: $p < 0.0001$, Control vs. Stress: $p = 0.93$, Interaction: $p = 0.60$). **(C)** Summary of cell firing in response to two different strengths of glutamate excitation. (Two-way ANOVA, Peak current: $p < 0.0001$, Control vs. Stress: $p = 0.0002$, Interaction: $p = 0.62$). n and N represent the number of cells and mice, respectively.

3.3 Repeated restraint stress decreases the neurons capacity to repetitively fire

To investigate stress-induced changes in the intrinsic excitability of PVN-CRH neurons, we examined their firing response to direct current injections in current clamp. The baseline membrane potential of individual cells was adjusted around − 68 mV by injecting constant current ranging between −10pA to −30pA. Thereafter the cells were artificially depolarized to trigger action potential firing with 10pA incremental steps of current injection (700ms) following a −20pA hyperpolarizing pre-pulse (300ms)(Figure 3.3 A, middle; sample traces from control (left) and stress (right)). Figure 3.3 B shows the average frequency of firing across a range of current injection steps (firing frequency-current relationship). We found that 21 day repeated restraint stress decreased the frequency of repetitive firing across the current injection steps compared to control (Figure 3.3, B; $p < 0.0001$, Dunnett's multiple comparisons test). This indicated that 21 day repeated stress robustly decreased the intrinsic excitability of PVN-CRH neurons. If this decrease in the intrinsic excitability of PVN-CRH contributes to the *in vivo* changes in the PVN-CRH neuron responsiveness to stress (as measured by c-fos induction), we predicted that the time course of the changes in the intrinsic excitability should follow that of c-fos response to restraint stress. Indeed, we found that neither a single acute stress (1 day) nor 7 day repeated stress was sufficient to change the firing frequency-current relationship (Figure 3.3, B and C; $p > 0.05$ for both 1 day and 7 day stress, Tukey's multiple comparisons test). Furthermore, the decrease in the firing frequency by 21 day repeated stress was reversible following 7 days of no stress period (recovery), as was the case for c-fos response (Figure 3.3, B and C, $p < 0.01$ vs 21 day, $p > 0.05$ vs control, Tukey's multiple comparisons test). These results suggested that the decrease in intrinsic excitability manifested by the decrease in firing frequency develops slowly after weeks of repetitive stress.

Figure 3.3
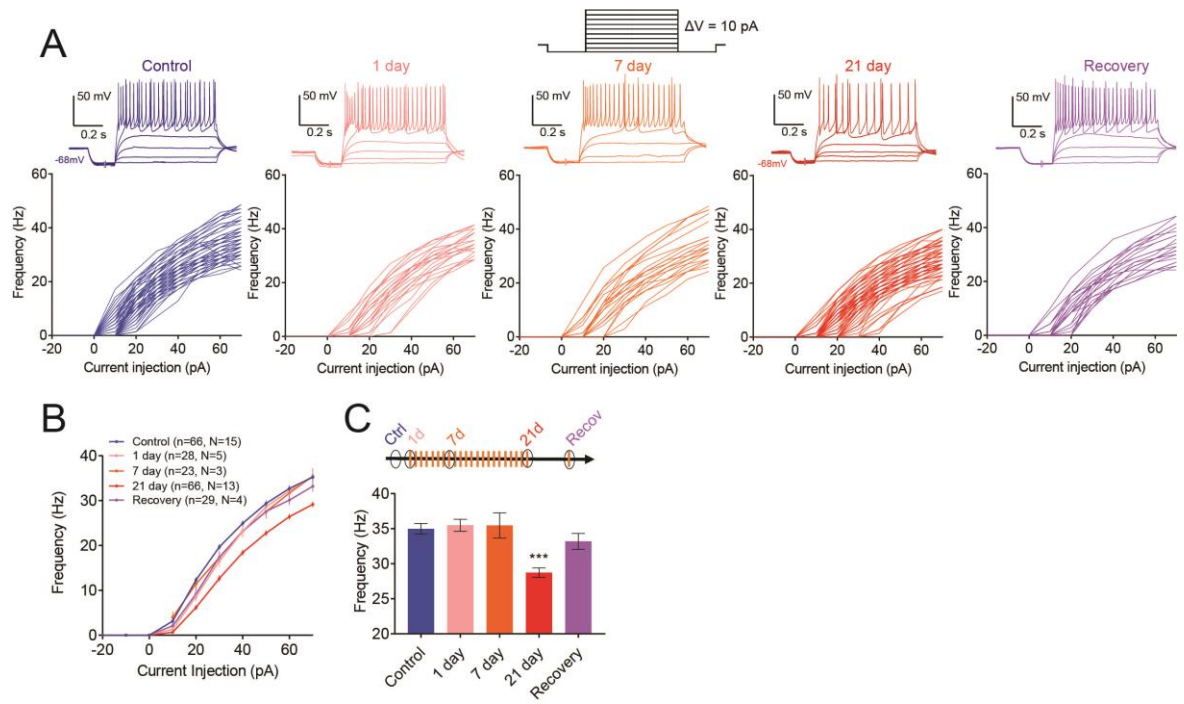
Figure 3.3. Repeated restraint stress decreases firing frequency of PVN-CRH neurons.

(A) **Top,** sample traces recorded from PVN-CRH neurons in slices from control, 1 day stressed, 7 day repeatedly stressed, 21 day repeatedly stressed, and 7 day no stress (recovery) after 21 day stress (left to right) mice. Current injection protocol (10pA increment from –20pA) is shown in the middle. **Bottom,** firing frequency of individual cells recorded in control (n = 66, N = 15), 1 day stressed (n = 28, N = 5), 7 day repeatedly stressed (n = 23, N = 3), 21 day repeatedly stressed (n = 66, N = 13), and recovery (n = 29, N = 4) mice. **(B)** Average graphs of firing frequency recorded across the time course of repeated restraint stress. Control, 1 day stressed, 7 day stressed, 21 day stressed, and 7 day no stress (recovery) after 21 day stress. (Two-way ANOVA, Current Injection: $p < 0.0001$; Control vs. Stress Groups: $p < 0.0001$; Interaction: $p < 0.0001$) **(C)** Top, experimental timeline. **Bottom,** summary bar graph of frequency at 70pA current injection derived from data shown in C. n and N represent the number of cells and mice, respectively. (One-way ANOVA, $p < 0.0001$; Tukey's post-hoc test 21 day stress vs control; *** $p < 0.001$).

3.4 Delay to spike increases after stress, but develops independently from the frequency of repetitive firing

Following stress, PVN-CRH neurons increase the delay before the first spike (firing latency) via voltage-dependent rapidly activating and rapidly inactivating K^+ currents (I_A; Senst, Baimoukhametova, Sterley, & Bains, 2016b). This raised a possibility that stress-induced delay in firing latency contributed to the observed decrease in the firing frequency. To address this, we analyzed firing latency in the same set of data we analyzed for firing frequency in Figure 3.3. Importantly, the current clamp protocol for the firing frequency measurement favors the I_A-mediated firing latency as it included a hyperpolarizing pre-pulse ($-20pA$ for 300ms) that removes the inactivation of I_A (Cai, Li, & Sesti, 2007; Yellen, 2002), followed by steps of depolarization to elicit firing (+10pA steps for 700ms; Figure 3.4 A, middle; sample traces from control (left) and stress (right)). We found that 21 day repeated stress increased firing latency compared to control across all current injection steps (Figure 3.4 A,C, and D). However, the stress time course study revealed that, in contrast to firing frequency changes, a single acute stress (1 day) was sufficient to develop the delay as effectively as repeated stress for 7 and 21 days (Tukey's post-hoc test stress vs control: 1 day stress: p = 0.01, 7 day stress: p = 0.04, 21 day stress: p = 0.003; Figure 3.4, C and D). Additionally, the increase in spike latency was reversible following a 7 day no stress recovery period (Tukey's post-hoc test recovery vs control: p = 1.00). These results are similar to the firing latency increase mediated by I_A that rapidly develops following acute stressors (Senst et al., 2016b). Indeed, consistent with the predicted roles of I_A, a sub-threshold depolarization of the cell membrane (~ -50 mV), which inactivates I_A (Cai et al., 2007; Yellen, 2002), prior to the depolarizing steps significantly shortened the firing latency as compared to a hyperpolarized membrane potential (~ -80 mV) in both control and 21 day repeatedly stressed cells (Two-way ANOVA, Holding potential: p < 0.0001; Control vs. Stress Groups: p = 0.01; Interaction: p = 0.49; Figure 3.3, B, lower left corner). Likewise, firing latency was sensitive to 4-aminopyridine (4-AP, 5mM) that blocks I_A at 1mM concentrations (Alexander et al., 2015), shortening the delay in both control and stressed cells to a similar level (Two-way ANOVA, 4-AP: p = 0.02; Control vs. Stress Groups: p

= 0.28; Interaction: p = 0.004; Figure 3.3, B, lower right corner). The same 4-AP treatment, however, did not normalize the stress-induced difference in firing frequency, further negating the roles of I_A in the decrease of firing frequency. Rather, 4-AP decreased firing frequency in both control and 21 day repeated stress groups (Two-way ANOVA, 4AP: p < 0.0001, Control vs. Stress: p = 0.04, Interaction: p = 0.36; Figure 3.4, E). These results indicated that different mechanisms underlie the stress-induced increase in firing latency and decrease in firing frequency. In line with this idea, we found no correlation between the first spike firing latency and firing frequency in any groups (Figure 3.4, F, R^2 < 0.01 and p > 0.05 for all groups).

Furthermore, habituation of PVN-CRH neurons to repeated restraint stress required weeks to develop, as observed through c-fos induction. With regards to this finding, the firing frequency decrease showed temporal correlation to habituation and the firing latency did not, suggesting that the firing frequency likely plays a major role in habituation. In the following section of the paper, we address the mechanisms underlying the stress-induced decrease in firing frequency as a neurophysiological correlate for PVN-CRH neurons' habituation to repeated stress.

Figure 3.4
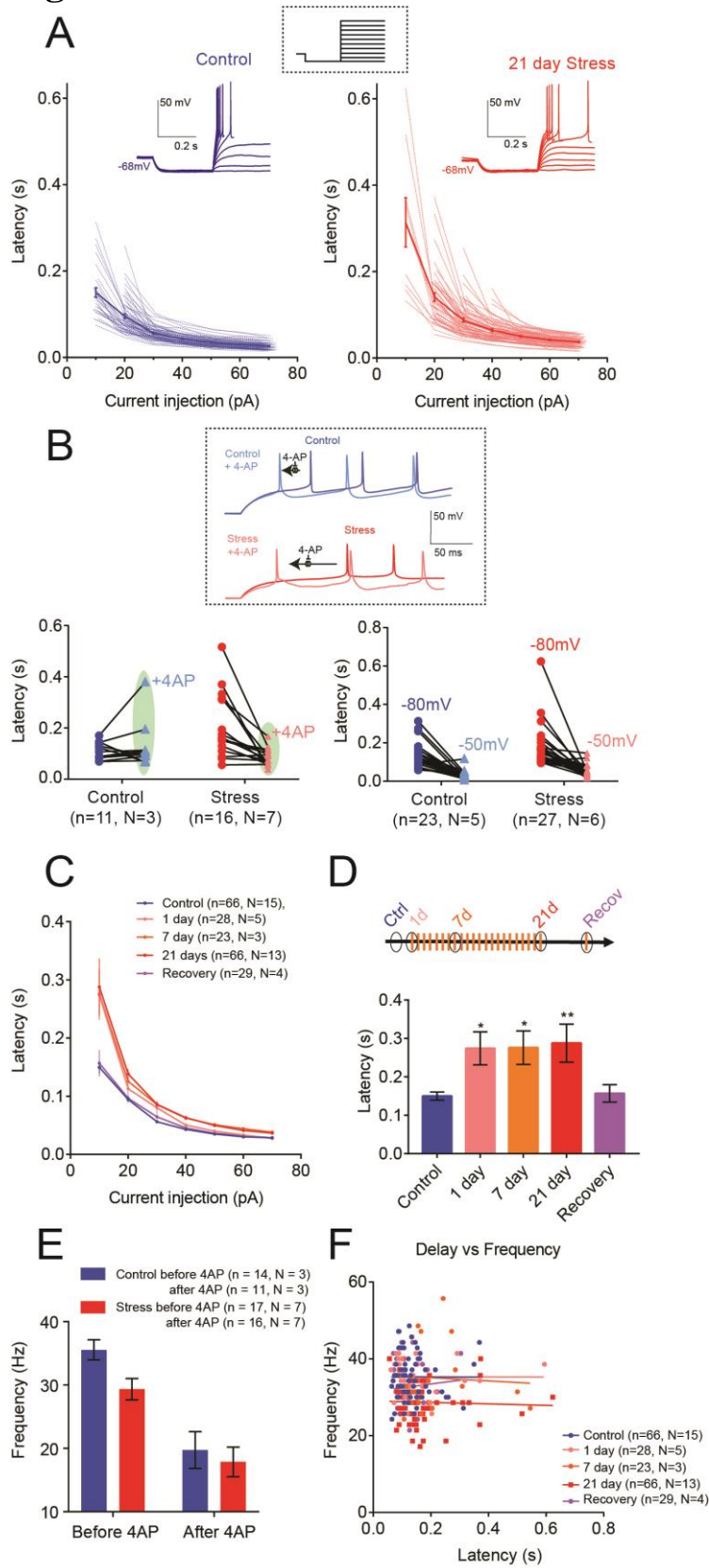
Figure 3.4 Stress-induced increase in firing latency does not correlate with spike frequency change.

Data set shown in Figure 3.3 is analyzed for firing latency. **(A) Top,** sample traces depicting firing latency recorded from PVN-CRH neurons in slices from control (left) and 21 day repeatedly stressed (right) mice. Current injection protocol (10pA increment from -20pA) is shown in the middle. **Bottom,** graphs for firing latency of individual cells. Control (n = 66, N =15) and 21 day repeatedly stressed (n = 66, N = 13) mice. **(B) Top,** sample traces for firing latency before and after bath application of 4AP (5 mM). **Bottom left**, summary plots for firing latency before and after 4AP application. Control (n = 11, N = 3) and 21 day stressed (n = 16, N = 7) mice. (Two-way ANOVA, 4AP: $p = 0.02$, Control vs. Stress: $p = 0.28$, Interaction: $p = 0.004$) **Bottom right,** summary plots for firing latency from the holding potential with (-80 mV) and without (-50 mV) hyperpolarization. Control (n = 23, N = 5) and 21 day stressed (n = 27, N = 6) mice. (Two-way ANOVA, Holding potential: $p < 0.0001$, Stress: $p = 0.014$, Interaction: $p = 0.49$). **(C)** Average graphs for firing latency. Control, 1 day stressed (n = 28, N = 5), 7 day stressed (n = 23, N = 3), 21 day stressed and 7 day no stress (recovery) after 21 day stress (n = 29, N = 4). **(D) Top,** experimental timeline. Bottom, summary bar graph of latency at 10pA current injection extracted from C. (One-way ANOVA, $p < 0.0001$; * $p < 0.05$, ** $p < 0.001$ Tukey's post-hoc test vs Control). **(E)** Frequency decreases in both stress and control cells after application of 4AP (Two-way ANOVA, 4AP: $p < 0.0001$, Control vs. Stress: $p = 0.04$, Interaction: $p = 0.36$). **(F)** Plots of spike delay against frequency. Spike delay does not correlate with repetitive firing frequency (control: $R^2 < 0.001$, $p = 0.97$; 1 day: $R^2 < 0.001$, $p = 0.99$; 7 days: $R^2 = 0.003$, $p = 0.79$; stress $R^2 = 0.001$, $p = 0.78$; recovery: $R^2 = 0.007$, $p = 0.68$). n and N represent the number of cells and mice, respectively.

3.5 The decrease in the frequency of repetitive firing does not depend on intracellular calcium.

A common mechanism to increase the frequency of repetitive firing is the activation of Ca^{2+} dependent potassium channels (Capel & Terrar, 2015; Peron & Gabbiani, 2009; Smith, Nelson, & Lac, 2002). As the first step to tease out the mechanism for the decrease in firing frequency, we tested the contribution of intracellular Ca^{2+}. To do this we included BAPTA (10 mM), a fast-acting Ca^{2+} chelator and EGTA (10 mM), a slow-acting Ca^{2+} chelator in the internal solution of the patch pipette. Including BAPTA and EGTA in the patch pipette did not affect the spike frequency in both control and stress conditions (Two-way ANOVA, Ca^{2+} chelator: $p = 0.20$, Control vs. Stress: $p < 0.0001$, Interaction: $p = 0.36$; Figure 3.6). These results unequivocally excluded the roles of Ca^{2+} in the stress-induced decrease of firing frequency.

Figure 3.5
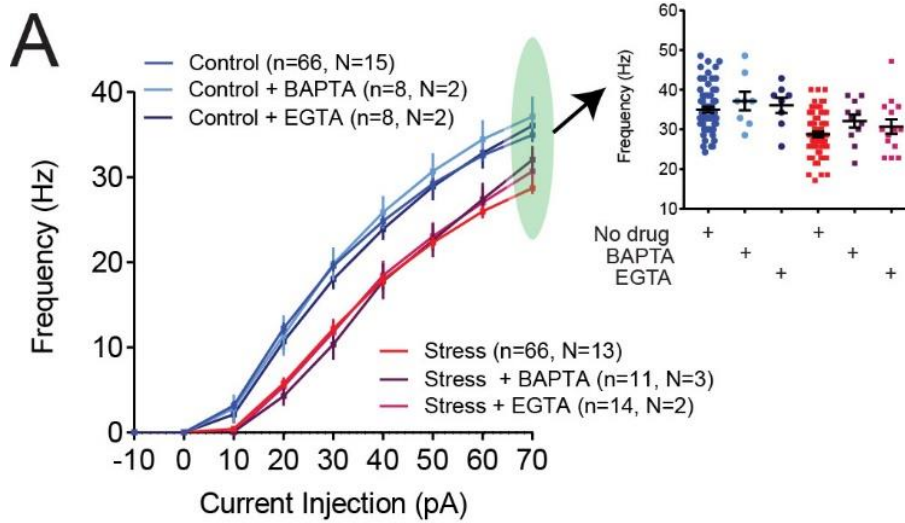
Figure 3.5 The decrease in firing frequency does not depend on intracellular Ca^{2+}.

(A) Summary graphs for the recordings using intracellular solution containing high concentration of BAPTA (10 mM) and EGTA (10 mM) obtained from PVN-CRH neurons in slices from control and 21 day stressed mice. The recordings using a regular intracellular solution (containing 0.1 mM EGTA) are adopted from Figure 3.3. Top right panes show a summary plot at 70pA current injection. (Two-way ANOVA, Ca^{2+} chelator: $p = 0.20$, Stress: $p < 0.0001$, Interaction: $p = 0.93$). n and N represent the number of cells and mice, respectively.

3.6 Repeated restraint stress decreases sub-threshold whole-cell membrane resistance.

The traces of current clamp data we analyzed for spike frequency and first spike latency showed that the membrane voltage changes with current steps below firing threshold were smaller in 21 day repeated stress than control, raising the possibility that 21 day repeated stress decreased sub-threshold membrane resistance (Figure 3.6.1, A). To test this, we plotted the voltage-current relationship for the current clamp data analyzed for spike frequency and first spike latency (Figure 3.6.1, B) and calculated the sub-threshold membrane resistance from the slope between 0pA and 10pA current injections (Figure 3.6.1, C). We found that 21 day repeated stress significantly decreased the subthreshold membrane resistance (Unpaired t-test, $p < 0.0001$). In line with this observation, rheobase (the current injection required to trigger the very first spike) was significantly higher in 21 day repeated stress than control (Unpaired t-test, $p < 0.0001$; Figure 3.6.2, C). On the other hand, the action potential amplitude and spike threshold were not significantly different between control and 21 day repeated stress (Unpaired t-test, $p = 0.31$ and $p = 0.22$, respectively; Figure 3.6.2, A and B), indicating that the increase in rheobase is primarily attributable to the decrease in sub-threshold membrane resistance. We also found a significant decrease in input resistance in stressed cells (Unpaired t-test, $p < 0.0001$) corresponding to the decrease in membrane resistance (Figure 3.6.2, F). Additionally we found that action potential firing at resting membrane potential ($I = 0$) was significantly less for stressed cells (Unpaired t-test, $p < 0.0001$), despite no major significant difference in resting membrane potential (Unpaired t-test, $p = 0.09$; Figure 3.6.2, E and D, respectively). These findings point to a mechanism that can decrease cell excitability without altering many basic action potential ion channel parameters (e.g. sodium channels and delayed-rectifier potassium channels).

Figure 3.6.1
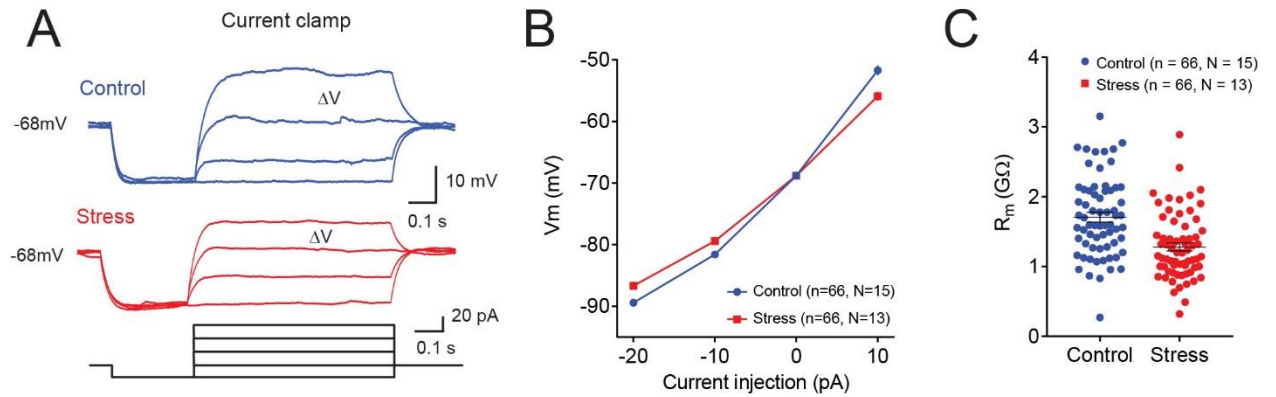
Figure 3.6.1 Repeated restraint stress decreases sub-threshold whole-cell membrane resistance.

Membrane response to subthreshold current injections are analyzed from the data set shown in Figure 3.2. **(A)** Sample traces. **(B)** A summary of the current-voltage relationship. **(C)** A summary plot of membrane resistance calculated at +10pA current injection when depolarized from 0pA. **(C)** Control cells show a higher membrane resistance compared to stress. Control (n = 66, N = 15) and 21 day stressed (n = 66, N = 13); Unpaired t-test, p < 0.0001.
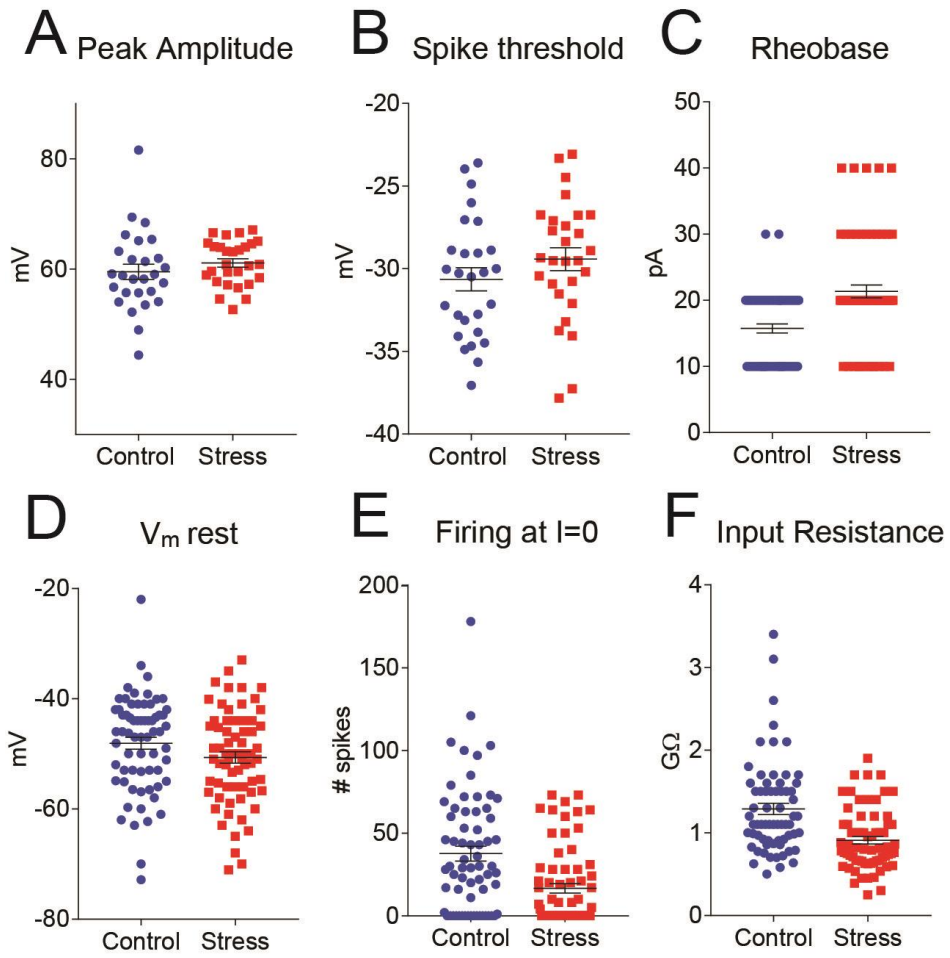
Figure 3.6.2

Figure 3.6.2 Repeated restraint stress increases rheobase current without changing firing threshold.

Various different parameters were measured under control and stress conditions. **(A)** Peak amplitude: control (n = 27, N = 6) and 21 day stressed (n = 28, N = 6) mice. (Unpaired t-test, p = 0.31). **(B)** Spike threshold: control (n = 27, N = 6) and 21 day stressed (n = 28, N = 4; unpaired t-test, p = 0.22). **(C)** Rheobase: control (n = 66, N = 15) and 21 day stressed (n = 66, N = 13) mice. (Unpaired t-test, p < 0.0001). **(D)** V_m rest: control (n = 66, N = 15) and 21 day stressed (n = 66, N = 13) mice. (Unpaired t-test, p = 0.09). **(E)** Firing at I = 0: control (n = 66, N = 15) and 21 day stressed (n = 66, N = 13) mice. (Unpaired t-test, p < 0.0001). **(F)** Input Resistance: control (n = 66, N = 15) and 21 day stressed (n = 66, N = 13) mice. (Unpaired t-test, p < 0.0001). n and N represent the number of cells and mice, respectively.

3.7 Voltage-dependent, non-inactivating conductance correlates with firing frequency.

To further examine stress-induced changes in membrane properties underlying firing frequency changes, subsets of cells in both stress naïve (control) and 21 day repeated stress groups recorded with current clamp were subsequently studied with voltage-clamp. In this subset of cells, we confirmed that the firing frequency was significantly lower in 21 day repeated stress than control groups (Unpaired t-test, p < 0.0001). We then analyzed the voltage clamp recordings and examined macroscopic outward currents elicited by depolarizing steps from a holding potential of −80 mV, and analyzed three different phases of the currents that we refer to here as 1) rapidly activating and rapidly inactivating current (Figure 3.7, B), 2) transient current (Figure 3.7, E) and 3) sustained, non-inactivating current (Figure 3.7, H). The rapidly activating and rapidly inactivating current showed a low activation threshold (~ −50 mV, Figure 3.7, B and C), likely representing the I_A underlying the first spike latency (Cai et al., 2007; Yellen, 2002) . In line with the stress-induced increase in the first spike latency, 21 day repeated stress groups showed a significant increase in this current. On the other hand, the transient current that was activated at voltages higher than −20 mV was not different between control and 21 day repeated stress groups (Figure 3.7, E and F). The most prominent stress-induced change was observed in the sustained current (Figure 3.7, H). Within a low voltage range (−80 to −40 mV), the sustained current was small but active, showing a linear I-V relationship. Consistent with the current-clamp data, 21 day repeated stress increased this sub-threshold current. Furthermore, at membrane potentials more positive than −30 mV, an additional current was activated, and again 21 day repeated stress increased this current. The Conductance-Current (G-I) plot revealed a prominent stress-induced increase in membrane conductance mediating the sustained current at the membrane voltage higher than −20 mV (Figure 3.7, C, F and I).

With relevance to the stress-induced spike frequency change, we found a significant correlation between the sustained current conductance (calculated from the voltage steps between −20 and −10 mV) and spike frequency in both control and 21 day repeated stress groups (control: $R^2 = 0.17$, p = 0.04; stress: $R^2 = 0.25$, p=0.005; Figure

3.7, J). By contrast, neither the rapidly activating and inactivating, nor transient conductance significantly correlated with the spike frequency (control: $R^2 = 0.02$, p = 0.46 ; stress: $R^2 = 0.05$, p = 0.21 and control: $R^2 < 0.001$, p = 0.98; stress: $R^2 = 0.10$, p = 0.75, respectively; Figure 3.7, D and G, respectively). These results pointed to the roles of high voltage activated, non-inactivating conductance in mediating the stress-induced decrease in the spike firing frequency.

Figure 3.7
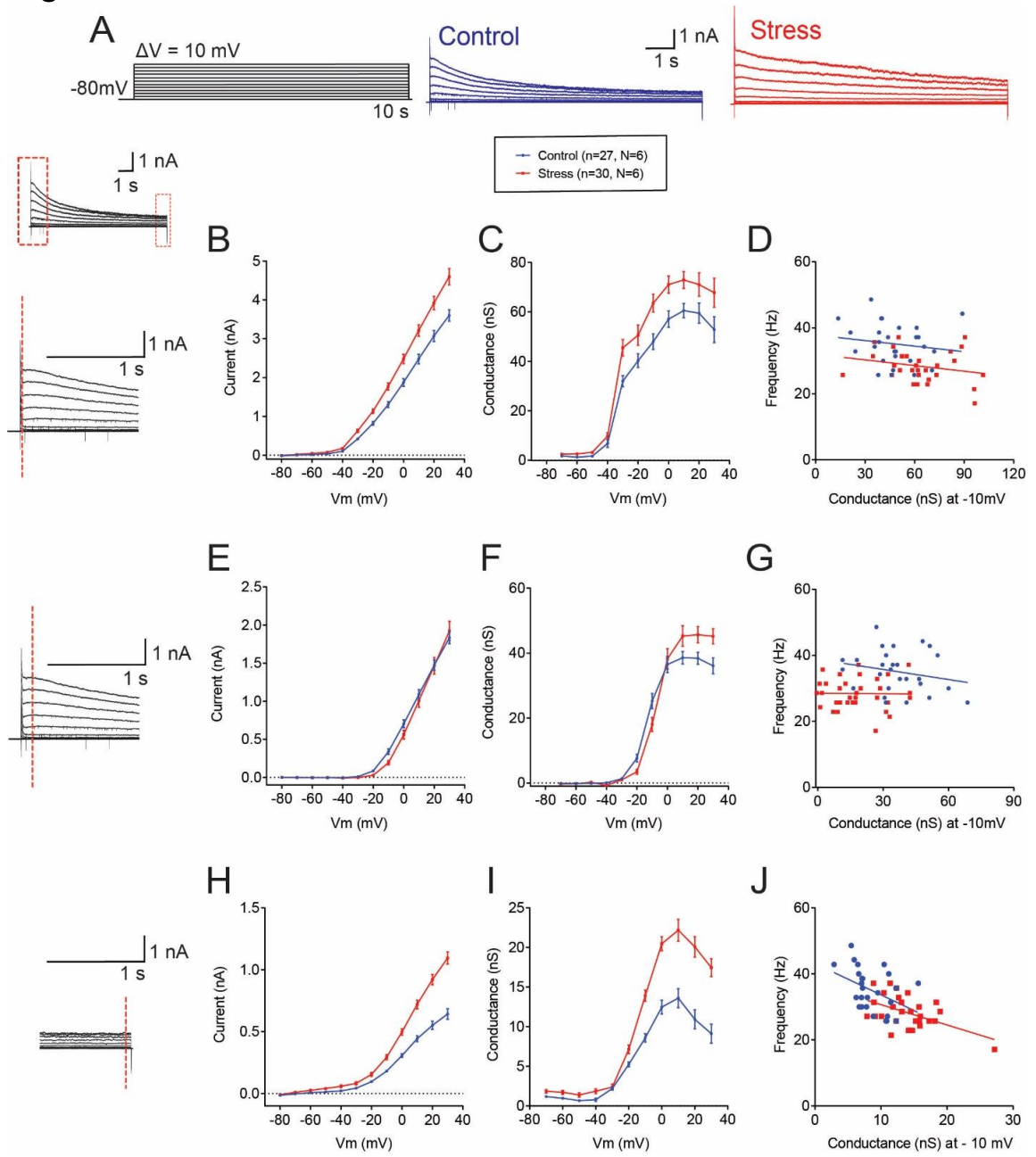
Figure 3.7 Voltage-dependent, non-inactivating conductance correlates with firing frequency.

(A) Sample traces for current responses to a voltage step protocol (+10 mV step from −80 mV) in cells from control and 21 day stressed mice. **(B-D)** Rapidly activating and inactivating currents, **(E-G)** inactivating currents, and **(H-J)** non-inactivating currents are measured between t = 0.003 - 0.0031, t = 0.116 - 0.117 seconds and t = 9.996 - 9.997 seconds after the onset of voltage steps, respectively. Note that conductance (measured for the step from −20 mV to −10 mV) significantly correlated with the firing frequency only for non-inactivating currents **(J)** control: $R^2 = 0.17$, $p = 0.04$; stress: $R^2 = 0.25$, $p = 0.005$, but not for rapidly activating and inactivating currents **(D)** control: $R^2 = 0.02$, $p = 0.46$; stress: $R^2 = 0.05$, $p = 0.21$; and inactivating currents **(G)** control: $R^2 < 0.001$, $p = 0.98$; stress: $R^2 = 0.10$, $p = 0.75$. Current conductance was taken at -10mV for all three time points.

3.8 Repeated stress does not change conductance density

We next calculated current density by dividing the whole cell current with the cell capacitance (C_m), which is proportional to cell surface area, to normalize potential contributions of changes in neuronal size to the observed stress-induced changes in the whole-cell current (Haedo & Golowasch, 2006; Iwasaki, Chihara, Komuta, Ito, & Sahara, 2008; Khorkova & Golowasch, 2007; Royeck et al., 2008). Interestingly, we found that the normalization with C_m eliminated, for the most part, the stress-induced changes (Figure 3.8). The comparison of G-I plots between whole-cell and density best demonstrated the difference: the normalization eliminated the stress-induced differences in subthreshold range (-80 - -30 mV) as well as the voltage-dependent conductance increase (-30 mV). Only the high voltage range change still remained. To add, the conductance density did not correlate with the firing frequency (control: $R^2 = 0.04$, p = 0.33; stress: $R^2 = 0.01$, p = 0.57). These findings suggest that the difference in the whole-cell currents/conductances and their effects on firing frequency were primarily due to stress-induced changes in C_m, and therefore possibly neuronal size.

Figure 3.8
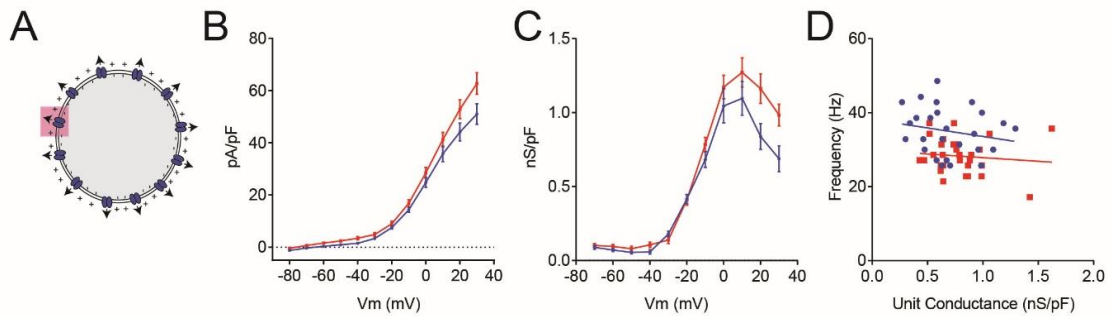
Figure 3.8 Repeated stress does not change conductance density.

(A) Schematics for conductance density. Density is represented by the pink square showing that calculations represent an amount of current per unit area. **(B-D)** Stress-induced changes of non-inactivating current **(B)** and conductance **(C)** normalized by cell capacitance. **(D)** Conductance density does not correlate with firing frequency for control (n = 27, N = 6): $R^2 = 0.04$, p = 0.33; nor stress (n = 30, N = 6): $R^2 = 0.01$, p = 0.57.

3.9 Cell capacitance and cell surface area correlates to repetitive firing frequency in stress cells.

The direct comparison of C_m revealed that 21 days of repeated restraint stress significantly increased C_m compared to control (14.3 ± 0.46 vs 19.0 ± 0.59 pF; Unpaired t-test: $p < 0.0001$; Figure 3.9 A). We found that C_m and firing frequency significantly correlated in 21 day repeated stress group ($R^2 = 0.19$, $p = 0.0002$), and there was a similar trend in the control group (control: $R^2 = 0.03$, $p = 0.19$; Figure 3.9, B). Additionally, we saw matching trends when averaging the capacitance values for individual animals (Figure 3.9, C and D). These results suggested that 21 day repeated restraint stress increased the neuronal size, and this structural plasticity might be the contributing factor to the changes in their excitability and the firing frequency. To directly investigate the relationship between cell size and firing frequency, we next measured the surface area of cells from control and 21 day repeated stress groups, by filling cells with biocytin (0.5%) during electrophysiological recordings. We obtained capacitance and spike frequency measures for the cells that we collected. We obtained confocal images (Leica TCS SP8, 63x magnification) of our slices and used Imaris software to quantify the cell body size (surface area, Figure 3.9 G). When we compared the average surface area for stressed cells to control cells, the two groups did not significantly differ (Unpaired t-test: $p = 0.26$). Interestingly, however, the surface area from the biocytin filled cells correlated with the frequency of repetitive firing for stress ($R^2 = 0.55$, $p = 0.004$), and had a trend to correlate for control ($R^2 = 0.21$, $p = 0.08$). When we compared the filled surface area to the capacitance, we again saw that surface area and capacitance correlated well in stress ($R^2 = 0.63$, $p = 0.001$), however does not correlate in control ($R^2 = 0.06$, $p = 0.38$). It is interesting to note that the surface area does not change between the two groups; however when you introduce a stressor, the surface area and capacitance correlates well with frequency.

Figure 3.9
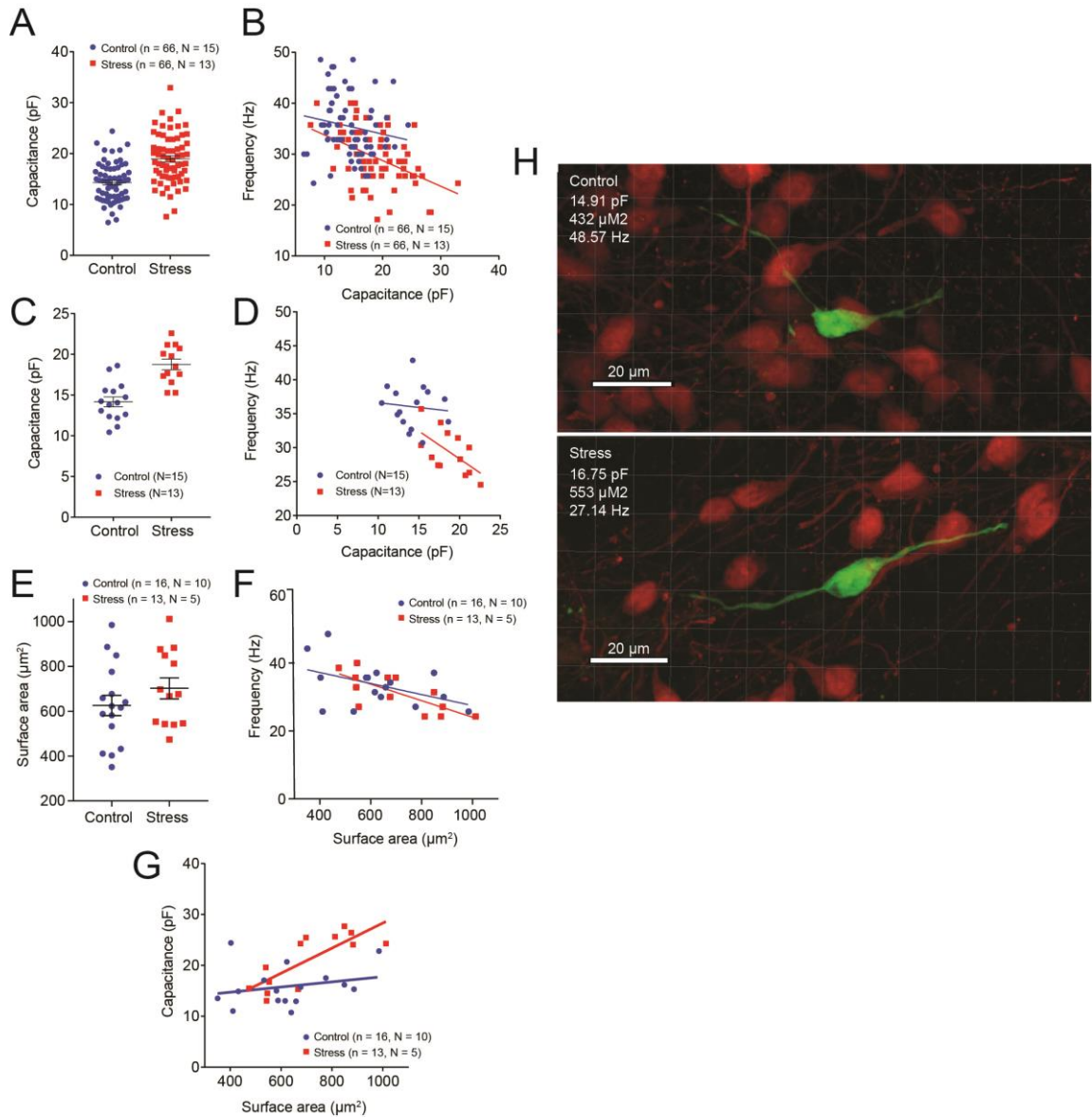
Figure 3.9 Repeated stress increases cell capacitance but not cell soma surface area. Both capacitance and cell soma surface area correlate to the frequency of firing.

Capacitance, which serves as a proxy for cell size ($1pF = 100\mu m^2$), correlates to the frequency of repetitive firing. **(A)** The capacitance recorded from stressed cells is significantly larger (Unpaired t-test: $p < 0.001$) than control cells. **(B)** The capacitance of the cell has a tendency to correlate to the frequency of repetitive firing in control cells and significantly correlates in stress cells (control: $p = 0.19$; stress: $p < 0.001$). **(C)** The average capacitance for each animal is significantly larger in stressed animals compared to control animals (Unpaired t-test: $p < 0.001$). **(D)** The average capacitance for each animal correlates to the frequency of repetitive firing in the stressed group ($R^2 = 0.35$, $p = 0.03$) but not control ($R^2 = 0.01$, $p = 0.71$). **(E)** The average surface area for stressed cells does not significantly differ from control cells (Unpaired t-test: $p = 0.26$). **(F)** The surface area (μm^2) from the biocytin filled cells, correlates to the frequency of repetitive firing for stress ($R^2 = 0.55$, $p = 0.004$), and has a trend to correlate for control ($R^2 = 0.21$, $p = 0.08$). **(G)** The surface area (μm^2) from the biocytin filled cells, correlates to capacitance for stress ($R^2 = 0.63$, $p = 0.001$), however does not correlate in control ($R^2 = 0.06$, $p = 0.38$). **(H)** Examples of biocytin filled cells from the control and stress groups.

Chapter 4

4. Discussion

This study revealed that PVN-CRH neurons robustly decreased their intrinsic excitability along the time course that parallels the development of c-fos response habituation to repeated restraint stress. More specifically, the plasticity of intrinsic excitability was characterized by two changes: an increase in rheobase (i.e. the amount of excitatory current required to trigger an action potential) and a decrease in the frequency of repetitive firing throughout a duration of excitatory current injection. Importantly, we did not find any change in the threshold for action potential, suggesting that the decrease in firing is not due to voltage-gated sodium channels. In line with this finding, the decrease of intrinsic excitability was best correlated with the decrease in whole-cell membrane resistance. By Ohm's law, a decrease in membrane resistance indicates that the same amount of charge transfer across the membrane (i.e. current injection during current clamp experiments or ionic flow by synaptic transmission under natural conditions) will generate a smaller membrane depolarization. With regards to information processing at PVN-CRH neurons, these changes predict that PVN-CRH neurons respond less to low-level excitatory inputs, likely from mild, repeated stressors.

To investigate the mechanism underlying the decrease in whole-cell membrane resistance and firing frequency we first examined the contribution of voltage-dependent transient inactivating potassium (I_A) conductance. Although repeated stress increased I_A conductance, this change did not correlate with the decrease in firing frequency. By contrast, an increase in sustained non-inactivating current strongly correlated with the decrease in firing frequency. To examine whether this difference was due to an upregulation of ion channels, we measured the difference in conductance density between groups by dividing the conductance by the capacitance, which serves as a proxy for cell size. This resulted in no difference in conductance density between stress and control, suggesting that cell size difference was the major determinant for the decrease in the whole-cell membrane resistance and firing frequency. In line with this idea, we found that repeated stress increased cell capacitance, and that the capacitance increase inversely correlated with the decrease in whole-cell membrane resistance and firing frequency.

Structural analysis of the cells failed to detect the expected increase in cell surface area despite the increase in capacitance. However, the cell surface area negatively correlated with the firing frequency of the cells, supporting the role of cell size change in controlling the intrinsic excitability of neurons during stress. Future directions related to this project include establishing the mechanisms by which cell surface area can change after stress, and subsequently using *in vivo* stress studies to examine whether preventing these neurophysiological changes contributes to stress susceptibility. The failure to adapt to stressors that are not inherently harmful is bio-energetically costly and can be linked to stress-related psychiatric conditions such as anxiety, post-traumatic stress and depression. By understanding the basic biological phenomenon during stress habituation, we can better understand neuronal changes that promote stress resilience.

4.1 C-fos expression in PVN-CRH neurons as a neuronal correlates for the HPA axis habituation

The activities of PVN-CRH neurons *in vivo* have been assessed by measuring the expression of immediate early genes, most commonly c-fos (Ceccatelli, Villar, Goldstein, & Hökfelt, 1989; Figueiredo, Bruestle, Bodie, Dolgas, & Herman, 2003; Girotti et al., 2006a; G. E. Hoffman, Smith, & Verbalis, 1993; Kovács, 2008). However, it is important to note that c-fos mRNA or protein expression does not directly represent the activity levels of neurons but its upregulation generally reflects high-levels of neuronal activity driven by stimuli. As noted by Kovács in her review (2008), "*If c-fos were indeed a general marker of normal neuronal activity and if depolarization per se induced its expression, c-fos should have been detected in millions of neurons throughout the brain under basal conditions.*" By contrast, under non-stress, baseline conditions, c-fos expression is scarce across the brain and almost undetectable in the PVN; on the other hand, c-fos is robustly induced in various brain areas including the PVN by a stimulus such as restraint stress used in my study. While the patterns of neural activities and signals required for c-fos induction are not entirely clear, it has been shown using neuronal cultures that various depolarizing agents, such as glutamate, NMDA, AMPA and high K^+ induce c-Fos in Ca^{2+} dependent manner (Herrera & Robertson, 1996). Using *in vivo* electrophysiology in anesthetized animals, it has also been shown that activity

promoting a high frequency discharge in neurons is followed by induction of c-fos in the hippocampus (Douglas, Dragunow, & Robertson, 1988). Thus, it is generally believed that c-fos upregulation represents a high-level of neuronal activity; this high-level of neuronal activity is advantageous to investigate stress-related activities in relevant circuits.

The transient nature of c-fos upregulation also made it useful to study neuronal activity driven by a recent experience/stimulus. The expression of c-fos mRNA first appears about 5-10 minutes after the stimulus with the peak expression occurring at approximately 30-60 minutes, whereas the expression for c-fos protein begins at 30-45 minutes after the stimulus is delivered and its peak expression is at approximately 90-120 minutes (Kovács, 2008; Kovacs & Sawchenko, 1996). Accordingly, c-fos has been successfully used as a tool to probe the activation of PVN neurons following various types of stressors including cold (Pacák & Palkovits, 2001), foot-shock (Li & Sawchenko, 1998), immobilization (Ceccatelli et al., 1989), restraint (Viau & Sawchenko, 2002), and novelty (Cullinan, Herman, Battaglia, Akil, & Watson, 1995). One interesting study found that after cat exposure (predator stress), rats did not display any c-fos induction in the PVN despite showing elevation of other stress-induced markers (i.e. CRH mRNA) (Figueiredo, Bodie, Tauchi, Dolgas, & Herman, 2003). On the other hand, predator odor (2,5-dihydro-2,4,5-trimethylthiazoline) exposure robustly induces c-fos in the PVN in rats and mice (Asok, Ayers, Awoyemi, Schulkin, & Rosen, 2013; Janitzky, D'Hanis, Kröber, & Schwegler, 2015). These results point to a potential mechanism that represses the transcriptional activation of c-fos associated specifically with cat exposure. The repression of c-fos transcription/translation is an important issue to consider when questioning the mechanisms by which neuronal adaptation occurs during repeated stress. While a number of studies have shown the decrease of c-fos induction in PVN neurons in association with the HPA axis habituation to repeated stress (see below), it is possible that c-fos induction levels could decrease independently from changes in the PVN neuronal activity. In other words, HPA axis habituation could involve molecular mechanisms that repress transcription/translation of c-fos downstream of neuronal excitation. One example is that GCs can act on glucocorticoid receptor to decrease the expression of c-fos following stress (Imaki et al., 1995). In this regard, the

present study is the first to show a decrease in neuronal excitability, which correlates with the time course of c-fos adaptation during repeated stress. One important direction of future study is to investigate the relationship between the heterogeneity in the excitability of PVN-CRH neurons (as I found in this study) and the heterogeneity in the c-fos expression levels as has been reported in several studies (Miklós & Kovács, 2003; Roberts et al., 1993). One way we can address this in the future is with the availability of a transgenic mouse that expresses GFP under c-fos promoter activity (Barth, Gerkin, & Dean, 2004); this will allows us to target c-fos high/low expressing neurons during ex-vivo, in slice electrophysiology experiments.

Measuring the level of CRH neuron activity has not been limited to studies examining c-fos. Other stress-related transcripts in CRH neurons such as CRH hnRNA, AVP hnRNA and CRH mRNA are closely tied to an increase in immediate early gene (IEG) activity such as c-fos. One study has shown that the induction of c-fos mRNA after stress precedes an increase in CRH mRNA levels (Imaki, Shibasaki, Hotta, & Demura, 1992), suggesting that neuronal activation is associated with an increase in the demand of stress-related proteins. Kovacs and Sawchenko (1996) discussed that in response to stress, CRH hnRNA are first quickly generated, followed by IEG mRNA (such as c-fos), then IEG protein, and finally by CRH mRNA, without the peaks of these transcript expressions overlapping (Figure 4.1). The timing of the peak response in the sequence of the transcriptional events make it difficult to examine all stress-related transcription at the same time; however, studies suggest that stress-related transcripts can also be reflective of neuronal activation. In one example, Ma, Levy, and Lightman (1997) showed that CRH transcripts (CRH hnRNA and CRH mRNA) gradually attenuate from baseline stress levels in response to subsequent exposures of repeated restraint stress. Thus, during habituation, CRH transcript levels mirror the attenuation of c-fos transcript levels, suggesting a role for both in representing neuronal activation.

Figure 4.1
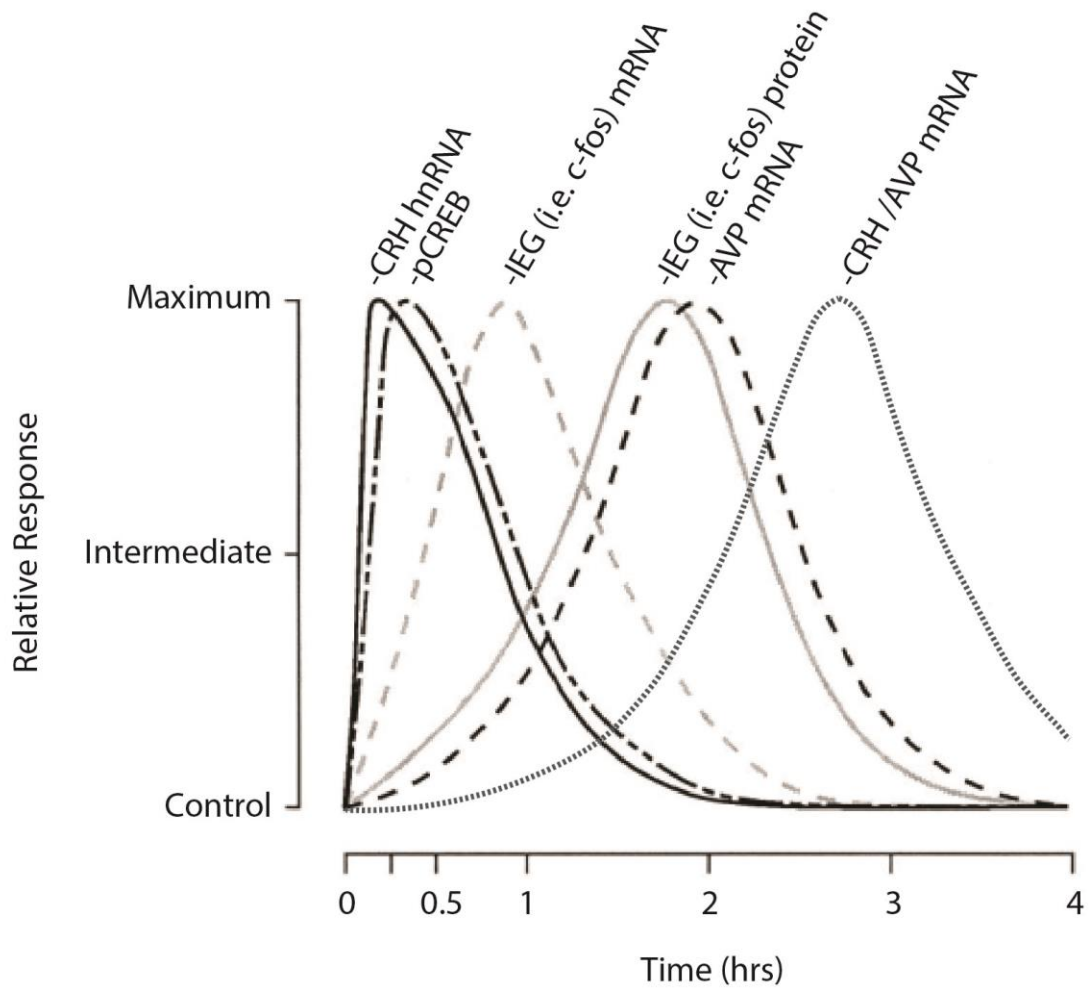
Figure 4.1 Stress-induced sequence of RNA/protein transcription/translation.

Stress elicits various indices of synaptic/transcriptional activation in CRH-PVN neurons. The timing of these indices vary and it is important to acknowledge when the peaks of these indices occur for successful ex-vivo stress-marker examinations. Early indices include CRH hnRNA (a primary transcript) and transcription factor pCREB, which peak 15-30 minutes after stress onset. Next, immediate early gene (IEG) mRNA (i.e. c-fos mRNA) peaks around 1 hour after stress onset. IEG protein and vasopressin (AVP) hnRNA are the next stress indices to peak around 2 hours. Finally, CRH and/or AVP mRNA peak around 2-3 hours after stress exposure.

Modified from "Sequence of stress-induced alterations in indices of synaptic and transcriptional activation in parvocellular neurosecretory neurons," by K. J. Kovacs & P. E Sawchenko. 1996. *Journal of Neuroscience*. *16*(1): 262–273. Copyright (1996) Journal of Neuroscience. Reprinted with permission.

There is evidence to suggest that susceptibility or resilience to stress may be inferred using the levels of stress related transcripts. Swaab, Bao and Lucassen (2005) reported in their review that the total amount of CRH mRNA in the PVN of depressed patients is significantly higher than control, indicating that the inability to tune CRH mRNA transcription appropriately may be indicative of a non-resilient phenotype. Future studies in animal models of stress can work to link c-fos and CRH transcriptional activity, neuronal excitability levels in the PVN, and behavioural phenotypes to elucidate a bio-behavioural model of resilience.

4.1.1 Differences between mouse and rat models of habituation using c-fos

My c-fos expression study essentially confirms previous studies conducted in rats that reported habituation of c-fos response in PVN neurons to repeated restraint or other homotypic stressors (Bonaz & Rivest, 1998; Girotti et al., 2006b; Ons, Rotllant, Marín-Blasco, & Armario, 2010; Uchida et al., 2008; Umemoto, Noguchi, Kawai, & Senba, 1994), and, to our best knowledge, is the first to report c-fos habituation in mice. Importantly, my study revealed two inter-species differences in the time course of the habituation of PVN-CRH neurons. First, mice were substantially slower than rats in developing the habituation of c-fos response. Published reports in rats consistently show that c-fos response in PVN neurons develops after 6-12 days of repeated restraint (Bonaz & Rivest, 1998; Girotti et al., 2006b; Ons et al., 2010; Uchida et al., 2008; Umemoto et al., 1994). On the other hand, in mice, I found that 7 days of repeated restraint was not sufficient to cause the habituation of PVN-CRH neurons that was evident after 21 days. This slow habituation is consistent with the difference in time required for the habituation of the hormonal (CORT) response to repeated stress: in rats, CORT response is significantly attenuated by 3 days and completely abolished by 7 days (Bhatnagar, Huber, Nowak, & Trotter, 2002b; Girotti et al., 2006b; Melia et al., 1994; Uchida et al., 2008), whereas in mice the CORT response only partially decreases over 14 days of repeated restraint (Kim & Han, 2006). Second, the habituation has been shown to be long-lasting after the termination of repeated stress in rats whereas in mice we found that it quickly reverses. Bhatnagar and colleagues (2002b) reported that in rats, habituation to repeated

restraint, which was formed after 8 days of repeated restraint stress, was still evident on 21 days after the last stress challenge (i.e. no stress recovery period). On the other hand, my findings in mice showed that the habituation, which developed after 21 days of repeated restraint stress, was fully recovered 7 days after the termination of repeated stress. While much of what we know about the function of the HPA axis and chronic stress models have been derived from studies using rats, more and more recent studies, including my thesis, use mice due to the availability of various transgenic lines and other research tools. My results provided an example for the importance of examining potential species-dependent differences when transferring stress-models established in rats to mice. Difference in rats and mice may help point to the mechanism that forms and retains stress memory for habituation.

4.2 Homotypic stress habituation occurs in various brain areas.

The activation of the HPA axis results from a cascade of information processing (i.e., signal transduction) from the perception of sensory information to the neuroendocrine, hormonal signaling cascade. Accordingly, a reduction in the sensitivity to stress-relevant signals at any information-processing node, both up-stream and down-stream of PVN-CRH neurons, likely contributes to the development of habituation to a repeated stressor. Indeed, several studies have shown that the neuroendocrine habituation to repeated stress is accompanied by a reduction of c-fos induction at multiple brain regions, including the sensory cortex (Girotti et al., 2006b), medial amygdala (X. Chen & Herbert, 1995) and multiple subcortical brain regions (Bonaz & Rivest, 1998; Stamp & Herbert, 1999). Moreover, habituation also develops for other physiological (i.e., heart rate, body temperature) (Stamp & Herbert, 1999) and behavioral (struggling during restraint) changes (Grissom, Kerr, & Bhatnagar, 2008; Kearns & Spencer, 2013), indicating brain-wide changes in the sensitivity to repeated stressor. Thus, it is likely that the stress sensitivity of the HPA axis to repeated stress is attenuated at multiple levels including the excitability of PVN-CRH neurons as I demonstrated in this study.

4.3 Synaptic plasticity at PVN-CRH neurons during chronic stress

Synaptic plasticity is an important mechanism that provides flexibility in neural circuits and ultimately behavior. With regard to the plasticity of the HPA axis, emerging evidence supports the importance of synaptic plasticity at PVN-CRH neurons (Bains, Cusulin, & Inoue, n.d.). Kuzmiski and colleagues (2010), showed that a single acute stressor primes glutamate synapses to undergo short-term potentiation (STP) in response to a subsequent burst of high-frequency afferent synapse stimulation. Additionally, Flak, Ostrander, Tasker and Herman (2009) showed an increase in the particles immune-positive for vesicular glutamate transporter 2 (vGLUT2, a glutamatergic synaptic protein) apposing to CRH neurons in the PVN after chronic variable stress, suggesting a structural change to glutamatergic synapses. These findings suggest that glutamate synapses are actively involved in stress-related activity-dependent plasticity. However, it is important to note that both acute stress and chronic variable stress do not represent paradigms for stress habituation, and glutamate synapse plasticity associated with habituation is likely distinct from other stress models. To my best knowledge, there is no published work that has examined synaptic plasticity at PVN-CRH neurons in a habituation model. In my undergraduate honours thesis project, I examined vGLUT2 expression on PVN neurons following 21 days repeated restraint and found no change in their expression levels compared to control. This finding provided preliminary evidence that unlike chronic variable stress, repeated restraint stress does not upregulate vGLUT2. In line with the lack of detectable histological changes in glutamate synapses, I did not find changes in the function of glutamate synapse under the experimental conditions I employed in my thesis work as the amplitude of eEPSCs were similar between control and after 21 day repeated stressed.

4.4 Plasticity of intrinsic excitability of PVN-CRH neurons

This study revealed that PVN-CRH neurons can robustly decrease their intrinsic excitability following 21 days of repeated restraint stress. The neuronal changes that followed the timeline of habituation included an increase in rheobase and a decrease in firing frequency in response to controlled current injections. The best intrinsic excitability

correlate to these changes was the decrease in whole-cell membrane resistance, which indicates that more current is necessary to depolarize stressed cells to the same extent as control cells. A decreased membrane resistance predicts that in response to low-level excitatory input, like that of mild chronic stress, PVN-CRH neurons should respond less. If this adaptation mechanism should promote resilience to stress, it is important that these neurons also maintain the capacity to respond optimally (i.e., at full capacity) to a novel/high-level stressor. When we examined the capacity of these neurons to fire action potentials during a sufficiently high incoming signal (which can be generated by more intense stressors and/or novel, heterotypic stressors), stressed neurons maintained the capacity to fire at levels similar to control (Figure 4.2). Therefore, intrinsic, neurophysiological changes that reduce the activation of these neurons upon re-exposure to the restraint stress serve as an important, adaptive mechanism for habituation. Meanwhile, these intrinsic excitability changes can maintain the neurons adaptive function of firing at high excitability levels when exposed to a novel and/or more intense stressor.

Figure 4.2
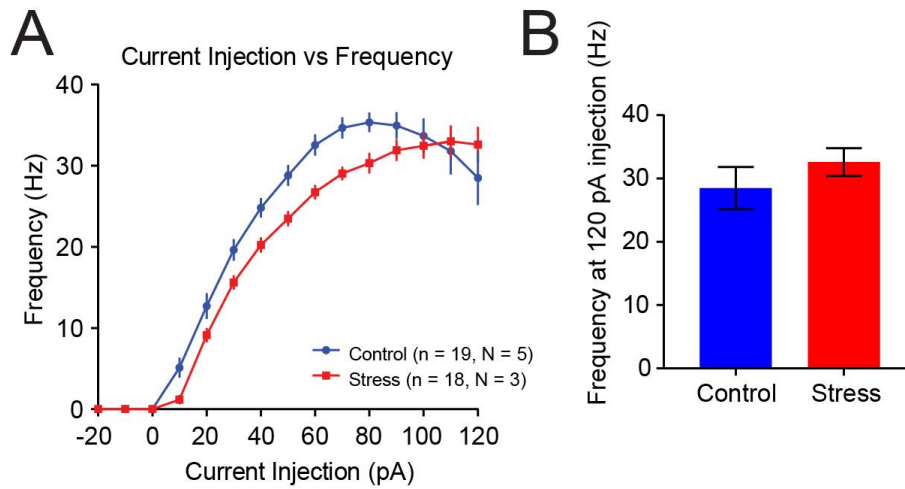
Figure 4.2 Stressed cells retain the capacity to fire as much as control cells.

(A) Current injection vs. firing frequency graph showing that at lower current injections (10 pA – 80 pA), stressed cells fire less, yet when you inject a high amount of current (> 80 pA), they maintain their capacity to fire at the same level as control, suggesting a mechanism by which they can normally respond to novel stressors (Two-way ANOVA, Current injection: $p < 0.001$, Control vs. Stress: $p = 0.02$, Interaction: $p < 0.001$). **(B)** Comparison of firing frequencies at 120pA between stress and control. Unpaired t-test: $p = 0.31$.

4.5 Homeostatic plasticity

Cell autonomous changes in intrinsic excitability is a fundamental way by which neurons maintain their activity levels within a certain range, a phenomenon generally called homeostatic plasticity (Desai, Rutherford, & Turrigiano, 1999; O'Leary, van Rossum, & Wyllie, 2010; Poolos, Migliore, & Johnston, 2002; Senst et al., 2016a). For example, it has been shown that in primary culture of cortical neurons, pharmacological blockade of action potentials with tetrodotoxin (TTX) for a duration of time (24 h) causes up-regulation of sodium channel (I_{Na}) density in the treated neurons, which increases their excitability (Desai et al., 1999). Conversely, when neurons are treated with high K^+ culture media, which induces sustained depolarization, the treated neurons decrease their membrane resistance resulting in an increase in rheobase as well as a decrease in the frequency of repetitive firing. Given that the activity of PVN-CRH neurons increases during stress exposure, the decrease in their intrinsic excitability following repetitive stress exposure can be considered a form of homeostatic plasticity *in vivo*. Although the mechanisms by which intrinsic excitability changes affect behavioural output are largely unknown, data from various fields have pointed to intrinsic excitability changes as being fundamental to behavioural changes related to learning (Rabinak, Zimmerman, Chang, & Orsini, 2008; Sehgal, Ehlers, & Moyer, 2014), central nervous system disorders (Beck & Yaari, 2008), pain (Camp, 2012; Snowball & Schorge, 2015) and drug addictions (Kourrich, Calu, & Bonci, 2015).

Our results support the idea that the brain undergoes homeostatic plasticity changes in order to promote optimal levels of functioning. After chronic exposure to repeated stress, we see that CRH neurons adapt in two fundamental ways. First, they show a delay to first spike, which is a rapidly induced effect promoted by Kv4 (I_A) potassium channels. Second, only after 21 days of repeated restraint stress, we see a decrease in the frequency of repetitive firing in response to an artificial current depolarization, as shown by a decrease in the input-output curve. We failed to reverse the stress-induced changes in the input-output curve by using various channel blockers (Table 1), indirectly supporting the importance of cell size in regulating the whole-cell membrane resistance associated with 21 day of restraint stress.

Table 1

Different drugs used to investigate the change in firing frequency

Drug, CONC, Internal solution vs External aCSF, Company	Effect of Drug	Frequency Reversal?
4-aminopyridine (4-AP), 5mM, external, Sigma	Non-selective voltage-dependent K^+-channel blocker	No
BAPTA, 10mM, internal, Sigma	Fast-acting, calcium chelator	No
EGTA, 10mM, internal, Sigma	Slow-acting, calcium chelator	No
Apamin, 100nM in external, Sigma	Highly selective inhibitor of the small-conductance Ca^{2+}-activated K^+-channel ($K_{Ca}2$, SK)	No
Penitrem A, 1µM in external, Sigma	Potent and selective blocker of BK_{Ca} ($K_{Ca}1.1$) channels	No
Niflumic Acid, 100µM, in external, Sigma	Blocker of endogenous calcium activated chloride channels (CaCCs)	No
Barium, 2.5mM, replaced Ca2+ in external, Sigma	Substitute for calcium to make a calcium-free aCSF	No
Tetraethylammonium (TEA), 1mM, in external, Sigma	Non-selective K^+ channel blocker	No
TRAM34, 1mM, in external, Sigma	Potent and highly selective IK_{Ca} ($K_{Ca}3.1$) channel blocker	No
Guanxitoxin, 5nM - 100nM, in external, Almone Labs	Gating modifier of $K_v2.1$, $K_v2.2$ and $K_v4.3$ channels	No
Cadmium, 10µM, in external aCSF, Sigma	Nonselective calcium channel blocker	No

4.6 Size principle

In the motor system, there is a textbook example that smaller motor units respond to lower stimuli whereas larger units have a higher excitation threshold (Houk & Henneman, 1967). The inverse relationship between the size of neuron and their excitability is termed "size principle" and is related to various aspects of motor regulation such as the amount of input required to elicit an action potential, the mean rate firing of the of the cell and even the rate at which the cell synthesizes proteins (Enoka & Stuart, 1984). Additionally, Houk and Henneman (1967), mentioned that an increase in cell size decreases input resistance, and so despite motor neurons of different sizes having similar voltage thresholds, the size of the cell is the factor that is important in determining neuronal recruitment. My finding of the inverse relationship between C_m and whole-cell membrane resistance is consistent with the size principle. Similarly, Canto and colleagues (2016) recently found that the size of neuronal soma and C_m inversely correlated with the membrane resistance in cerebellar motor neurons. CRH neurons of the hypothalamus are responsible for processing complex information relating to stress; therefore, the fine-tuning of the passive, integrative capacities of individual CRH neurons can help diversify the capacity of these CRH neurons to process stress related information. A decrease in membrane resistance as a result of an increase in cell size is one mechanism by which CRH neurons can tune their response outputs. Together, both synaptic and intrinsic excitability changes to CRH neurons work to assimilate stress information and shape neuronal signal transduction.

4.7 Basis for capacitance change

The electrophysiological measurement of C_m is commonly used to estimate the total cell surface area (hence our interest in cell size). This is based on the several assumptions such as that specific membrane capacitance is similar among different neurons ($\sim 1\ \mu F/cm^2$) and that cell membrane is isopotential. My data for the robust increase in C_m after chronic stress suggested that there is an increase in cell surface area, and as a consequence, a decrease in the intrinsic excitability. To directly measure the cell size and its relationship with intrinsic excitability, I imaged the PVN-CRH neurons after

patch-clamp recordings. While, the cell surface area and firing frequency of the cells showed the expected inverse correlation, 21 day of restraint stress did not increase the surface area (despite the increase in C_m). One possibility is that the stress-induced cell size change may take place primarily in distal dendrites, which was not included in cell surface area measurements but could influence the C_m measurement. More specifically, we were able to visualize the cell soma and the proximal dendrites, but distal dendrites were not visible in many cells. In the future, we will work on refining our cell filling methods (i.e., increasing biocytin filling time) in order to better capture the distal dendrite of the cell to address the possible changes in distal dendrite morphology.

In addition to the lack of stress-induced increase, cell surface area showed expected correlation with C_m only in stress group but not in control group. The reasons for the lack of the changes in cell surface area are currently unclear. Structural changes of the cell will affect the efficacy of space clamp, and as a result, will affect the C_m readout. For example, complex structures such as compartmentalized structures in the cell body and dendrite will distort the relationship between cell surface area and C_m readout. However, while quantifying filled cell images, I did not notice any obvious changes in cell shape. Alternatively, I speculate that stress may change the properties of cell membrane that influence the specific capacitance (capacitance per area membrane). Various mechanisms, such as cell membrane thickness (White, 1970), changes in the cell membrane composition (Valincius et al., 2008), membrane surface folds, can influence specific capacitance. One possibility is that glial cells that adhere to neuronal membrane may affect the specific capacitance of the cell and stress affects the glial adherence to PVN-CRH neurons. Supporting this idea, structural plasticity of glial has been shown to occur in the PVN during lactation to help synchronize oxytocin neuron bursting activity (Tasker, Oliet, Bains, Brown, & Stern, 2012), pointing to a potential mechanism to control the output of CRH neurons.

To further speculate on possible changes in neuronal cell size, the literature describes a variety of cell surface area changes that can contrarily influence neuronal excitability such as: the development of dendritic spines (Matus, 2000; Padival, Quinette, & Rosenkranz, 2013), changes in proximal dendrite diameter (Mitra, Adamec, &

Sapolsky, 2009), how far away spines are from the cell soma, and the size of the cell soma itself (Padival et al., 2013). It is well documented that chronic elevated glucocorticoids can lead to dendritic shortening in the medial prefrontal cortex (Cook & Wellman, 2004; Radley et al., 2006) and the hippocampus (Vyas, Mitra, Shankaranarayana Rao, & Chattarji, 2002), and dendritic growth in the amygdala (Vyas et al., 2002) leading to hypo-activity and hyper-activity in these regions, respectively. More specifically, it appears that an up-regulation of dendritic spines in the amygdala contributes to hyper-excitable changes in the amygdala after stress; also, if these spines are located further from the cell soma, they appear to be more excitable (Padival et al., 2013). Opposed to chronic glucocorticoids, Mitra and colleagues (2009) showed that when rats were able to adapt to a chronic predator stress, as confirmed by resilient behavioural data, they exhibited a phenotypic change that promoted less activity in the amygdala; for example, adapting rats showed more densely packed and shorter dendrites in the amygdala compared to non-adapting or control rats. In an intriguing hypothesis proposed by Gorman and Docherty (2010), a way that neurons might protect themselves from apoptosis is by retracting their dendrites and decreasing their spine numbers to decrease the number of exposed glutamate receptors. Therefore, it is possible that one mechanism by which neurons protect themselves from the maladaptive consequences of repeated stress is to modify their neuronal cell properties to decrease the membrane resistance which can decrease the effectiveness of signal propagation. It is important to mention that the results we have mentioned in this study might be an underestimation of the neurophysiological changes occurring with habituation to chronic stress since we do not have any identification method that can eliminate maladapted animals. Since hyperactivity of CRH neurons in response to non-threatening, repetitive stress would have detrimental physiological and psychological consequences, changes in neuronal surface area properties that have the capacity to reduce the effect of incoming stress signals, can serve as a mechanism for habituation and therefore resilience to stress.

4.8 Stress inoculation, HPA axis habituation and resilience to stress

There is evidence to suggest that exposure to a stressor throughout life can promote adaptive responses to future life stressors. Russo and colleagues (2012) called this "stress inoculation". Stress inoculation is suggested to promote stress resilience by encouraging more optimal behaviours and performance during normal levels of stress and by increasing the capacity to manage higher levels of stress (Russo et al., 2012). Research has begun to look at the effects of moderate life stress on promoting future stress resilience. For example, Parker and colleagues (2004) were the first to demonstrate that moderate stress in squirrel monkeys actually increases their resilience to subsequent stressors, which was shown by an increase in healthy behaviours (increased exploration, food consumption and decreased maternal clinging) and lower CRH and cortisol levels after stress. This promotes the idea that moderate life stressors can in fact serve an adaptive function for the future.

Another study by Sasse and colleagues (2008) shows that the act of habituating to a stressor promotes more efficient habituation to future stressors. Exercise, such as wheel running in rodents, is a physical stressor that induces catabolic requirements and activates the HPA axis (Stranahan, Lee, & Mattson, 2008). Sasse and colleagues (2008) showed that rats subjected to chronic, voluntary wheel running showed habituation at the level of the HPA axis to the exercise and also showed facilitated habituation to a subsequent novel stressor (audiogenic stress). This result promotes the idea that mild stressors such as exercise can prepare the body to manage subsequent stressors. In the field of psychiatry, exercise has been endorsed as a treatment for symptoms of major depression and anxiety (Babyak et al., 2000; Carek, Laibstain, & Carek, 2011; Ekkekakis & Murri, 2017).

The stress-induced capacity to better manage and habituate to future stressors suggests that there are stress-induced neurophysiological changes at stress neurons that promote facilitated habituation. Here, I propose that the neurophysiological changes we see in CRH neurons during habituation promote resilience towards a chronic repeated stressor and possibly towards future stress encounters as well. An increase in the delay

before spiking and a decrease in the frequency of firing in response to neuronal depolarization might be able to explain a shift in the capacity to manage more stress. Also, at higher levels of excitatory input, these habituated neurons show the capacity to maintain control levels of excitability. This suggests that these CRH neurons are tuned to be able to manage the chronic stress (i.e., decrease their responsiveness), and perform more optimally to a higher level of stress (i.e., perform at baseline stress levels). Alone, these results suggest that CRH neurons gain the capacity to respond in an adaptive manner to subsequent stressors, promoting stress resiliency. It would be interesting to investigate whether these neurophysiological changes prime more efficient habituation to stressors following the first habituated stressor, since that too would indicate a more efficient and resilient stress-response system.

4.9 Conclusion

The purpose of this project was to investigate the neurophysiological underpinnings for the habituation of the HPA axis to repeated stress. My thesis revealed that PVN-CRH neurons robustly decreased their intrinsic excitability with the time course that parallels the development of c-fos response habituation to repeated restraint. Importantly, the decrease in the intrinsic excitability was best correlated with the C_m, and likely the change in cell size, resulting in the decrease in whole-cell membrane resistance. With regards to information processing at PVN-CRH neurons, these changes predict that PVN-CRH neurons respond less to low-level excitatory inputs, likely from mild, repeated stressors. At the same time, these CRH neurons maintained the capacity to respond at a high level during a high excitatory input. In certain situations, the inability of the HPA axis to dynamically adapt can be detrimental and can become the driving factor for different psychiatric disorders (Watson & Mackin, 2009). Optimally tuning the stress response can promote future stress resiliency, therefore understanding the mechanism of the how the HPA axis habituates after chronic stress can also help us better understand the mechanisms underlying both stress resilience and stress susceptibility.

Bibliography

Abou-Samra, A. B., Harwood, J. P., Manganiello, V. C., Catt, K. J., & Aguilera, G. (1987). Phorbol 12-myristate 13-acetate and vasopressin potentiate the effect of corticotropin-releasing factor on cyclic AMP production in rat anterior pituitary cells. Mechanisms of action. *The Journal of Biological Chemistry*, *262*(3), 1129–1136.

Aguilera, G. (1994a). Regulation of pituitary ACTH secretion during chronic stress. *Frontiers in Neuroendocrinology*, *15*(4), 321–350. https://doi.org/10.1006/frne.1994.1013

Aguilera, G. (1994b). Regulation of pituitary ACTH secretion during chronic stress. *Frontiers in Neuroendocrinology*, *15*(4), 321–350. https://doi.org/10.1006/frne.1994.1013

Alexander, S. P., Catterall, W. A., Kelly, E., Marrion, N., Peters, J. A., Benson, H. E., … CGTP Collaborators. (2015). The Concise Guide to PHARMACOLOGY 2015/16: Voltage-gated ion channels. *British Journal of Pharmacology*, *172*(24), 5904–5941. https://doi.org/10.1111/bph.13349

Asok, A., Ayers, L. W., Awoyemi, B., Schulkin, J., & Rosen, J. B. (2013). Immediate early gene and neuropeptide expression following exposure to the predator odor 2,5-dihydro-2,4,5-trimethylthiazoline (TMT). *Behavioural Brain Research*, *248*, 85–93. https://doi.org/10.1016/j.bbr.2013.03.047

Babyak, M., Blumenthal, J. A., Herman, S., Khatri, P., Doraiswamy, M., Moore, K., … Krishnan, K. R. (2000). Exercise treatment for major depression: maintenance of therapeutic benefit at 10 months. *Psychosomatic Medicine*, *62*(5), 633–638.

Bains, J. S., Cusulin, J. I. W., & Inoue, W. (2015). Stress-related synaptic plasticity in the hypothalamus. *Nature Reviews. Neuroscience*, *16*(7), 377–388. https://doi.org/10.1038/nrn3881

Bains, J. S., Follwell, M. J., Latchford, K. J., Anderson, J. W., & Ferguson, A. V. (2001). Slowly inactivating potassium conductance (I(D)): a potential target for stroke therapy. *Stroke*, *32*(11), 2624–2634.

Bains, J. S., Wamsteeker Cusulin, J. I., & Inoue, W. (n.d.). Rules of Synaptic Engagement and Plasticity in Hypothalamic Stress Command Neurons. *Nature Reviews Neuroscience*.

Barth, A. L., Gerkin, R. C., & Dean, K. L. (2004). Alteration of Neuronal Firing Properties after In Vivo Experience in a FosGFP Transgenic Mouse. *Journal of Neuroscience*, *24*(29), 6466–6475. https://doi.org/10.1523/JNEUROSCI.4737-03.2004

Beck, H., & Yaari, Y. (2008). Plasticity of intrinsic neuronal properties in CNS disorders. *Nature Reviews Neuroscience*, *9*(5), 357–369. https://doi.org/10.1038/nrn2371

Bhatnagar, S., & Dallman, M. (1998). Neuroanatomical basis for facilitation of hypothalamic-pituitary-adrenal responses to a novel stressor after chronic stress. *Neuroscience*, *84*(4), 1025–1039.

Bhatnagar, S., Huber, R., Nowak, N., & Trotter, P. (2002a). Lesions of the posterior paraventricular thalamus block habituation of hypothalamic-pituitary-adrenal responses to repeated restraint. *Journal of Neuroendocrinology*, *14*(5), 403–410.

Bhatnagar, S., Huber, R., Nowak, N., & Trotter, P. (2002b). Lesions of the Posterior Paraventricular Thalamus Block Habituation of Hypothalamic-Pituitary-Adrenal Responses to Repeated Restraint. *Journal of Neuroendocrinology*, *14*(5), 403–410. https://doi.org/10.1046/j.0007-1331.2002.00792.x

Biag, J., Huang, Y., Gou, L., Hintiryan, H., Askarinam, A., Hahn, J. D., … Dong, H.-W. (2012). Cyto- and chemoarchitecture of the hypothalamic paraventricular nucleus in the C57BL/6J male mouse: a study of immunostaining and multiple fluorescent tract tracing. *The Journal of Comparative Neurology*, *520*(1), 6–33. https://doi.org/10.1002/cne.22698

Billington, C. J., Briggs, J. E., Harker, S., Grace, M., & Levine, A. S. (1994). Neuropeptide Y in hypothalamic paraventricular nucleus: a center coordinating energy metabolism. *American Journal of Physiology - Regulatory, Integrative and Comparative Physiology*, *266*(6), R1765–R1770.

Bonaz, B., & Rivest, S. (1998). Effect of a chronic stress on CRF neuronal activity and expression of its type 1 receptor in the rat brain. *The American Journal of Physiology*, *275*(5 Pt 2), R1438-1449.

Bourque, C. W. (2008). Central mechanisms of osmosensation and systemic osmoregulation. *Nature Reviews. Neuroscience; London*, *9*(7), 519–31. https://doi.org/http://dx.doi.org/10.1038/nrn2400

Brown, E. S., Varghese, F. P., & McEwen, B. S. (2004). Association of depression with medical illness: does cortisol play a role? *Biological Psychiatry*, *55*(1), 1–9. https://doi.org/10.1016/S0006-3223(03)00473-6

Buttgereit, F., Burmester, G.-R., & Lipworth, B. J. (2009). Inflammation, glucocorticoids and risk of cardiovascular disease. *Nature Clinical Practice. Rheumatology*, *5*(1), 18–19. https://doi.org/10.1038/ncprheum0963

Cai, S.-Q., Li, W., & Sesti, F. (2007). Multiple modes of a-type potassium current regulation. *Current Pharmaceutical Design*, *13*(31), 3178–3184.

Cain, D. W., & Cidlowski, J. A. (2017). Immune regulation by glucocorticoids. *Nature Reviews. Immunology*, *17*(4), 233–247. https://doi.org/10.1038/nri.2017.1

Camp, A. J. (2012). Intrinsic Neuronal Excitability: A Role in Homeostasis and Disease. *Frontiers in Neurology*, *3*. https://doi.org/10.3389/fneur.2012.00050

Canto, C. B., Witter, L., & De Zeeuw, C. I. (2016). Whole-Cell Properties of Cerebellar Nuclei Neurons In Vivo. *PloS One*, *11*(11), e0165887. https://doi.org/10.1371/journal.pone.0165887

Capel, R. A., & Terrar, D. A. (2015). Cytosolic calcium ions exert a major influence on the firing rate and maintenance of pacemaker activity in guinea-pig sinus node. *Frontiers in Physiology*, *6*. https://doi.org/10.3389/fphys.2015.00023

Carek, P. J., Laibstain, S. E., & Carek, S. M. (2011). Exercise for the Treatment of Depression and Anxiety. *The International Journal of Psychiatry in Medicine*, *41*(1), 15–28. https://doi.org/10.2190/PM.41.1.c

Ceccatelli, S., Villar, M. J., Goldstein, M., & Hökfelt, T. (1989). Expression of c-Fos immunoreactivity in transmitter-characterized neurons after stress. *Proceedings of the National Academy of Sciences*, *86*(23), 9569–9573.

Chen, X., & Herbert, J. (1995). Regional changes in c-fos expression in the basal forebrain and brainstem during adaptation to repeated stress: Correlations with cardiovascular, hypothermic and endocrine responses. *Neuroscience*, *64*(3), 675–685. https://doi.org/10.1016/0306-4522(94)00532-A

Chen, Y., Molet, J., Gunn, B. G., Ressler, K., & Baram, T. Z. (2015). Diversity of Reporter Expression Patterns in Transgenic Mouse Lines Targeting Corticotropin-Releasing Hormone-Expressing Neurons. *Endocrinology*, *156*(12), 4769–4780. https://doi.org/10.1210/en.2015-1673

Cook, S. C., & Wellman, C. L. (2004). Chronic stress alters dendritic morphology in rat medial prefrontal cortex. *Journal of Neurobiology*, *60*(2), 236–248. https://doi.org/10.1002/neu.20025

Covington, H. E., Lobo, M. K., Maze, I., Vialou, V., Hyman, J. M., Zaman, S., … Nestler, E. J. (2010). Antidepressant Effect of Optogenetic Stimulation of the Medial Prefrontal Cortex. *Journal of Neuroscience*, *30*(48), 16082–16090. https://doi.org/10.1523/JNEUROSCI.1731-10.2010

Cullinan, W. E., Herman, J. P., Battaglia, D. F., Akil, H., & Watson, S. J. (1995). Pattern and time course of immediate early gene expression in rat brain following acute stress. *Neuroscience*, *64*(2), 477–505. https://doi.org/10.1016/0306-4522(94)00355-9

Cunningham, E. T., Bohn, M. C., & Sawchenko, P. E. (1990). Organization of adrenergic inputs to the paraventricular and supraoptic nuclei of the hypothalamus in the rat. *The Journal of Comparative Neurology*, *292*(4), 651–667. https://doi.org/10.1002/cne.902920413

Daftary, S. S., Boudaba, C., & Tasker, J. G. (2000). Noradrenergic regulation of parvocellular neurons in the rat hypothalamic paraventricular nucleus. *Neuroscience*, *96*(4), 743–751. https://doi.org/10.1016/S0306-4522(00)00003-8

Dallman, M. F., Akana, S. F., Jacobson, L., Levin, N., Cascio, C. S., & Shinsako, J. (1987). Characterization of corticosterone feedback regulation of ACTH secretion. *Annals of the New York Academy of Sciences*, *512*, 402–414.

Dallman, M. F., Akana, S. F., Strack, A. M., Hanson, E. S., & Sebastian, R. J. (1995). The neural network that regulates energy balance is responsive to glucocorticoids

and insulin and also regulates HPA axis responsivity at a site proximal to CRF neurons. *Annals of the New York Academy of Sciences*, *771*, 730–742.

de Kloet, E. R., Joëls, M., & Holsboer, F. (2005). Stress and the brain: from adaptation to disease. *Nature Reviews. Neuroscience*, *6*(6), 463–475. https://doi.org/10.1038/nrn1683

De Kloet, E. R., Vreugdenhil, E., Oitzl, M. S., & Joëls, M. (1998). Brain corticosteroid receptor balance in health and disease. *Endocrine Reviews*, *19*(3), 269–301. https://doi.org/10.1210/edrv.19.3.0331

Desai, N. S., Rutherford, L. C., & Turrigiano, G. G. (1999). Plasticity in the intrinsic excitability of cortical pyramidal neurons. *Nature Neuroscience*, *2*(6). Retrieved from https://pdfs.semanticscholar.org/6fe6/943b760b257f4dc3f28b4052c9645d69e2bd.pdf

Douglas, R. M., Dragunow, M., & Robertson, H. A. (1988). High-frequency discharge of dentate granule cells, but not long-term potentiation, induces c-fos protein. *Brain Research*, *464*(3), 259–262.

Ekkekakis, P., & Murri, M. B. (2017). Exercise as antidepressant treatment: Time for the transition from trials to clinic? *General Hospital Psychiatry*. https://doi.org/10.1016/j.genhosppsych.2017.04.008

Epel, E. S., McEwen, B., Seeman, T., Matthews, K., Castellazzo, G., Brownell, K. D., … Ickovics, J. R. (2000). Stress and body shape: stress-induced cortisol secretion is consistently greater among women with central fat. *Psychosomatic Medicine*, *62*(5), 623–632.

Figueiredo, H. F., Bodie, B. L., Tauchi, M., Dolgas, C. M., & Herman, J. P. (2003). Stress integration after acute and chronic predator stress: differential activation of central stress circuitry and sensitization of the hypothalamo-pituitary-adrenocortical axis. *Endocrinology*, *144*(12), 5249–5258. https://doi.org/10.1210/en.2003-0713

Figueiredo, H. F., Bruestle, A., Bodie, B., Dolgas, C. M., & Herman, J. P. (2003). The medial prefrontal cortex differentially regulates stress-induced c-fos expression in the forebrain depending on type of stressor. *European Journal of Neuroscience*, *18*(8), 2357–2364. https://doi.org/10.1046/j.1460-9568.2003.02932.x

Flak, J. N., Ostrander, M. M., Tasker, J. G., & Herman, J. P. (2009). Chronic stress-induced neurotransmitter plasticity in the PVN. *The Journal of Comparative Neurology*, *517*(2), 156–165. https://doi.org/10.1002/cne.22142

Gianferante, D., Thoma, M. V., Hanlin, L., Chen, X., Breines, J. G., Zoccola, P. M., & Rohleder, N. (2014). Post-stress rumination predicts HPA axis responses to repeated acute stress. *Psychoneuroendocrinology*, *49*, 244–252. https://doi.org/10.1016/j.psyneuen.2014.07.021

Gimpl, G., & Fahrenholz, F. (2001). The Oxytocin Receptor System: Structure, Function, and Regulation. *Physiological Reviews*, *81*(2), 629–683.

Girotti, M., Pace, T. W. W., Gaylord, R. I., Rubin, B. A., Herman, J. P., & Spencer, R. L. (2006a). Habituation to repeated restraint stress is associated with lack of stress-induced c-fos expression in primary sensory processing areas of the rat brain. *Neuroscience*, *138*(4), 1067–1081. https://doi.org/10.1016/j.neuroscience.2005.12.002

Girotti, M., Pace, T. W. W., Gaylord, R. I., Rubin, B. A., Herman, J. P., & Spencer, R. L. (2006b). Habituation to repeated restraint stress is associated with lack of stress-induced c-fos expression in primary sensory processing areas of the rat brain. *Neuroscience*, *138*(4), 1067–1081. https://doi.org/10.1016/j.neuroscience.2005.12.002

Gorman, J. M., & Docherty, J. P. (2010). A hypothesized role for dendritic remodeling in the etiology of mood and anxiety disorders. *The Journal of Neuropsychiatry and Clinical Neurosciences*, *22*(3), 256–264. https://doi.org/10.1176/appi.neuropsych.22.3.256

Grissom, N., & Bhatnagar, S. (2009). Habituation to repeated stress: get used to it. *Neurobiology of Learning and Memory*, *92*(2), 215–224. https://doi.org/10.1016/j.nlm.2008.07.001

Grissom, N., Kerr, W., & Bhatnagar, S. (2008). Struggling behavior during restraint is regulated by stress experience. *Behavioural Brain Research*, *191*(2), 219–226. https://doi.org/10.1016/j.bbr.2008.03.030

Gutnick, M. J., & Yarom, Y. (1989). Low threshold calcium spikes, intrinsic neuronal oscillation and rhythm generation in the CNS. *Journal of Neuroscience Methods*, *28*(1), 93–99. https://doi.org/10.1016/0165-0270(89)90014-9

Haedo, R. J., & Golowasch, J. (2006). Ionic Mechanism Underlying Recovery of Rhythmic Activity in Adult Isolated Neurons. *Journal of Neurophysiology*, *96*(4), 1860–1876. https://doi.org/10.1152/jn.00385.2006

Herman, J. P., & Cullinan, W. E. (1997). Neurocircuitry of stress: central control of the hypothalamo-pituitary-adrenocortical axis. *Trends in Neurosciences*, *20*(2), 78–84.

Herman, J. P., Figueiredo, H., Mueller, N. K., Ulrich-Lai, Y., Ostrander, M. M., Choi, D. C., & Cullinan, W. E. (2003). Central mechanisms of stress integration: hierarchical circuitry controlling hypothalamo-pituitary-adrenocortical responsiveness. *Frontiers in Neuroendocrinology*, *24*(3), 151–180.

Herrera, D. G., & Robertson, H. A. (1996). Activation of c-fos in the brain. *Progress in Neurobiology*, *50*(2–3), 83–107.

Hewitt, S. A., & Bains, J. S. (2006). Brain-Derived Neurotrophic Factor Silences GABA Synapses Onto Hypothalamic Neuroendocrine Cells Through a Postsynaptic

Dynamin-Mediated Mechanism. *Journal of Neurophysiology*, *95*(4), 2193–2198. https://doi.org/10.1152/jn.01135.2005

Hewitt, S. A., Wamsteeker, J. I., Kurz, E. U., & Bains, J. S. (2009). Altered chloride homeostasis removes synaptic inhibitory constraint of the stress axis. *Nature Neuroscience*, *12*(4), 438–443. https://doi.org/10.1038/nn.2274

Hoffman, G. E., Smith, M. S., & Verbalis, J. G. (1993). c-Fos and Related Immediate Early Gene Products as Markers of Activity in Neuroendocrine Systems. *Frontiers in Neuroendocrinology*, *14*(3), 173–213. https://doi.org/10.1006/frne.1993.1006

Hoffman, N. W., Tasker, J. G., & Dudek, F. E. (1991). Immunohistochemical differentiation of electrophysiologically defined neuronal populations in the region of the rat hypothalamic paraventricular nucleus. *The Journal of Comparative Neurology*, *307*(3), 405–416. https://doi.org/10.1002/cne.903070306

Hoyda, T. D., & Ferguson, A. V. (2010). Adiponectin Modulates Excitability of Rat Paraventricular Nucleus Neurons by Differential Modulation of Potassium Currents. *Endocrinology*, *151*(7), 3154–3162. https://doi.org/10.1210/en.2009-1390

Imaki, T., Shibasaki, T., Hotta, M., & Demura, H. (1992). Early induction of c-fos precedes increased expression of corticotropin-releasing factor messenger ribonucleic acid in the paraventricular nucleus after immobilization stress. *Endocrinology*, *131*(1), 240–246. https://doi.org/10.1210/endo.131.1.1612001

Imaki, T., Xiao-Quan, W., Shibasaki, T., Yamada, K., Harada, S., Chikada, N., … Demura, H. (1995). Stress-induced activation of neuronal activity and corticotropin-releasing factor gene expression in the paraventricular nucleus is modulated by glucocorticoids in rats. *The Journal of Clinical Investigation*, *96*(1), 231–238. https://doi.org/10.1172/JCI118026

Inoue, W., Baimoukhametova, D. V., Füzesi, T., Cusulin, J. I. W., Koblinger, K., Whelan, P. J., … Bains, J. S. (2013). Noradrenaline is a stress-associated metaplastic signal at GABA synapses. *Nature Neuroscience*, *16*(5), 605–612. https://doi.org/10.1038/nn.3373

Itoi, K., Talukder, A. H., Fuse, T., Kaneko, T., Ozawa, R., Sato, T., … Sakimura, K. (2014). Visualization of corticotropin-releasing factor neurons by fluorescent proteins in the mouse brain and characterization of labeled neurons in the paraventricular nucleus of the hypothalamus. *Endocrinology*, *155*(10), 4054–4060. https://doi.org/10.1210/en.2014-1182

Iwasaki, S., Chihara, Y., Komuta, Y., Ito, K., & Sahara, Y. (2008). Low-Voltage-Activated Potassium Channels Underlie the Regulation of Intrinsic Firing Properties of Rat Vestibular Ganglion Cells. *Journal of Neurophysiology*, *100*(4), 2192–2204. https://doi.org/10.1152/jn.01240.2007

Janitzky, K., D'Hanis, W., Kröber, A., & Schwegler, H. (2015). TMT predator odor activated neural circuit in C57BL/6J mice indicates TMT-stress as a suitable

model for uncontrollable intense stress. *Brain Research*, *1599*, 1–8. https://doi.org/10.1016/j.brainres.2014.12.030

Kant, G. J., Bunnell, B. N., Mougey, E. H., Pennington, L. L., & Meyerhoff, J. L. (1983). Effects of repeated stress on pituitary cyclic AMP, and plasma prolactin, corticosterone and growth hormone in male rats. *Pharmacology Biochemistry and Behavior*, *18*(6), 967–971. https://doi.org/10.1016/S0091-3057(83)80022-7

Kearns, R. R., & Spencer, R. L. (2013). An unexpected increase in restraint duration alters the expression of stress response habituation. *Physiology & Behavior*, *122*, 193–200. https://doi.org/10.1016/j.physbeh.2013.03.029

Khorkova, O., & Golowasch, J. (2007). Neuromodulators, Not Activity, Control Coordinated Expression of Ionic Currents. *Journal of Neuroscience*, *27*(32), 8709–8718. https://doi.org/10.1523/JNEUROSCI.1274-07.2007

Kim, K.-S., & Han, P.-L. (2006). Optimization of chronic stress paradigms using anxiety- and depression-like behavioral parameters. *Journal of Neuroscience Research*, *83*(3), 497–507. https://doi.org/10.1002/jnr.20754

Kirschbaum, C., Prüssner, J. C., Stone, A. A., Federenko, I., Gaab, J., Lintz, D., … Hellhammer, D. H. (1995). Persistent high cortisol responses to repeated psychological stress in a subpopulation of healthy men. *Psychosomatic Medicine*, *57*(5), 468–474.

Kiss, A., & Aguilera, G. (1993). Regulation of the hypothalamic pituitary adrenal axis during chronic stress: responses to repeated intraperitoneal hypertonic saline injection. *Brain Research*, *630*(1–2), 262–270.

Kourrich, S., Calu, D. J., & Bonci, A. (2015). Intrinsic plasticity: an emerging player in addiction. *Nature Reviews. Neuroscience*, *16*(3), 173–184. https://doi.org/10.1038/nrn3877

Kovács, K. J. (2008). Measurement of Immediate-Early Gene Activation- c-fos and Beyond. *Journal of Neuroendocrinology*, *20*(6), 665–672. https://doi.org/10.1111/j.1365-2826.2008.01734.x

Kovacs, K. J., & Sawchenko, P. E. (1996). Sequence of stress-induced alterations in indices of synaptic and transcriptional activation in parvocellular neurosecretory neurons. *Journal of Neuroscience*, *16*(1), 262–273.

Kudielka, B. M., Bellingrath, S., & Hellhammer, D. H. (2006). Cortisol in burnout and vital exhaustion: an overview. *Giornale Italiano Di Medicina Del Lavoro Ed Ergonomia*, *28*(1 Suppl 1), 34–42.

Kuzmiski, J. B., Marty, V., Baimoukhametova, D. V., & Bains, J. S. (2010). Stress-induced priming of glutamate synapses unmasks associative short-term plasticity. *Nat Neurosci*, *13*(10), 1257–1264. https://doi.org/10.1038/nn.2629

Latchford, K. J. (2008, January 18). *Electrophysiological Effects of Angiotensin II on Hypothalamic Paraventricular Nucleus Neurons of the Rat* (Thesis). Retrieved from https://qspace.library.queensu.ca/handle/1974/995

Lee, A. K., Tse, F. W., & Tse, A. (2015). Arginine Vasopressin Potentiates the Stimulatory Action of CRH on Pituitary Corticotropes via a Protein Kinase C–Dependent Reduction of the Background TREK-1 Current. *Endocrinology*, *156*(10), 3661–3672. https://doi.org/10.1210/en.2015-1293

Lehmann, M. L., & Herkenham, M. (2011). Environmental Enrichment Confers Stress Resiliency to Social Defeat through an Infralimbic Cortex-Dependent Neuroanatomical Pathway. *Journal of Neuroscience*, *31*(16), 6159–6173. https://doi.org/10.1523/JNEUROSCI.0577-11.2011

Levy, B. H., & Tasker, J. G. (2012). Synaptic regulation of the hypothalamic-pituitary-adrenal axis and its modulation by glucocorticoids and stress. *Frontiers in Cellular Neuroscience*, *6*, 24. https://doi.org/10.3389/fncel.2012.00024

Li, H.-Y., & Sawchenko, P. e. (1998). Hypothalamic effector neurons and extended circuitries activated in "neurogenic" stress: A comparison of footshock effects exerted acutely, chronically, and in animals with controlled glucocorticoid levels. *The Journal of Comparative Neurology*, *393*(2), 244–266. https://doi.org/10.1002/(SICI)1096-9861(19980406)393:2<244::AID-CNE8>3.0.CO;2-2

Loewen, S. P., & Ferguson, A. V. (2017). Adropin acts in the rat paraventricular nucleus to influence neuronal excitability. *American Journal of Physiology - Regulatory, Integrative and Comparative Physiology*, *312*(4), R511–R519. https://doi.org/10.1152/ajpregu.00517.2016

Luther, J. A., Daftary, S. S., Boudaba, C., Gould, G. C., Halmos, K. C., & Tasker, J. G. (2002). Neurosecretory and non-neurosecretory parvocellular neurones of the hypothalamic paraventricular nucleus express distinct electrophysiological properties. *Journal of Neuroendocrinology*, *14*(12), 929–932.

Luther, J. A., & Tasker, J. G. (2000). Voltage-gated currents distinguish parvocellular from magnocellular neurones in the rat hypothalamic paraventricular nucleus. *The Journal of Physiology*, *523*(1), 193–209. https://doi.org/10.1111/j.1469-7793.2000.t01-1-00193.x

Ma, X.-M., Levy, A., & Lightman, S. L. (1997). Rapid changes in heteronuclear RNA for corticotrophin-releasing hormone and arginine vasopressin in response to acute stress. *Journal of Endocrinology*, *152*(1), 81–89. https://doi.org/10.1677/joe.0.1520081

Marty, V., Kuzmiski, J. B., Baimoukhametova, D. V., & Bains, J. S. (2011). Short-term plasticity impacts information transfer at glutamate synapses onto parvocellular neuroendocrine cells in the paraventricular nucleus of the hypothalamus. *The Journal of Physiology*, *589*(Pt 17), 4259–4270. https://doi.org/10.1113/jphysiol.2011.208082

Matus, A. (2000). Actin-Based Plasticity in Dendritic Spines. *Science*, *290*(5492), 754–758. https://doi.org/10.1126/science.290.5492.754

McEwen, B. S. (2000). The neurobiology of stress: from serendipity to clinical relevance. *Brain Research*, *886*(1–2), 172–189.

McEwen, B. S. (2012). Brain on stress: how the social environment gets under the skin. *Proceedings of the National Academy of Sciences of the United States of America*, *109 Suppl 2*, 17180–17185. https://doi.org/10.1073/pnas.1121254109

McEwen, B. S., & Seeman, T. (1999). Protective and damaging effects of mediators of stress. Elaborating and testing the concepts of allostasis and allostatic load. *Annals of the New York Academy of Sciences*, *896*, 30–47.

Melia, K. R., Ryabinin, A. E., Schroeder, R., Bloom, F. E., & Wilson, M. C. (1994). Induction and habituation of immediate early gene expression in rat brain by acute and repeated restraint stress. *The Journal of Neuroscience: The Official Journal of the Society for Neuroscience*, *14*(10), 5929–5938.

Membrane Test Algorithms. (n.d.). Retrieved June 25, 2017, from http://mdc.custhelp.com/app/answers/detail/a_id/17006/session/L2F2LzEvdGltZS8xNDk4MzY1MjAxL3NpZC9ucmo1LVpsbg%3D%3D

Miklós, I. H., & Kovács, K. J. (2003). Functional heterogeneity of the responses of histaminergic neuron subpopulations to various stress challenges. *European Journal of Neuroscience*, *18*(11), 3069–3079. https://doi.org/10.1111/j.1460-9568.2003.03033.x

Mitra, R., Adamec, R., & Sapolsky, R. (2009). Resilience against predator stress and dendritic morphology of amygdala neurons. *Behavioural Brain Research*, *205*(2), 535–543. https://doi.org/10.1016/j.bbr.2009.08.014

Munck, A., Guyre, P. M., & Holbrook, N. J. (1984). Physiological Functions of Glucocorticoids in Stress and Their Relation to Pharmacological Actions*. *Endocrine Reviews*, *5*(1), 25–44. https://doi.org/10.1210/edrv-5-1-25

Natelson, B. H., Ottenweller, J. E., Cook, J. A., Pitman, D., McCarty, R., & Tapp, W. N. (1988). Effect of stressor intensity on habituation of the adrenocortical stress response. *Physiology & Behavior*, *43*(1), 41–46. https://doi.org/10.1016/0031-9384(88)90096-0

Nunn, N., Womack, M., Dart, C., & Barrett-Jolley, R. (2011). Function and pharmacology of spinally-projecting sympathetic pre-autonomic neurones in the paraventricular nucleus of the hypothalamus. *Current Neuropharmacology*, *9*(2), 262–277. https://doi.org/10.2174/157015911795596531

O'Leary, T., van Rossum, M. C. W., & Wyllie, D. J. A. (2010). Homeostasis of intrinsic excitability in hippocampal neurones: dynamics and mechanism of the response to chronic depolarization. *The Journal of Physiology*, *588*(Pt 1), 157–170. https://doi.org/10.1113/jphysiol.2009.181024

Ons, S., Rotllant, D., Marín-Blasco, I. J., & Armario, A. (2010). Immediate-early gene response to repeated immobilization: Fos protein and arc mRNA levels appear to be less sensitive than c-fos mRNA to adaptation. *The European Journal of*

Neuroscience, *31*(11), 2043–2052. https://doi.org/10.1111/j.1460-9568.2010.07242.x

Pacák, K., & Palkovits, M. (2001). Stressor Specificity of Central Neuroendocrine Responses: Implications for Stress-Related Disorders. *Endocrine Reviews*, *22*(4), 502–548. https://doi.org/10.1210/er.22.4.502

Padival, M., Quinette, D., & Rosenkranz, J. A. (2013). Effects of repeated stress on excitatory drive of basal amygdala neurons in vivo. *Neuropsychopharmacology: Official Publication of the American College of Neuropsychopharmacology*, *38*(9), 1748–1762. https://doi.org/10.1038/npp.2013.74

Parker, K. J., Buckmaster, C. L., Schatzberg, A. F., & Lyons, D. M. (2004). Prospective Investigation of Stress Inoculation in Young Monkeys. *Archives of General Psychiatry*, *61*(9), 933–941. https://doi.org/10.1001/archpsyc.61.9.933

Peron, S., & Gabbiani, F. (2009). Spike frequency adaptation mediates looming stimulus selectivity in a collision-detecting neuron. *Nature Neuroscience*, *12*(3), 318–326. https://doi.org/10.1038/nn.2259

Poolos, N. P., Migliore, M., & Johnston, D. (2002). Pharmacological upregulation of h-channels reduces the excitability of pyramidal neuron dendrites. *Nature Neuroscience*, *5*(8), 767–774. https://doi.org/10.1038/nn891

Price, C. J., Hoyda, T. D., Samson, W. K., & Ferguson, A. V. (2008). Nesfatin-1 Influences the Excitability of Paraventricular Nucleus Neurones. *Journal of Neuroendocrinology*, *20*(2), 245–250. https://doi.org/10.1111/j.1365-2826.2007.01641.x

Rabinak, C. A., Zimmerman, J. M., Chang, C., & Orsini, C. A. (2008). Bidirectional Changes in the Intrinsic Excitability of Infralimbic Neurons Reflect a Possible Regulatory Role in the Acquisition and Extinction of Pavlovian Conditioned Fear. *Journal of Neuroscience*, *28*(29), 7245–7247. https://doi.org/10.1523/JNEUROSCI.2130-08.2008

Radley, J. J., Rocher, A. B., Miller, M., Janssen, W. G. M., Liston, C., Hof, P. R., … Morrison, J. H. (2006). Repeated stress induces dendritic spine loss in the rat medial prefrontal cortex. *Cerebral Cortex (New York, N.Y.: 1991)*, *16*(3), 313–320. https://doi.org/10.1093/cercor/bhi104

Roberts, M. M., Robinson, A. G., Fitzsimmons, M. D., Grant, F., Lee, W. S., & Hoffman, G. E. (1993). c-fos expression in vasopressin and oxytocin neurons reveals functional heterogeneity within magnocellular neurons. *Neuroendocrinology*, *57*(3), 388–400.

Royeck, M., Horstmann, M.-T., Remy, S., Reitze, M., Yaari, Y., & Beck, H. (2008). Role of Axonal NaV1.6 Sodium Channels in Action Potential Initiation of CA1 Pyramidal Neurons. *Journal of Neurophysiology*, *100*(4), 2361–2380. https://doi.org/10.1152/jn.90332.2008

Russo, S. J., Murrough, J. W., Han, M.-H., Charney, D. S., & Nestler, E. J. (2012). Neurobiology of resilience. *Nature Neuroscience*, *15*(11), 1475–1484. https://doi.org/10.1038/nn.3234

Sapolsky, R. M., Romero, L. M., & Munck, A. U. (2000). How do glucocorticoids influence stress responses? Integrating permissive, suppressive, stimulatory, and preparative actions. *Endocrine Reviews*, *21*(1), 55–89.

Sasse, S. K., Greenwood, B. N., Masini, C. V., Nyhuis, T. J., Fleshner, M., Day, H. E. W., & Campeau, S. (2008). Chronic voluntary wheel running facilitates corticosterone response habituation to repeated audiogenic stress exposure in male rats. *Stress*, *11*(6), 425–437. https://doi.org/10.1080/10253890801887453

Sawchenko, P. E., & Swanson, L. W. (1982). The organization of noradrenergic pathways from the brainstem to the paraventricular and supraoptic nuclei in the rat. *Brain Research*, *257*(3), 275–325.

Sehgal, M., Ehlers, V. L., & Moyer, J. R. (2014). Learning enhances intrinsic excitability in a subset of lateral amygdala neurons. *Learning & Memory*, *21*(3), 161–170. https://doi.org/10.1101/lm.032730.113

Senst, L., Baimoukhametova, D., Sterley, T.-L., & Bains, J. S. (2016a). Sexually dimorphic neuronal responses to social isolation. *ELife*, *5*, e18726. https://doi.org/10.7554/eLife.18726

Senst, L., Baimoukhametova, D., Sterley, T.-L., & Bains, J. S. (2016b). Sexually dimorphic neuronal responses to social isolation. *ELife*, *5*, e18726. https://doi.org/10.7554/eLife.18726

Simmons, D. M., & Swanson, L. W. (2009). Comparison of the spatial distribution of seven types of neuroendocrine neurons in the rat paraventricular nucleus: toward a global 3D model. *The Journal of Comparative Neurology*, *516*(5), 423–441. https://doi.org/10.1002/cne.22126

Smith, M. R., Nelson, A. B., & Lac, S. du. (2002). Regulation of Firing Response Gain by Calcium-Dependent Mechanisms in Vestibular Nucleus Neurons. *Journal of Neurophysiology*, *87*(4), 2031–2042. https://doi.org/10.1152/jn.00821.2001

Snowball, A., & Schorge, S. (2015). Changing channels in pain and epilepsy: Exploiting ion channel gene therapy for disorders of neuronal hyperexcitability. *FEBS Letters*, *589*(14), 1620–1634. https://doi.org/10.1016/j.febslet.2015.05.004

Stamp, J. A., & Herbert, J. (1999). Multiple immediate-early gene expression during physiological and endocrine adaptation to repeated stress. *Neuroscience*, *94*(4), 1313–1322.

Stern, J. E. (2001). Electrophysiological and morphological properties of pre-autonomic neurones in the rat hypothalamic paraventricular nucleus. *The Journal of Physiology*, *537*(Pt 1), 161–177.

Stetler, C., & Miller, G. E. (2011). Depression and hypothalamic-pituitary-adrenal activation: a quantitative summary of four decades of research. *Psychosomatic Medicine*, *73*(2), 114–126. https://doi.org/10.1097/PSY.0b013e31820ad12b

Stranahan, A. M., Lee, K., & Mattson, M. P. (2008). Central Mechanisms of HPA Axis Regulation by Voluntary Exercise. *NeuroMolecular Medicine*, *10*(2), 118–127. https://doi.org/10.1007/s12017-008-8027-0

Swaab, D. F., Bao, A.-M., & Lucassen, P. J. (2005). The stress system in the human brain in depression and neurodegeneration. *Ageing Research Reviews*, *4*(2), 141–194. https://doi.org/10.1016/j.arr.2005.03.003

Tanaka, H., Shimizu, N., & Yoshikawa, N. (2017). Role of skeletal muscle glucocorticoid receptor in systemic energy homeostasis. *Experimental Cell Research*. https://doi.org/10.1016/j.yexcr.2017.03.049

Tasker, J. G., & Dudek, F. E. (1991). Electrophysiological properties of neurones in the region of the paraventricular nucleus in slices of rat hypothalamus. *The Journal of Physiology*, *434*, 271–293.

Tasker, J. G., Oliet, S. H. R., Bains, J. S., Brown, C. H., & Stern, J. E. (2012). Glial regulation of neuronal function: from synapse to systems physiology. *Journal of Neuroendocrinology*, *24*(4), 566–576. https://doi.org/10.1111/j.1365-2826.2011.02259.x

Taylor, M. M., Yuill, E. A., Baker, J. R., Ferri, C. C., Ferguson, A. V., & Samson, W. K. (2005). Actions of neuropeptide W in paraventricular hypothalamus: implications for the control of stress hormone secretion. *American Journal of Physiology - Regulatory, Integrative and Comparative Physiology*, *288*(1), R270–R275. https://doi.org/10.1152/ajpregu.00396.2004

Thompson, R. F., & Spencer, W. A. (1966). Habituation: a model phenomenon for the study of neuronal substrates of behavior. *Psychological Review*, *73*(1), 16–43.

Uchida, S., Nishida, A., Hara, K., Kamemoto, T., Suetsugi, M., Fujimoto, M., … Watanabe, Y. (2008). Characterization of the vulnerability to repeated stress in Fischer 344 rats: possible involvement of microRNA-mediated down-regulation of the glucocorticoid receptor. *The European Journal of Neuroscience*, *27*(9), 2250–2261. https://doi.org/10.1111/j.1460-9568.2008.06218.x

Ulrich-Lai, Y. M., & Herman, J. P. (2009). Neural regulation of endocrine and autonomic stress responses. *Nature Reviews. Neuroscience*, *10*(6), 397–409. https://doi.org/10.1038/nrn2647

Umemoto, S., Noguchi, K., Kawai, Y., & Senba, E. (1994). Repeated stress reduces the subsequent stress-induced expression of Fos in rat brain. *Neuroscience Letters*, *167*(1–2), 101–104.

Valincius, G., Heinrich, F., Budvytyte, R., Vanderah, D. J., McGillivray, D. J., Sokolov, Y., … Lösche, M. (2008). Soluble Amyloid β-Oligomers Affect Dielectric Membrane Properties by Bilayer Insertion and Domain Formation: Implications

for Cell Toxicity. *Biophysical Journal*, *95*(10), 4845–4861. https://doi.org/10.1529/biophysj.108.130997

van den Pol, A. N., Wuarin, J. P., & Dudek, F. E. (1990). Glutamate, the dominant excitatory transmitter in neuroendocrine regulation. *Science (New York, N.Y.)*, *250*(4985), 1276–1278.

Viau, V., & Sawchenko, P. E. (2002). Hypophysiotropic neurons of the paraventricular nucleus respond in spatially, temporally, and phenotypically differentiated manners to acute vs. repeated restraint stress: Rapid publication. *The Journal of Comparative Neurology*, *445*(4), 293–307. https://doi.org/10.1002/cne.10178

Vyas, A., Mitra, R., Shankaranarayana Rao, B. S., & Chattarji, S. (2002). Chronic stress induces contrasting patterns of dendritic remodeling in hippocampal and amygdaloid neurons. *The Journal of Neuroscience: The Official Journal of the Society for Neuroscience*, *22*(15), 6810–6818. https://doi.org/20026655

Walker, C.-D., Toufexis, D. J., & Burlet, A. (2001). Chapter 7 Hypothalamic and limbic expression of CRF and vasopressin during lactation: implications for the control of ACTH secretion and stress hyporesponsiveness. *Progress in Brain Research*, *133*, 99–110. https://doi.org/10.1016/S0079-6123(01)33008-X

Wamsteeker Cusulin, J. I., Füzesi, T., Watts, A. G., & Bains, J. S. (2013). Characterization of corticotropin-releasing hormone neurons in the paraventricular nucleus of the hypothalamus of Crh-IRES-Cre mutant mice. *PloS One*, *8*(5), e64943. https://doi.org/10.1371/journal.pone.0064943

Watson, S., & Mackin, P. (2009). HPA axis function in mood disorders. *Psychiatry*, *8*(3), 97–101. https://doi.org/10.1016/j.mppsy.2008.11.006

White, S. H. (1970). A Study of Lipid Bilayer Membrane Stability Using Precise Measurements of Specific Capacitance. *Biophysical Journal*, *10*(12), 1127–1148. https://doi.org/10.1016/S0006-3495(70)86360-3

Yellen, G. (2002). The voltage-gated potassium channels and their relatives. *Nature*, *419*(6902), 35–42. https://doi.org/10.1038/nature00978

Yuill, E. A., Hoyda, T. D., Ferri, C. C., Zhou, Q.-Y., & Ferguson, A. V. (2007). Prokineticin 2 depolarizes paraventricular nucleus magnocellular and parvocellular neurons. *European Journal of Neuroscience*, *25*(2), 425–434. https://doi.org/10.1111/j.1460-9568.2006.05293.x

Ziegler, D. R., & Herman, J. P. (2000). Local integration of glutamate signaling in the hypothalamic paraventricular region: regulation of glucocorticoid stress responses. *Endocrinology*, *141*(12), 4801–4804.

Appendices

Appendix A

License Number	4175061052789
License date	Aug 23, 2017
Licensed Content Publisher	Nature Publishing Group
Licensed Content Publication	Nature Reviews Neuroscience
Licensed Content Title	Stress-related synaptic plasticity in the hypothalamus
Licensed Content Author	Jaideep S. Bains, Jaclyn I. Wamsteeker Cusulin, Wataru Inoue
Licensed Content Date	Jun 19, 2015
Licensed Content Volume	16
Licensed Content Issue	7
Type of Use	reuse in a dissertation / thesis
Requestor type	academic/educational
Format	print and electronic
Portion	figures/tables/illustrations
Number of figures/tables/illustrations	1
High-res required	no
Figures	Figure 2
Author of this NPG article	no
Your reference number	
Title of your thesis / dissertation	Neuronal Correlates for Neuroendocrine Habituation to Repeated Stress
Expected completion date	Aug 2017
Estimated size (number of pages)	100
Requestor Location	N/A
Billing Type	Invoice
Billing Address	N/A

Appendix B

This Agreement between Miss. Sara Matovic ("You") and John Wiley and Sons ("John Wiley and Sons") consists of your license details and the terms and conditions provided by John Wiley and Sons and Copyright Clearance Center.

License Number	4175061412067
License date	Aug 23, 2017
Licensed Content Publisher	John Wiley and Sons
Licensed Content Publication	Journal of Physiology
Licensed Content Title	Voltage-gated currents distinguish parvocellular from magnocellular neurones in the rat hypothalamic paraventricular nucleus
Licensed Content Author	Jason A. Luther,Jeffrey G. Tasker
Licensed Content Date	Feb 1, 2001
Licensed Content Pages	17
Type of use	Dissertation/Thesis
Requestor type	University/Academic
Format	Print and electronic
Portion	Figure/table
Number of figures/tables	1
Original Wiley figure/table number(s)	Figure 1
Will you be translating?	No
Title of your thesis / dissertation	Neuronal Correlates for Neuroendocrine Habituation to Repeated Stress
Expected completion date	Aug 2017
Expected size (number of pages)	100
Requestor Location	N/A
Publisher Tax ID	EU826007151
Billing Type	Invoice
Billing Address	N/A

Appendix C

This is a License Agreement between Miss. Sara Matovic ("You") and Society for Neuroscience ("Society for Neuroscience") provided by Copyright Clearance Center ("CCC"). The license consists of your order details, the terms and conditions provided by Society for Neuroscience, and the payment terms and conditions.

All payments must be made in full to CCC. For payment instructions, please see information listed at the bottom of this form.

License Number	4177830433100
License date	Aug 23, 2017
Licensed content publisher	Society for Neuroscience
Licensed content title	The journal of neuroscience : the official journal of the Society for Neuroscience
Licensed content date	Jan 1, 1981
Type of Use	Thesis/Dissertation
Requestor type	Academic institution
Format	Print, Electronic
Portion	chart/graph/table/figure
Number of charts/graphs/tables/figures	1
Title or numeric reference of the portion(s)	Figure 9
Title of the article or chapter the portion is from	Sequence of stress-induced alterations in indices of synaptic and transcriptional activation in parvocellular neurosecretory neurons
Editor of portion(s)	N/A
Author of portion(s)	K. J. Kovacs & P. E Sawchenko
Volume of serial or monograph.	16(1): 262–273
Page range of the portion	Pg 47-48 of Figure section (Figure 4.1)
Publication date of portion	October 2017
Rights for	Main product and any product related to main product
Duration of use	Current edition and up to 5 years
Creation of copies for the disabled	no
With minor editing privileges	yes
For distribution to	Canada
In the following language(s)	Original language of publication
With incidental promotional use	no
The lifetime unit quantity of new product	Up to 499
Made available in the following markets	None - Masters thesis
Specified additional information	I would like to edit the figure to include the CRH mRNA they mention in the Figure legend. I am using this in my thesis to describe stress-related transcripts.
The requesting person/organization is:	Sara Matovic / University of Western Ontario
Order reference number	
Author/Editor	Sara Matovic
The standard identifier of New Work	N/A
Title of New Work	Neuronal Correlates for Neuroendocrine Habituation to Repeated Stress
Publisher of New Work	Scholarship@Western
Expected publication date	Sep 2017
Estimated size (pages)	100

Curriculum Vitae

<div align="center">

SARA MATOVIC

</div>

EDUCATION

University of Western Ontario, London, ON
M.Sc. Neuroscience **2018 (convocation)**
Thesis: "Neuronal Correlates for Neuroendocrine Habituation to Repeated Stress"

University of Western Ontario, London, ON
B.Sc. Neuroscience **2015**
Honors Thesis: "Synaptic Changes in the Hypothalamus after Chronic Stress"
Western Scholar, Deans Honors List 2010-2015

AWARDS

OUA Coach of the Year (Varsity Women's Rowing) **2017**
Went undefeated at OUA regatta in all lightweight women's categories.
Award selected by vote from all university head coaches.

NSERC Research Grant (CGS - M) **Sept. 2016 – August 2017**
National Research award valued at $17,500 over 3 terms.
Awarded based on academic and research merit.

Ontario Graduate Scholarship (OGS – M) **Sept. 2015 - August 2016**
Provincial Research award valued at $15,000 over 3 terms.
Awarded based on academic and research merit.

UWO Continuing Admissions Scholarship **2010 - 2015**
Valued at $2,500 per year. Awarded based on minimum application average of 94%.

The Purple Blanket Athletic Honor **2015**
Prestigious University Athletics Award (12 athletes awarded from all teams). Achieved
"superior distinction at the Provincial/National level of competitions as representatives of Western".

Queen Elizabeth Aiming for the Top Scholarship **2010 – 2014**
Valued at $3,500 per year for four years. Awarded for academic excellence in high school.

E.F Lepine Memorial Award and Gordon Risk (OSOTF) Fund Award **2014**
Valued at $1,000 each. Based on academic achievement and athletic leadership.

Dorothy Thompson Award **2012/2013**
Valued at $1,000. Awarded to those demonstrating academic achievement and leadership
qualities on an intercollegiate athletic team.

Quest for Gold (Rowing) **2012 – 2014**
Valued at $5,000 per year. Awarded to athletes who have met a certain sport specific
standard to allow them to continue their pursuit of excellence in sport while fulfilling educational goals.

RESEARCH WORK AND MAJOR VOLUNTEER EXPERIENCE

Support Line Volunteer – Canadian Mental Health Association, London, ON **Feb. 2017 - present**
Empathetic listening, assessing suicide/possible harm to self/others, encouraging
help and support in various ways.

Volunteer Rowing Coach – Western University and UWO Boat Club, London, ON **May 2016 - present**
Empowering female athletes to become confident and strategic. Striving for
excellence through teamwork and commitment at provincial and national level.

Inoue Lab Summer Research Trainee – Western University, London, ON **May 2015 – August 2015**
Pre-graduate project, received intensive training for patch clamp electrophysiology.

Memory and Emotion Work Study Research Assistant **Jan. 2013 – Dec. 2013**
Worked with a Master's student to look at the role of affective signals in face
recognition. Techniques: EMG, ECG, galvanic skin response.

TECHNICAL SKILLS/TRAINING
- Standard First Aid & CPR-C; Mental Health First Aid; SafeTalk
- Familiar with basic computer programming in Matlab/python
- Immunohistochemistry and confocal microscopy
- Whole-cell patch clamp electrophysiology
- Animal behavior techniques: open field, forced swim, elevated plus maze, y-maze, light/dark box
- DREADDS (tamoxifen and CNO injections)

PUBLICATIONS AND CONFERENCES (PRIMARY AUTHOR)

Society for Neuroscience Conference
Abstract Publication + Poster Presentation   **November 2016**
Neuronal correlates for neuroendocrine adaptation to repeated stress.

Physiology Day
Poster Presentation (with Best Poster Award)   **November 2016**
Neuronal correlates for stress adaptation.

Robarts Research Day
Oral Presentation + Poster Presentation   **June 2016**
Neuronal correlates for neuroendocrine adaptation to repeated stress.

Canadian Association for Neuroscience
Abstract Publication + Poster Presentation   **May 2016 and May 2017**
Neuronal correlates for bi-directional adaptation of the hypothalamic-pituitary-
adrenal (HPA axis) during chronic stress. *Travel award received.*

London Health Research Day
Platform Presentation + Abstract Publication.   **March 2016**
Neuronal correlates for bi-directional adaptation of the hypothalamic-pituitary-
adrenal (HPA axis) during chronic stress.

Southern Ontario Neuroscience Association
Poster Presentation   **May 2016**
Neuronal correlates for neuroendocrine adaptation to repeated stress.

Western Student Research Conference
Poster Presentation   **March 2015**
Glutamatergic changes in the paraventricular nucleus after chronic stress.

London Health Research Day
Abstract Publication + Poster Presentation   **March 2015**
Synaptic changes in the hypothalamus after chronic stress.

LEADERSHIP ROLES/EXTRACURRICULAR ACHIEVEMENTS

Mustang Athlete Student Council President	2015-2016
UWO Rowing Executive: VP alumni relations, VP Gala	2013-2015
Mustang Athlete Student Council – Rowing representative	2013-2015
Ontario University and Canadian University Rowing Champion	2012-2015
UWO Lightweight Women's Rowing Captain	2012-2014
Head of the Charles (International) Rowing Champion	2012, 2013
National Development Center Ontario Athlete	2012
Most Valuable Player (Rowing)	2011, 2013